THE INTERFEROMETRY OF REVERSED AND NON-REVERSED SPECTRA

PART II

By CARL BARUS
Hazard Professor of Physics and Dean of the Graduate Department in Brown University



Published by the Carnegie Institution of Washington
Washington, 1917

CARNEGIE INSTITUTION OF WASHINGTON

Publication No. 249, Part II

PRINTED BY J. B. LIPPINCOTT COMPANY
AT THE WASHINGTON SQUARE PRESS
PHILADELPHIA, U. S. A.

CONTENTS.

CHAPTER I.—*Methods for Reversed and Non-Reversed Spectrum Interferometry.*

PAGE.

1. Introductory..... 9
2. Apparatus. Figs. 1, 2, 3..... 9
3. Measurements. First- and second-order spectra. Tables 1, 2. Figs. 4, 5..... 11
4. Continued. First-order spectra..... 13
5. Continued. Second-order spectra. Table 3..... 14
6. Theory. Fig. 6..... 14
7. Compensator measurements. Sharp wedge..... 15
8. Continuation. Revolving plate. Table 4. Fig. 7..... 16
9. Continuation. Air column. Tables 5, 6..... 18
10. Continuation. Babinet compensator. Fig. 8..... 19
11. Micrometer displacement of the second grating, G' (fig. 3). Table 7..... 20
12. Prism method. Reflection. Table 8. Figs. 9, 10, 11..... 21
13. Prismatic refraction. Figs. 12, 13..... 25
14. Prism methods without grating. Figs. 14, 15, 16..... 26
15. Displacement parallel to rays. Table 9..... 28
16. Breadth of efficient wave-fronts. Apparent uniformity of wave-trains. Rotation of fringes. Figs. 17, 18..... 30
17. Film grating. Figs. 19, 20..... 32
18. Non-reversed spectra. Figs. 21, 22, 23, 24..... 34
19. Non-reversed spectra. Restricted coincidence. Figs. 25, 26..... 38
20. The same, continued. Homogeneous light. Dissimilar gratings..... 43
21. The same, continued. Duplicate fringes. Figs. 27, 28, 29..... 45
22. The same. Prismatic adjustment. Figs. 30, 31..... 48
23. Apparent lengths of uniform wave-trains. Tables 10, 11. Figs. 32, 33, 34..... 52
24. Normal displacement of mirrors ($\delta=0$). Figs. 35, 36, 37..... 55
25. Diffraction at M, N, replacing reflection. Table 12. Figs. 38, 39..... 57
26. Experiments with the concave grating..... 59
27. Polarization. Figs. 40, 41..... 60

CHAPTER II.—*The Interferences of Inverted Spectra.*

28. Introductory..... 62
29. Apparatus. Non-inverted spectra. Fig. 42..... 62
30. Apparatus and results for inverted spectra. Figs. 43, 44, 45..... 64
31. Wave-fronts narrowed. Table 13. Figs. 46, 47, 48..... 65
32. Inverted spectra. Further measurements. Table 14..... 67
33. Rotation of fringes. Fig. 49..... 69
34. Range of displacement varying with orientation of reflector P'..... 70
35. Range of displacement varying with dispersion..... 72
36. Spectra both reversed and inverted. Figs. 50, 51..... 73
37. Experiments with the concave grating..... 74
38. Conclusion. General methods. Fig. 52..... 75
39. Displacement interferometry. Equations. Fig. 53..... 77
40. Continued. Reversed spectra, etc. Tables 15, 16..... 80

CHAPTER III.—*Elongation of Metallic Tubes by Pressure and the Mesurement of the Bulk Modulus by Displacement Interferometry.*

41. General method and apparatus. Fig. 54..... 84
42. Remarks on the displacement interferometer. Figs. 55, 56..... 85
43. Observations. Thick steel tube..... 86
44. Further experiments. Tables 17, 18. Fig. 57..... 87
45. Brass tube. Tables 19, 20. Figs. 58, 59, 60, 61..... 90
46. Thin steel tube. Table 21..... 92
47. Conclusion. Thermodynamic application. Fig. 62..... 93

CHAPTER IV.—*Refractivity Determined, Irrespective of Form, by Displacement Interferometry.*

PAGE.
48. Introductory 95
49. Preliminary experiments. Figs. 63, 64 95
50. Apparatus 96
51. Equations. Table 22 97
52. Observations. Tables 23, 24. Figs. 65, 66 99
53. Dispersion constants. Tables 25, 26. Fig. 67 100
54. Further observations. Tables 27, 28. Figs. 68, 69 102
55. Conclusion. Table 29 105

CHAPTER V.—*Displacement Interferometry in Connection with U-Tubes. Jamin's Interferometer.*

56. Introduction. Figs. 70, 71, 72 107
57. Apparatus. Michelson interferometer 107
58. Equations 109
59. Observations 110
60. Jamin's interferometer. Figs. 73, 74, 75, 76 111
61. Vertical displacement of ellipses. Figs. 77, 78 114
62. Displacement interferometer. Jamin type. Tables 30, 31, 32, 33. Fig. 79 115
63. Broad slit interferences. Achromatic fringes 120
64. Wide slit. Homogeneous light. Sodium flame. Figs. 80, 81, 82, 83, 84, 85 121
65. Vertical displacement. Table 34. Fig. 86 126
66. Angular displacement of fringes. Table 35. Fig. 87 128

CHAPTER VI.—*The Displacement Interferometry of Small Angles and of Long Distances. Complementary Fringes.*

67. Parallel rays retracing their path. Figs. 88, 89, 90, 91, 92 130
68. Groups of achromatic fringes. Table 36. Fig. 93 133
69. Measurement of small angles without auxiliary mirror. Table 37 134
70. Complementary fringes. Figs. 94, 95 135
71. Equations 138
72. Separated rigid vertical system. Figs. 96, 97 139
73. The displacement interferometry of long distances 141
74. Theory. Table 38 142

PREFACE.

In the present volume I have pursued the work on the interferences of reversed and non-reversed spectra, begun in my last report (Carnegie Inst. Wash. Pub. No. 249, 1916), in a variety of promising directions, such as the original investigation suggested. It will be remembered that the reversal (180°) here contemplated takes place on a transverse line of the spectrum (*i.e.*, a line parallel to the Fraunhofer lines), which thereby becomes a line of symmetry for the phenomena. The apparatus has been extensively modified, so as to admit of measurements relating to individual fringes. The object of such quantitative work, however, is to furnish a guide for the development of the experiments and to corroborate equations, not to collate standard data. These could hardly be satisfactorily obtained, moreover, unless the work were done with optical plates and mirrors, whereas the work in this volume and the preceding has been done with ordinary window-plate and usually with film gratings.

A large part of Chapter I is devoted to the treatment of prismatic methods, developed with the additional purpose of securing a greater intensity of light. A very curious intermediate case between the interferences of reversed and non-reversed spectra is the pronounced interference of spectra from the same source, but of different lengths (dispersion) between red and violet. The phenomena of crossed rays find a parallel occurrence in the present paper, in the behavior of duplicated fringes, when similar gratings or prisms disperse and subsequently recombine a beam of white light. A type of fringes is detected which depends merely on the grating space and is independent of wave-length. An interesting question as to the limits of micrometer displacement within which fringes of any kind are discernible (observations which were at first supposed to be due to the degree of uniformity of interfering wave-trains) is eventually shown to be a necessary result of dispersion. Finally, the direct interference of divergent rays obtained from polarizing media is exhibited.

In Chapter II the interferences of inverted spectra, a subject merely touched in the preceding volume, are given greater prominence. In this case one of the two spectra from the same source is inverted (180°) relatively to the other on a longitudinal axis (*i.e.*, an axis normal to the Fraunhofer lines), which thus becomes a line of symmetry. In the development of the subject, spectra half reversed and spectra both reversed and inverted are treated successfully. In the latter case the conditions of interference are fulfilled at but a single point in the whole area of the spectrum field; and yet the phenomenon is pronounced and not very difficult to realize. The limits of micrometer displacement within which interferences may be obtained are again determined. At the end of the chapter it was thought useful to collate available equations in the treatment of phenomena of the present kind.

The third and fourth chapters are incidental applications of the displacement interferometer and contain experiments on the expansion of metal tubes by internal pressure and on a promising method of measuring the refraction of glass, irrespective of form. To carry out the experiments in the last case with requisite rigor, optic plate-glass apparatus would unquestionably be essential. Nevertheless the tentative data obtained are noteworthy.

I have begun in Chapter V the development of displacement interferometry in connection with the older Jamin-Mach interferometer, an instrument which has certain peculiar advantages and is in a measure complementary to the Michelson interferometer. The work was undertaken in connection with the micromeasurement of the difference of heights of communicating columns of liquids, though the latter had to be abandoned in consequence of the excessive tremor in a laboratory surrounded by active city traffic. I shall hope, however, to carry out such work elsewhere.

The chief result of Chapter V is the detection of the achromatic interferences, as I have called them for convenience—interferences which are ultimately colors of thin plates seen at oblique incidence; but with the new interferometer, and obtained with white light, they are peculiarly straight and vivid and resemble a narrow group of sharp Fresnellian fringes with the central member nearly in black and white. They are capable of indefinite magnification and their displacement equivalent is a fraction of a mean wavelength per fringe. Notwithstanding their strength and clearness, they are so mobile in connection with micrometric displacement that in general it would be almost hopeless to attempt to find them but for the fact that they coincide in adjustment with the centered ellipses or hyperbolæ of the spectrum fringes of the displacement interferometer.

The fine white slit-image which is dispersed to produce the latter carries the achromatic fringes when the slit is indefinitely broadened or removed. Once found, moreover, they are not sensitive to small differences of adjustment if a change of focal plane is admissible. The chapter shows a curious method for the measurement of vertical displacements, possibly available for the detection of ether drag, which, though just insufficient in connection with the spectrum fringes, would be promising in connection with the achromatic fringes. Finally, the chapter contains some repetitions of the old experiments of Fizeau on the periodic evanescence of fringes due to the sodium lines. Curiously enough, the achromatic fringes also show periodic recurrence sometimes, which as yet remains unexplained.

The peculiar adaptability of the new interferometer to the measurement of small angles, either in a horizontal or a vertical plane, is developed in the final chapter. The ratio of the angular displacement of fringes to the angle to be measured (*i.e.*, the rotation either of the paired mirrors or of an auxiliary mirror in the apparatus) may be made enormously large, and the paper shows cases in which, with strong luminous fringes, the angle to be measured is magnified 500 times. Moreover, this is by no means a limiting performance. Again, while angles as small as a few tenths of a second or less are measured, angles

as large as several degrees come naturally within the scope of the method. Similar remarks may be made with respect to the ratio of angular displacement and micrometer displacement. Given, therefore, an apparatus which measures very small angles without constraint or forced approximations, the measurement of long distances is the next result in order; for it is merely necessary to place the angle to be measured at the apex of the distance triangle on the length of the ray parallelogram as a base. This may be done in a variety of ways, some of which are shown in the chapter. The sensitiveness may again be made remarkably large.

The fringes here in question are preferably the very luminous achromatic fringes. They have been identified as ultimately colors of thin plates, but they look like Fresnel's fringes. In connection with this work, however, another type of fringes was detected obtainable with a fine slit, white light, and in case of centered spectrum fringes when the ocular of the telescope (or the eye) is out of focus. These are actually Fresnellian interferences, but being made up of broad concentric hyperbolic areas, brilliantly complementary in color, they resemble the lemniscates of biaxial crystals without the shadows.

My thanks are due Miss Lena F. Uhlig, who has assisted me efficiently in the preparation of this volume for the press.

Carl Barus.

Brown University,
Providence, Rhode Island, June 1917.

CHAPTER I.

METHODS FOR REVERSED AND NON-REVERSED SPECTRUM INTERFEROMETRY.

1. Introductory.—Thus far it has been impossible to use the fringes of reversed spectra individually, because of the tremor of the apparatus. It is therefore desirable to endeavor to obviate this annoyance as far as possible, and the end would appear to be most easily obtainable if the distances corresponding to the same path-difference are made smaller. At the same time the results for small distances will be interesting for this very reason in contrast to the long-distance methods.

Furthermore, the development of different methods, with a consideration of the peculiarities of each, will constitute an essential contribution to the theory of the phenomena; for from this the degree of importance which is to be attached to the original diffraction at the slit of the collimator (*i.e.*, the limiting angle at the slit, within which diffracted rays must lie to be subsequently capable of interference, whether reversed or inverted) will appear in its relations to the total dispersion of the system. The slit, however fine, is still a wave-front of finite breadth.

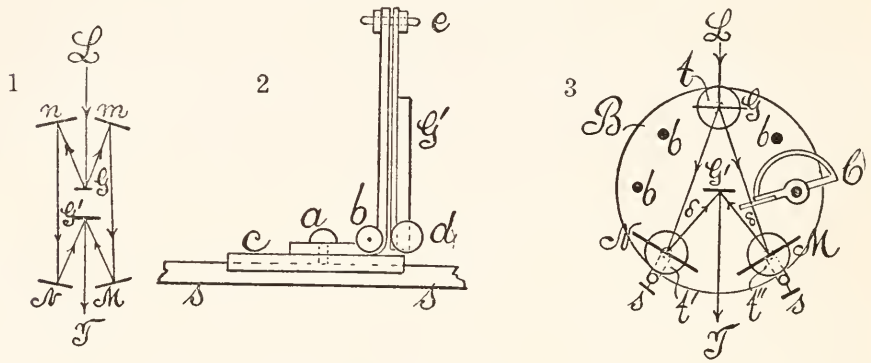
2. Apparatus.—In the first experiment, the device with two identical reflecting gratings, GG', figure 1, was firmly mounted on a massive spectrometer, the four mirrors, m, n, M, N, being specially attached. White light received from the collimator L after two dispersions was viewed at the telescope T. Both gratings were on a slide ss, enlarged in figure 2, set in the direction LT of the previous figure. The carriage c, figure 2, was provided with universal joints (a with a vertical axis, b and e with horizontal axes normal to each other), while the swiveling of the grating G was controlled by set-screws at d, relative to the axle at e.

Unfortunately, the displacement of the mirror M, figure 1 (on a micrometer), passes the corresponding pencil across the face of the grating G' and thus virtually includes a fore-and-aft motion of the latter. Thus the fringes pass, with rotation, from very fine, hair-like striations, through a horizontal maximum of coarseness, back to vertical lines again, when homogeneous light and a wide slit are employed. The annoyances due to tremor, however, were not overcome. Moreover, there is difficulty in obtaining Fraunhofer lines normal to the longitudinal axis of the spectrum. This method was therefore abandoned.

The design shown in figure 3, with a transmitting grating at G (grating space $D = 352 \times 10^{-6}$ cm.) and a stronger reflecting grating at G' ($D = 200 \times 10^{-6}$ cm.), was next tested, M being the micrometer mirror. The mean distance of M from N was about 15 cm., from MN to G' about 10 cm. and to G 40 cm.

Later these distances were enlarged. First-order spectra were used and the fringes obtained easily and brilliantly, particularly with mercury light, in both green and yellow. They rotated as above, admitted a displacement M of about 1 cm. But they were still too mobile to be used individually.

The same design, figure 3, was now mounted on a round, heavy block of cast iron B, 30 cm. in diameter and 4 cm. thick, the distance G to MN being about 20 cm. A number of screw-sockets, b, b, were drilled into B on the right and left, for mounting subsidiary apparatus. G' as before was on the universal slide (fig. 2), movable in the direction LT. The tablets t, t', etc., of G, M, N, and G' were mounted tentatively on standards of gas-pipe 1.5 cm. in external diameter and 6 cm. long. Slight pressure by the finger-tips showed a passage of several fringes across the field, but the fringes were stationary in the absence of manual interferences and in spite of all laboratory tremors. A parallel arm of the same pipe was therefore firmly attached to the stem of

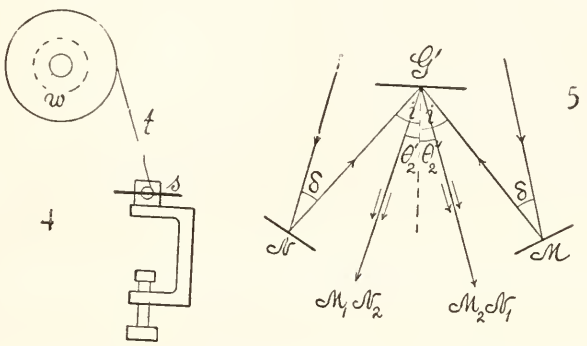


N and M, each arm terminating in a fine horizontal set-screw, s, s, below, adapted to push against the rim of the iron block. In this way adequately stationary conditions and an elastic fine adjustment for superposed longitudinal spectrum axes were both secured with advantage. Similar elastic adjustments have been recently applied. It was now possible to manipulate the micrometer at M by hand; but a glass-plate compensator C, rotated by a tangent screw over a graduated arc, was also convenient. Later other types were attached, including an air-compensator, in which path-difference was secured by exhausting the air within a closed pipe provided with glass-plate ends. These contrivances were eventually superfluous, however, as it was found that on reducing the rotation of the micrometer-screw the latter could be used at once.

In case of homogeneous light and a wide slit, fringes were visible in an ordinary telescope for a play of over 2 cm. of the micrometer-screw, passing, however, between extremes of fineness. The slit images are not of equal breadth, if first- and second-order spectra are superposed; but if the longitudinal axes are coincident, any position of the narrow image within the broader produces a wide vertical distribution of fringes, usually more or less horizontal. They are very easily found. The sodium flame is too feeble for use. The mercury

arc is unfortunately too flickering, so that the fringes jump about and are useless for measurement. Excellently sharp quiet fringes are obtained with sunlight (white), in which the cross-hatched interference pattern is nearly linear at the line of symmetry of the reversed spectra. The fringes climb very decisively up and down this line with the motion of the micrometer, reduced as suggested. The electric arc and a Nernst filament are equally available as a source of light. Finally, by suitably rotating the grating G', figure 2, on the axis e, by aid of the set of screws d, fringes whose distance apart is over one-third of the width of the telescope field may be obtained quite sharply. As this distance represents but 30×10^{-6} cm., there is no difficulty of realizing 10^{-6} cm. in case of these long fringes.

3. Measurements. First- and second-order spectra.—The steadiness of the fringes, even in an agitated location, induced me to make a few measurements for orientation. Accordingly, the Fraunhofer micrometer, reading to 10^{-4} cm., was provided at its screw-head with a light wooden wheel w, figure 4, about



10 cm. in diameter and 3 mm. thick. A groove was cut in the circumference of the wheel, so that a silk thread t could be wrapped around it. The other end of the thread was wound around a brass screw s, about 6 mm. in diameter, turning in a nut, preferably of fiber, which was fastened to the edge of the table by a small brass clamp. In this way it was possible to control the motion of individual fringes crossing a fiducial line in the field of the telescope. This simple device worked surprisingly well, a smoothly running micrometer being presupposed. In fact, it was possible to set a fringe to a few millionths of a centimeter. Later the micrometer-head was grooved and a finer turning-screw suitably attached to the base B of the apparatus. (*Cf.* § 70, below.)

The fringes should be widened as far as convenient, by rotating the grating on the axle e, figure 2, by aid of the set-screws d. In this case they climb up or down the transverse strip as s in figure 4 is slowly rotated. Fringes moving horizontally are not serviceable, because they are too near together. It is not difficult to obtain the single vertical line, black or bright, on suitable rotation about e. On either side of this transitional adjustment the fringes move vertically (climb or fall) in opposite directions for the same micrometer

displacement. The arrow-shaped forms are also often satisfactory, and may be obtained by adjusting the two bright patches on the reflecting grating into coincidence, by the eye, in the absence of the telescope. The grating G' is moved fore and aft for this purpose on the slide s, figure 2, until the two bright strips become one.

In making the first adjustment, I incidentally combined the first-order spectrum from N with the second-order spectrum from M, as shown in figure 5, under the impression that the wider D groups from the latter were due to slight curvatures of mirrors. The fringes were nevertheless easily found and showed no anomalies, except that observation had to be made near M or N.

It appears from figure 5 that the equations for this case imply

$$\sin i + \sin \theta''_2 = 2\lambda/D_2$$
$$\sin i - \sin \theta'_2 = \lambda/D_2$$

where the angles i and θ are equal ($\theta'_2 = \theta''_2$). Thus $\sin i = 3\lambda/2D_2$ and $\sin \theta = \lambda/2D_2$, D_2 being the grating constant ($D_2 = 200 \times 10^{-6}$ cm.).
Hence

$$\sin i = 0.4420 \quad \sin \theta_2 = 0.1423$$
$$i = 26°14' \qquad \theta_2 = 8°11'$$

while from the first grating, $D_1 = 352 \times 10^{-6}$ cm., $\theta_1 = 9°38'$; whence

$$\sigma = i + \theta_1 = 35°52' \qquad \delta = i - \theta = 16°36'$$

The trial readings given in table 1 of the micrometer for a passage of 20 fringes each were found without special precautions, which is equivalent

TABLE 1.

Scale parts.	10^{-3} cm.
19.7	9.85
21.0	10.5
22.2	11.1
23.4	11.7
24.6	12.3
25.8	12.9
27.0	13.5
28.2	14.1

to an average of $10^{-6} \times 30.1$ cm. per fringe. As the line of symmetry lay very near the two D_1D_2 doublets, this is obviously an approach to half a wave-length. For accurate work D_1D_2 and $D'_1D'_2$ should be superposed, in which case the fringes would lie between and actually correspond to their mean wave-length.

A number of measurements like the above were now made with different types of fringes. The mean values successively taken from 3 or 4 batches of 20 fringes each were

$$10^6 \delta e = 29.4,\ 30.0,\ 31.2,\ 30.6,\ 29.7,\ 30.1,\ 30.0,\ 30.0,\ 30.8 \text{ cm.}$$

The results were less decided when long fringes were used. The mean value of the 10 sets is thus $\delta e \times 10^6 = 30.19$ cm. per fringe. Actual or approximate coincidence of the D lines made no appreciable difference.

In the following results the reflection from the mirror M, figure 5, was used in the first order and from N in the second order, after leaving G'. Observations were made near N, figure 5. The displacement corresponding to 80 fringes was successively 0.0024, 0.0024, 0.0024, 0.0024 cm., so that the mean value

$$10^6 \delta e = 30.0 \text{ cm.}$$

agrees with the above.

Similar trial observations (combined first order from N and second order from M) were made with red light near the C line in series of 6 with a mean value $\delta e \times 10^6 = 34.0$ cm. Again, near the b line (green), giving $\delta e \times 10^6 = 27.2$ and 27.8 cm. per fringe. These should therefore be distributed in terms of wave-length, as in table 2.

TABLE 2.

	$10^6\lambda$	Ratio.	$10^6\delta e$	Ratio.
C	65.6 cm.	1.11	34.0 cm.	1.13
D	58.9	1.	30.2	1.
b	51.7	0.88	27.5	0.91

and they are as nearly as may be expected in the ratio in question, seeing that the total displacement for 60 fringes does not exceed 0.004 cm. For accurate data it would be necessary to count many hundreds of fringes, and to correct the δe values by multiplying by sec $(\theta_2 - \theta_1)/2$. I have not done this, as the red and green fringes are not so distinctly seen as the yellow.

4. Continued. First-order spectra.—The apparatus was now readjusted in such a way that first-order spectra were available from both mirrors. This puts the grating G' at a greater distance from the line M and N than before, for the angle θ_2 is smaller. A series of trial results were investigated in the same manner as above, the mean values from 4 successive pairs of 80 fringes each being, in three repetitions,

$$\delta e \times 10^6 = 29.0,\ 29.4,\ 29.5 \text{ cm.}$$

and from 5 pairs of 100 fringes each,

$$\delta e \times 10^6 = 29.1 \text{ cm.}$$

This makes an average of

$$\delta e \times 10^6 = 29.25 \text{ cm.}$$

somewhat smaller than half a wave-length of the D light used. Unfortunately, the screw at s (fig. 4) here worked jerkily, to which the low value is probably due.

In this case $\sin \theta_1 = \lambda/D_1$, where $D_1 = 352 \times 10^{-6}$ cm. or $\theta'_1 = 9°38'$; $\sin \theta'_2 = \lambda/D_2$, where $D_2 = 200 \times 10^{-6}$ cm. or $\theta'_2 = 17°9'$, whence

$$\sigma = 26°47' \quad \text{and} \quad \delta = 7°31'$$

In a later series of experiments, the play of the screw s was improved, so

that it ran more smoothly. The following values were found in two repetitions, from 4 pairs of 80 fringes each:

$$\delta e \times 10^6 = 30.1,\ 30.0 \text{ cm.}$$

and in 5 pairs of 100 fringes each,

$$\delta e \times 10^6 = 29.5 \text{ cm.}$$

If the mean value of these data is compounded with the above mean, the average is

$$\delta e \times 10^6 = 29.56 \text{ cm.}$$

5. Continued. Second-order spectra.—The same phenomenon was not sought in the two second-order spectra from G'. Magnificent arrows were obtained, useful throughout about 5 mm. of the micrometer-screw, after which they lost clearness. This limited range could no doubt be immensely increased if optical plate glass were employed in place of the ordinary plate used. The data for pairs of observations, including 60 or 80 fringes, were (5 repetitions) $\delta e \times 10^{-6} = 30.3,\ 30.5,\ 30.0,\ 30.8,\ 31.1$ cm. per fringe, giving a mean value of $\delta e \times 10^6 = 30.5$ cm. In the last two measurements the sodium doublets coincided.

In this case $\sin \theta''_2 = 2\lambda/D_2$, where $D_2 = 200 \times 10^{-6}$ cm. and $D_1 = 352 \times 10^{-6}$ cm. (first grating). Thus

$$\sigma = 45^\circ\ 44',\ \delta = 26^\circ 28'$$

If the above mean data are summarized the results appear as follows ($\lambda = 58.93 \times 10^{-6}$ cm.):

G first order, G' first order, mean $\delta e \times 10^6 = 29.56$ cm.
G first order, G' first and second order, mean $\delta e \times 10^6 = 30.2$ cm.
G first order, G' second order, mean $\delta e \times 10^6 = 30.5$ cm.

And if computed as $\delta e = \lambda/2 \cos \delta/2$, these become

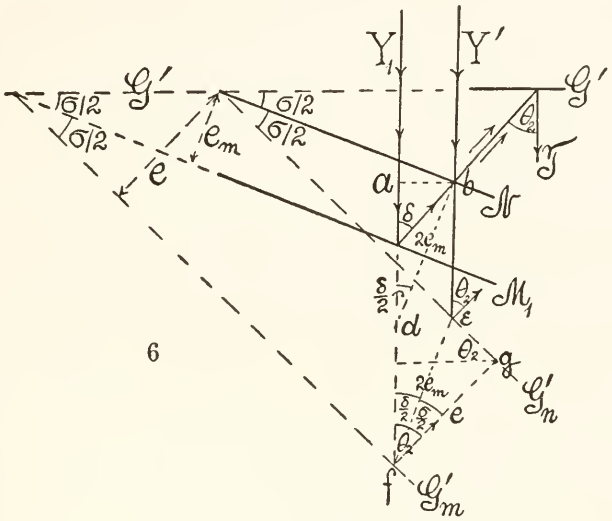
TABLE 3.

$\delta e \times 10^6$	Diff.
29.53 cm.	+0.03 cm.
29.78	+ .42
30.27	+ .23

The maximum error of 4×10^{-7} cm. is equivalent to but a little over 1 per cent of the distance between fringes, and it would be idle to suppose that the apparatus, figure 4, could be set more accurately. In fact, the largest error occurs in the second set, which were first made and in which the play of the apparatus was inadequately smooth.

6. Theory.—Hence the theory of the apparatus (fig. 6) may be regarded as justified. Here the rays Y and Y' come from the first grating (G transmitting), and after reflection from the opaque mirrors M and N (the former on a micrometer) impinge on the second reflecting grating G', with a smaller

grating space, and thereafter interfere along the line T, entering the telescope. To treat the case the mirrors M, etc., may be rotated on the axis T normal to G' in the position M_1. G'_n and G'_m show the reflections of G' in the mirrors



N and M_1. We thus have a case resembling the interferences of thin plates, and if e_m is the normal distance apart of the mirrors M_1 and N, the displacement Δe_m per fringe is given by

$$\lambda = 2\Delta e_m \cos \delta/2$$

where δ is the angle between the rays incident and reflected at the mirrors. This is the equation used above. If the mirrors and the reflections of the gratings G' make angles $\sigma/2$ and σ with G', the actual lengths of the rays (prolonged) before meeting to interfere terminate in e and f respectively. Let the image of G' be at a normal distance e apart. Then $e = 2e_m \cos \sigma/2$, for the figure $fdb\epsilon$ is a parallelogram. If the distance ϵg is called C we may also write

$$\lambda = e \cos \theta_2 + C \sin \theta_2$$

since $C = 2e_m \sin \sigma/2$ and the angle of diffraction $\theta_2 = (\sigma+\delta)/2$.

7. Compensator measurements. Sharp wedge.—With the object of testing the interferometer under a variety of conditions, measurements were made with a number of different compensators and the experience obtained may be briefly given here. The first of these was a very sharp wedge, such as may be obtained from ordinary plate glass. The piece selected, cut from an old mirror, on being calipered, showed the following dimensions: Length, 5 cm.; thickness at ends, 0.375 and 0.367 cm. Hence the angle of the wedge is $\alpha = 0.0016$ radian, or about 0.1°. No difficulty is experienced from the deviation of the rays for so small an angle, though sometimes the fringes are unequal and the lines presumably curved. This wedge was attached to a Fraunhofer micrometer moving horizontally, and the normality of the rays passing through

the glass was found by rotating it around an axis perpendicular to the rays until the direction of motion of the fringes was reversed. In view of the small angle α and the micrometric displacement, it was easy to count single fringes, or fractions as far as about 1/30 of a fringe, even though the beam traversed the glass twice. In the first experiment the following data of the horizontal displacement, r, of the wedge were found for successions of 7 fringes:

0.2044 cm.	0.2042	0.2043	0.2067
0.2058 cm.	0.1976	0.1946	0.18888

Mean, 0.2008 cm. Per fringe, $\delta r = 0.0287$ cm.

The last three results are low, the discrepancies probably resulting from slight wabbling of the micrometer slide. In another series made with care as to the normal adjustment, the horizontal displacement, r, of the wedge for successions of 11 parallel fringes was

0.3022 cm.	0.2997	0.2974	0.3002	0.2991	0.3078
0.3081 cm.	0.3101	0.3170	0.3183	0.3155	

Mean, 0.3014 cm. Per fringe, $\delta r = 0.0274$ cm.

If x be the distance from apex of the wedge, its thickness is $e = x\alpha$, or per fringe $\delta e = \alpha \delta x$. The index of refraction was found to be $\mu = 1.526$ by total reflection. Thus, without correcting for dispersion,

$$2(\mu - 1)\delta e = \lambda$$

and with the above values

$$\alpha = \frac{10^{-5} \times 5.893}{2 \times 0.526 \times 0.028} = 0.0020 \text{ radian}$$

This is larger than the calipered value because the rays go through the wedge twice obliquely. The reduction, however, would be too complicated here and will be treated later.

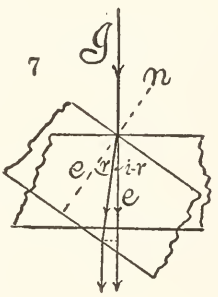
The irregularities above are referable to the micrometer, which was not very accurate, and no particular care was taken with details. The method is interesting as allowing of the complete control of a single fringe; *i.e.*, the equivalent of 30×10^{-6} cm. As this corresponds to 0.028 cm. on the micrometer, the displacement $\delta x = 0.001$ is equivalent to 10^{-6} cm. Furthermore, the method presents an expeditious means of finding $\alpha = \lambda / 2(\mu - 1)\delta x$ when α is very small.

8. Continuation. Revolving plate.—In the next place, the revolving compensator C, figure 3, was employed. This also proved to be an admirable device for controlling the fringes, and it was much more rapid than the preceding. Unfortunately the computation is inconvenient, as the normal position can not be ascertained with sufficient accuracy. To find it, the plate was revolved until the fringes changed their direction of motion. This is an indication of the insertion of the minimum thickness of glass, but is not sharp enough for precision. Hence data in A, table 4, are not coincident, i denoting the angle of incidence. Another somewhat better and thicker plate was now inserted with the results shown in B.

TABLE 4.

A. Same plate as in the preceding work, $e=0.370$ cm.					B. Thickness $e=0.489$ cm.				
No. of fringes.	i			i (probable value).	No. of fringes.	i			i (probable value).
0	0°	0°	0°	0°	0	0°	0°	0°	0°
10	4.4	5.8	7.3	5.4	10	6.0	5.5	4.9	5.2
20	7.4	8.0	9.5	7.8	20	7.9	7.3	7.0	6.8
30	9.6	9.7	11.1	9.5	30	9.5	8.9	8.5	8.3
40	11.4		12.6	11.0	40	10.9	10.3	9.9	9.6
50	13.0		13.8	12.3	..			...	

The second series here is practically the mean of the two, though the reason for these large discrepancies is not clear to me, even in consideration of the wedge-shaped plates. The mean of the results may, however, be used for computation.



The path-increment introduced by the glass of thickness $e=0.489$ cm. and index of refraction $\mu=1.526$, at an angle of incidence i and refraction r for n fringes, beginning at $i=0$, may be written (see fig. 7, where I is the incident ray)

$$n\lambda = e\mu\left(\frac{1}{\cos r} - 1\right) - e\left(\frac{\cos(i-r)}{\cos r} - 1\right)$$

This is a cumbersome equation. If the angles i are small, the cosines may be expanded and then approximately

$$2n\lambda = e\left((\mu-1)r^2 + (i-r)^2\right)$$

which, since $i=\mu r$ nearly, may be further simplified to

$$n\lambda = e(\mu-1)i^2/2\mu$$

Thus for the second set (mean)

$r=$	3.6°	4.8°	5.9°	6.8°
$10^5\lambda=$	6.7	6.4	6.9	6.5 cm.

The wave-length thus comes out very much too large, but in consideration of the inadequacy of the fiducial position, $i=0°$, this is not unexpected. Thus the probable values of i in the tables (computed from λ correct) agree with the third series. In addition to this the effect of slightly wedge-shaped plates, etc., can not be ignored. For the first set (mean values) the results are similar, being

$$10^5\lambda = 6.8 \quad 7.0 \quad 6.9 \quad 7.0 \quad 7.0 \text{ cm.}$$

if computed by the approximate equation. This is again too large, but the probable value of i computed from the correct λ, as before, agrees nearly with the first series of this set.

9. Continuation. Air column.—An air compensator was now installed consisting of a tube $e=15$ cm. long and about 2 cm. in diameter, closed with glass plates. The fringes were easily found and sharp. Unfortunately the pump was not quite tight, so that, on breaking the count of fringes at low pressures, it was difficult to state when the conditions had become isothermal. Hence the results in table 5 are rough. Temp. 19.7°.

TABLE 5.

No. of fringes.	Exhausted to (p).	$\frac{dp}{dn}$	$\lambda 10^6$
0	75.1 cm.		
30	41.8	11.1	59.7 cm.
67	0	11.1	60.0
0	75.1		
30	43.0	10.7	57.6
70	0	10.6	57.1
0	75.1		
40	32.1	10.7	57.8
68	0	11.2	60.0

The mean value thus appears as $\lambda=10^{-5}\times 5.88$ for sodium light. The equations used are

(1) $$n\lambda=e(\mu-1)$$

where n is the number of fringes counted, e the tube-length, and μ the index of refraction of air. Again,

(2) $$p=C(\mu-1)\vartheta$$

where p is the pressure, ϑ the absolute temperature, and the constant C computed from normal conditions (76 cm. and 0° C.) is (Mascart's values) $C=952.6$. Hence

(3) $$\lambda=\frac{e}{C}\frac{p}{n\vartheta}=\frac{e}{C}\frac{dp}{d(n\vartheta)}=\frac{e}{C\vartheta}\frac{dp}{dn}$$

when ϑ is constant. It is this assumption which is not quite guaranteed above. To obviate this in the following experiments, the total number of fringes were counted (table 6) from exhaustion to plenum. Their number was definite to the fraction of a fringe.

TABLE 6.

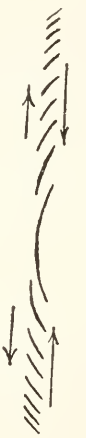
Temp. 19.3° C.; $C=15$ cm.			
No. of fringes.	Exhausted to (p).	$\frac{dp}{dn}$	$\lambda 10^6$
0	75.8 cm.		
69.5	0	1.090	58.8 cm.
0	75.8		
69.5	0	1.090	58.8
0	75.8		
69.5	0	1.090	58.8

These results are correct to 0.5 per cent and are as close as the estimation of p, c, ϑ, and fractions of a fringe will warrant. If results of precision were aimed at, a long tube should of course be used. What was particularly marked in these experiments was the motion of fringes in the passage from any approximately adiabatic to isothermal conditions and on approaching a plenum of air.

Since the refraction depends on density, there should not (apparently) be any motion at all; but the thin tube is always more nearly isothermal than the much larger barrel of the air-pump. As a consequence there is residual expansion from the former to the latter.

10. Continuation. Babinet compensator.—The behavior of an old Babinet compensator, placed nearly normal to one of the beams, figure 3, was peculiar, though the fringes were clear and easily controlled. The dimensions of the right-handed quartz wedge were roughly calipered and found to be: length, 4.2 cm.; thickness at ends, 1.017 and 0.934 cm. Thus there is a grade of $0.083/4.2 = 0.0193$, or something over 1° of arc. A vertical displacement of 2.5 cm. of this wedge was available behind the stationary counteracting left-handed wedge.

The fringes were not uniform and they required an inclination to the vertical of the rulings of the grating G'. The fringes were evidently curved lines, intersected by the vertical strip within which they are visible. Consequently they appeared as in figure 8, with linear elements in the middle, shortening into dots at either end of the strip. On motion of the compensator wedge they moved toward or from the center of symmetry, as is also indicated in the figure. Tiled forms were frequent. The most interesting feature, however, was their alternate appearance and evanescence in cycles. While the wedge was moved over 2.5 cm. of its length, 7 of these cycles appeared and vanished, each consisting of about 36 to 40 fringes. The disappearance was not always quite complete, but the fringes could not be restored by any adjustment for coincidence of spectra.



8

An attempt was made to find the angle of the quartz wedge by the first method. Data, 0.0023, 0.0024, 0.0024 cm., were found for the displacement of the micrometer per fringe. Hence, apart from dispersion,

$$\alpha = \frac{10^{-5} \times 5.893}{2 \times 0.5442 \times 0.0024} = 0.022 \text{ radian}$$

which, as in case of the glass plate, is again slightly above the calipered value.

In another somewhat thinner Babinet compensator the constants were: length, 3.35 cm.; thickness, small end, 0.494 cm., large end, 0.496 cm. The prism angle is $\alpha = 0.062/3.35 = 0.0185$ radian, also about 1°.

In this case there was no periodic phenomenon, but in its place the degree of longitudinal coincidence of the axes of the two spectra continually changed.

The fringes at once sharpened, however, on readjustment of either mirror, indicating a continuous small change of deviation, due to curvature, probably, in the quartz wedge. In the preceding periodic case, no readjustment of deviation sufficed to restore the fringes. The wedge was now detached and used alone. In spite of the relatively large angle (1°), no difficulty was experienced in adjusting or controlling the fringes; but the face curvature just suggested appeared as before, so that readjustment for varying wedge-angle was required from time to time.

11. Micrometer displacement of the second grating, G′ (fig. 3).—In the preceding report (Carnegie Inst. Wash. Publication 249, Chapter III, § 28) it was shown that if the angle between the gratings G and G' is φ and the angle between the mirrors M and N (which in a symmetrical adjustment would be $180°-(\theta_1+\theta_2)$, θ_1 and θ_2 being the angles of diffraction at G and G' for normal incidence at G) is decreased by α, so that the adjustment is non-symmetrical, then the displacement δe of the grating G' per fringe will be very nearly

$$\delta e = \frac{\lambda \cos^2 \theta_2}{2(\alpha - \varphi) \sin \theta_2}$$

if α and φ are small. Here α is effectively the angle between the mirrors M and N, since, if M is rotated 180° on the line of symmetry (normal to the grating G), the two mirrors would intersect at an angle α. The result of fore-and-aft motion thus depends on the angle $\alpha-\varphi$, and if $\alpha=\varphi$, $\delta e=\infty$ per fringe; *i.e.*, fore-and-aft motion would produce no result. This is necessarily

TABLE 7.

i = increasing; d = decreasing.		
No. of fringes.	Total displacement.	Mean δe displacement per fringe.
i 3	0.0234 cm.	0.0088 cm.
3	267	
3	293	
i 4	.0302	.0080
4	317	
4	318	
4	346	
4	330	
d 4	.0285	.0073
4	285	
4	287	
4	315	
4	288	

the case when but a single grating is used, as in the earlier methods. In the case of two gratings, however, it is not only difficult to make a perfectly symmetrical adjustment of mirrors and grating, but it would not be of any

special advantage. Hence the fore-and-aft displacement e of the grating G' will probably be accompanied by a slow motion of the fringes, from which the angle $\alpha - \varphi$ may be computed.

The experiments recorded in table 7 were made with the grating G' on a micrometer-slide moving normally to the face of the grating. With the mirrors, etc., placed so that optical paths were nearly equal, the adjustment screws on M and N sufficed to bring the fringes strongly into view. Successions of 3 and of 4 fringes were tested, as these required an adequately large displacement of the micrometer, which was moved both forward and backward.

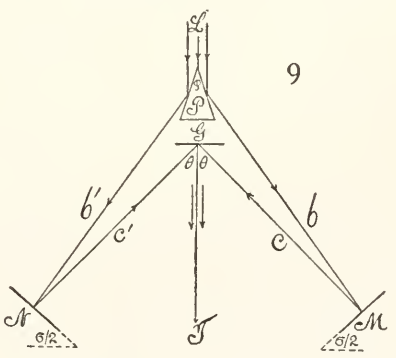
The mean of the three results is $\delta e = 0.008$ cm. per fringe. The data are not smooth, because the micrometer placed between the mirrors M and N is in an inconvenient position for manipulation. The different sets of values, moreover, correspond to different adjustments and therefore to slightly different values of $\alpha - \varphi$. As an order of values only is wanted, it was not considered worth while to remedy the deficiencies.

In accordance with the equation given, if $\delta e = 0.008$ cm., $\lambda = 58.9 \times 10^{-6}$ cm., $\theta_2 = 20°$ be inserted,

$$\alpha - \varphi = \frac{\lambda \cos^2 \theta_2}{2 \delta e \sin \theta_2} = 0.0095 \text{ radian} = 0.54°$$

The adjustment is thus about half a degree out of symmetry, a result which in case of improvised apparatus is inevitable and moreover without significance in the precision of the method.

12. Prism method. Reflection.—The grating G was now removed and replaced by a silvered prism, as shown in figure 9 (P, prism; M, N, mirrors; G, grating; T, telescope). A small prism angle, φ, is essential ($\varphi = 18°$, about), as a large divergence of rays would not be accommodated on the interferometer, figure 3. The fringes were found without difficulty, in the second order, the arc lamp being used. They are also easily distorted, if the edge of the prism is not parallel to the rulings of the grating. In such a case the symmetrical arrow-shaped forms become one-sided and, as it were, curved or faintly fringed beyond the limits of the strip. To get the best adjustment, the lamp should shed about the same amount of undeviated light from both faces of the prism, on a screen temporarily placed behind it. The illuminated strips on the grating must coincide to the eye while making the fore-and-aft adjustment. Finally, the grating is to be slowly rotated on the axis normal to itself, until fringes of satisfactory shape and size appear. Naturally this is done through the telescope, and a readjustment of the longitudinal axes



9

of the spectra is necessary after each step of rotation. Fringes so obtained are as good as those obtained by any other method.

The range within which the fringes are sharp is small, not exceeding 2 mm. of displacement of the micrometer mirror, M. A partial reason for this will appear from figure 9 and results from the fact that the illumination on the grating due to M moves laterally across the stationary strip due to N. Clearly if the latter were also on a micrometer it might, in turn, be displaced relatively to the direction of M and restore the fringes to full brilliancy. The range in this case may be increased till either illuminated strip gets beyond the edges of the grating. This test will presently be made.

If the prism angle is φ and the angle of diffraction for normal incidence is θ, the angle δ, between the incident and reflected ray at M, is

$$\delta = \theta - \varphi$$

Thus $e \tan \delta/2$ is the displacement of the strip of light on the mirror M, if e is the normal displacement of the latter. Hence the corresponding displacement x on the grating is

$$x = 2e \sin (\delta/2)/\cos \theta$$

If b be the distance from the prism to the light spot reflected on M, and c the distance from there to the bright spot on the grating, φ may be computed as

$$\sin \varphi = \frac{C \sin \theta}{b} = \frac{2\lambda c}{b}$$

for the spectra are in the second order.
The data are:

$$10^6\lambda = 58.93 \text{ cm.}; \quad b = 38.0 \text{ cm.}; \quad c = 20.4 \text{ cm.}; \quad D = 200 \times 10^{-6} \text{ cm.}$$

Whence

$$\varphi = 18^\circ\, 12' \qquad \theta = 36^\circ\, 6' \qquad \delta = 17^\circ\, 54'; \quad \delta/2 = 8^\circ\, 57'$$

Hence

$$x = \frac{25 \times 0.1556}{0.808} = 0.096 \text{ cm.}$$

if $e = 0.25$ cm., as found. Thus the rays of the same origin, or rays capable of interfering, are found in a vertical strip on the grating, not more than 1 mm. wide. It is interesting to note that the fringes vanish by becoming coarser and wider, corresponding to the narrowing of effective edges in contact.

The attempt to produce these fringes with homogeneous (sodium) light and a wide slit again failed, although much time was spent in the endeavor. Even with a narrow slit and accentuated sodium lines (impregnated arc) the phenomenon may be produced between the doublets, however close together, but it fails to appear with the same adjustment when two corresponding lines coincide. I was only able to produce it in a continuous spectrum, between the two doublets and with a fine slit. It is very important to ascertain the reason.

Both mirrors, M and N, were now placed on micrometers moving nearly normal to their faces. Beginning with a coincidence of the illuminated strips on the grating, the M micrometer was moved until the fringes disappeared. The N micrometer was then moved in the same direction, until the reappearing fringes passed through an optimum and finally vanished, in turn. Thereafter the M micrometer was displaced again, always in the given direction, and the same cycle repeated, etc. It was possible to pass through about 8 cycles with each micrometer before the illumination reached the edge of the grating, each cycle corresponding to a displacement of about 2 mm. for a single mirror; but a total displacement of 2.5 cm. was registered, which would obviously have been increased much further if the grating had been wider. The data given in table 8 give a concrete example:

TABLE 8.

Position of N.	Advance of N.	Remarks.	Position of N.	Advance of N.	Remarks.
2.42 cm.		Broad arrows	1.75 cm.		Vertical lines
2.20			1.54		
....	0.22 cm.	M advanced		0.21 cm.	M advanced
2.20		Narrow arrows	1.54		Vertical lines
1.98			1.37		
....	.24	M advanced		1.7	M advanced
1.98		Upright lines, inclination changed			
1.75					
....	.23	M advanced			

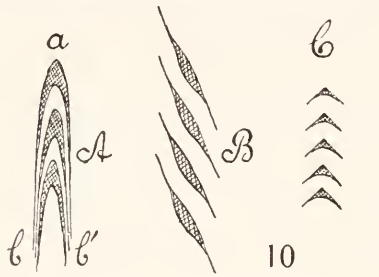
As both mirrors move in the same direction, the two illuminated strips on the grating gradually separate until they are quite distinct. Meanwhile the fringes pass with rotation from the original sagittate forms to very fine hair-like striations; whereas the part of the spectrum within which the former occur is less than the distance apart of the sodium lines (doublets), the hair-lines are visible within a strip of spectrum many times as broad as the sodium doublet. Ten such lines may be visible. In good adjustments the sagittate forms are seen to be a nest of very eccentric, identical hyperbolas, as in figure 10, A, arranged or strung on the same major axis. The vertices a are therefore thick and pronounced, but taper rapidly down into hair-lines, b, b', on both sides. Frequently but half of the coarse vertices, a, abundantly fringed on one side, b or b', appear. Nevertheless this does not seem to be an exhaustive description of the phenomena; for it is not uncommon, when partial hyperbolas appear, to find the striations (which are always faint) in the same direction on both sides, as in figure 10, B; *i.e.*, the striations are apt to be non-symmetrical on the two sides, as if they constituted a second diffraction phenomenon superimposed on the first phenomenon. Roof-shaped forms (fig. 10, C), strongly dotted, are also common, often irregularly awned.

Figure 11 may be consulted to further elucidate the subjects under consideration. G is the grating, PP' the principal plane of the objective of the telescope, a and b are two rays interfering at the focus f, and leaving the grating parallel and symmetrically placed to the axial ray of. The passage

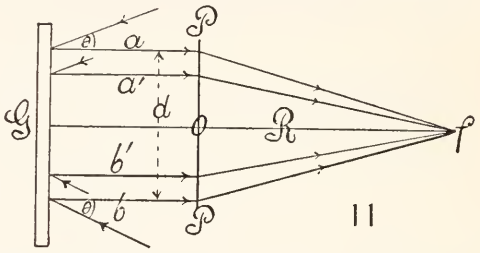
of the coarse sagittate phenomena into the hair-like striations, as a and b move farther apart, may then be accounted for in accordance with the general theory of diffraction; *i.e.*, if the distance apart of a and b is d and the principal focal distance *of* is R,

$$\frac{\lambda}{d} = \frac{z}{R}$$

where z is the distance between the two fringes of wave-length λ. Hence z will increase as d decreases, agreeing with the effect of fore-and-aft motion, or with the effect of simultaneous, large (2.5 cm.) displacement of both mirrors, neither of which destroys the symmetry of the interfering rays.



10



11

The motion of a single mirror, M or N, for instance, does destroy the symmetry, and it was shown in § 12 that the limiting range of displacement of 0.25 cm. moves either a or b 0.096 cm. out of symmetry. The interferences thus vanish without much changing in form or size, and vanish in all focal planes.

The breadth of the blades of light aa' and bb', figure 11, capable of interfering is x on the grating and

$$x \cos \theta = 0.096 \times 0.808 = 0.078 \text{ cm.}$$

normally. Since the rays are parallel after leaving the collimator, this would be about half the breadth of the effective beam on the objective of this appurtenance. Thus $2 \times 0.0776 = 0.155$ cm., increased by the width of the refracting edge of the prism, is the width of the strip of white light which, after separation by the knife-edge of the prism, furnished the two component beams which potentially interfere on recombination. It is reasonable to suppose that the elements of these beams come from a common source and that the width in question is produced by the diffraction of the slit.

This datum is more appropriately reduced to the angle at the slit α, within which lie the rays capable of interfering with each other after the interferometer cleavage. As the collimator used was $l = 22$ cm. from slit to lens,

$$\alpha = 2x \cos \theta / l = 0.155/22 = 0.0070$$

Hence the angular width of the wedge of white light, with its apex at the slit of the collimator and containing all the rays which can mutually interfere, is about 0.007 radian, or less than half a degree of arc. One would infer that a long (l) collimator (*i.e.*, one with weak objective) is advantageous, as the blade of parallel rays issuing is proportionally wide and the range of displace-

ment at M or N larger. Similarly, divergence subsequently imparted by dispersion (prism, grating), before the rays reach the mirrors, M, N, should have the same effect. The results obtained for dispersion bear this out, but not those for a long collimator. Moreover, the width of the slit, so long as the Fraunhofer lines do not vanish, is of no consequence. It thus seems tenable (to be carefully investigated below) that the positive effect of dispersion has a deeper significance, bearing directly on the structure of the interfering wave-trains—*i.e.*, the length of the coördinated, uniform wave-train is possibly greater as the dispersion to which the wave-train has been subjected is greater. Two parts of it will therefore fit over a correspondingly longer range of path-difference.

A number of other results point in the same direction. Thus, I may again point to the impossibility of obtaining fringes with homogeneous light and a wide slit, whereas two identical sodium lines (D_1 and D'_1), superposed, show the interferences strongly. The lines actually become helical in shape and much broader. The range of displacement of N may be decreased from 0.25 cm. to 0.10 cm. by narrowing the beam emerging from the collimator with a slotted screen, while the fringes themselves are coarsened by this process. With the screen removed the fringes are not only sharper and finer, but apparently they may be seen to slowly move laterally across the fiducial sodium lines. This is in accord with the increased range of displacement of the mirror. The observation, however, is complicated by the fact that the sodium doublets are not quite in the same focal plane. The fringes must, in a reduced case, lie midway between them, in the line of symmetry of the spectra.

13. Prismatic refraction.—The method indicated in figure 12 (P, prism; M,N, mirrors; G, grating; T, telescope) was next tested for small distances and the experiments begun in the third order of spectra of the grating G. The prism was a small right-angled sample, with faces only about 1 cm. square; but it sufficed very well. Its distance from the grating being about 13 cm. and the illuminated spots on the mirrors 18.8 cm. apart, the mirrors were nearly normal to each other. In fact, as θ in the third order is about 62° and i' about 28°, $\delta = 34°$ and $\sigma = 90°$. Hence, on displacing the micrometer mirrors M or N, the illuminated strips move relatively rapidly across the face of the grating. Nevertheless, the fringes are easily found and controlled. Their range of visibility is larger than in the cases of the preceding paragraph. They remain in view for normal displacement of M of 3 to 4 mm., passing from hair-like striations, through sharp arrows, back to the hair-like forms. The range has thus been increased by the dispersion. The arrows are of the type shown in figure 13, with reëntrant sides and part of the outline accentuated.

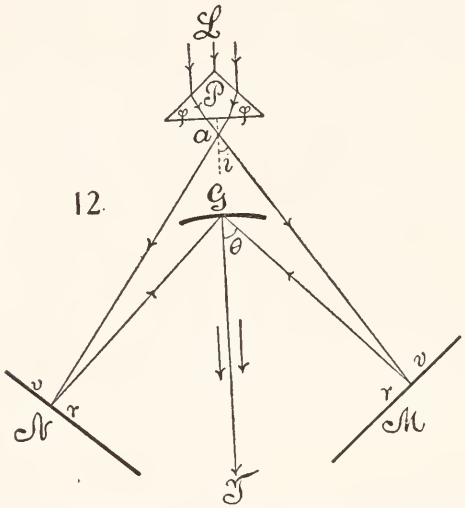
In the second order of spectra from G, the phenomena were much the same, but far more brilliant. The arrows were now evenly wedge-shaped and very slender. The fringes entered as nearly vertical hair-like striations, and, after

passing the optimum, vanished as inflated arrows. The range of visibility was, as before, about 3.5 mm., so that the change of order has not had any further marked effect, such as might be anticipated. As in the preceding paragraph, if the impinging collimated beam is narrowed, the range of visibility decreases; in fact, the arrows themselves are reduced to slightly oblique lines. Within the limits given the fringes are well adapted for interferometry.

First-order spectra are not available because of the large value of i' in the case of the right-angled prism.

Taking the results of the last two paragraphs together, the increase of the range of displacement is due to the dispersion of the prism. The breadth of the pencil, diffracted at the slit, after leaving the collimator and prism,

12.



13

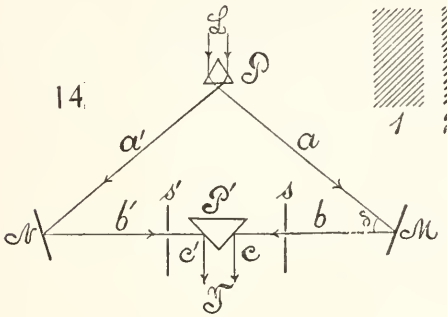


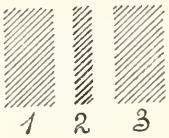
increases. It was shown in the earlier report that inversion of spectra on a longitudinal axis does not preclude the possibility of interference. Taken as a whole, therefore, the present results have a direct bearing on Huyghens's principle.

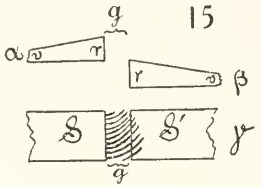
14. Prism methods without grating.—A more interesting method, in some respects, in which the grating is entirely dispensed with, is shown in figure 14. L is the beam of white light from a collimator, P a refracting prism (here with a 60° prism angle), M and N the opaque mirrors, with either or both on a micrometer, P' a silvered reflecting prism (here right-angled). The telescope is at T and should have high magnification. The rays L are refracted into $a\,b\,c$ and $a'\,b'\,c'$ and the two spectra observed by the telescope at T. Each of the prisms should be on 3 adjustment screws, as well as the mirrors. P must be revolvable slightly around a vertical axis and capable of fore-and-aft motion. P' is preferably a large prism placed on a tablet. The rays b and b' are made collinear before P' is inserted, and both the rays c and c' must come from near its edge.

The fringes are strong and large and lie within a remarkably wide transverse strip. This may be 10 or 20 times as wide as the $D_1 D_2$ doublets, which, in view of the small dispersion, are hardly separated. For the same reason, moreover, the range of displacement of M within which fringes are visible rarely reaches 0.5 mm. Within this the fringes grow from the fine hair-lines, usually oblique, to their maximum coarseness. Apart from the small range of displacement, these fringes are available for measurement. If both mirrors M and N are on micrometers, they may be brought forward or the reverse, alternately, and the range increased 5 or 10 times.

To change the form of the fringes, the first prism, P, may be tilted slightly on an axis parallel to LT, figure 14. The fringes then pass through a maximum in the vertical direction (linear phenomenon). Fore-and-aft motion of P rotates the fringes, partially, toward the horizontal; but, as a rule, the com-







ponent beams b and b' pass beyond the edge of P' and the fringes vanish. Just before this (the spectra separating), the strip within which the fringes lie widens enormously. In other words, the breadth of the phenomenon depends on diffraction, not on dispersion, so that even though the prism P scarcely separates the V lines, the striated strip has about the same width as when it is produced by highly resolving gratings.

It is preferable to use sunlight directly (without a long-focus condensing lens), as there is a superabundance of light. The best results are attained with a large collimator. A spectacle lens with a focal distance of 1 meter is excellent. The range of displacement of M is not increased, but the spectra and fringes become very sharp. If, with the large collimator, the spectra are just separated in the field of the telescope, by fore-and-aft motion of P, a magnificent display appears, resembling a thick, twisted golden cord. With further separation confocal elliptic fringes often cross the gap, as in figure 15. Here α and β are graphs suggesting the wave-lengths of the two spectra, g being the gap or deficient overlapping. The appearance in the telescope is shown at γ, S and S' being the spectra. When the fringes are erect, huge vertical furrows may lie in the gap. When the gap is closed, the linear phenomenon reappears. These enlarged fringes vanish, however, within 0.25 mm. of displacement at M. On the other hand, when the spectra are made

to overlap considerably (by fore-and-aft motion of P) the fringes become fine and vertical and the parallel blades of light, which interfere at the focus of the telescope, are 0.5 to 1 cm. apart at the objective.

In further experiments, screens s, s' (fig. 14) were placed in the paths of the pencils $b\,b'$, so that they were compelled to pass through vertical slits 0.5 mm. wide in the screens. In this way the interfering rays were identified. The first vertical hair-line fringes came from rays about 5 mm. behind the edge of the prism P'. Hence the pencils were here about 1.2 cm. apart when they entered the telescope. The largest and last of the fringes came from close to the edge of P'. The experiment was varied as follows: Supposing both screens s and s' placed as far to the rear as the visibility of fringes permits; let the former, s, be slowly pushed forward. The fringes then contract from the very broad set, figure 16, case 1, to the strong and narrow set 2 (which is a mere line for a full wave-front), and then expand again to case 3. If, now, s is left in place and s' moved forward slowly in the same way, the identical contraction and expansion, cases 1, 2, 3, are reproduced. The screen s' may then be left in place and s in turn slowly moved forward with the same results, etc. (there may be 6 alternations), until finally the effective parts of the pencils b and b' are beyond the edge of the prism P'. In case 2 the two slits s and s' are obviously symmetrical to the interfering rays, whereas in cases 1 and 3 the diagonally opposite edges of the slits s and s' limit the efficient pencils to a sheet. If the edge of the prism were truly a knife-edge, the last fringes would be very large, since the distance cc', figure 14, would vanish. If the fringes are vertical (obtained by tilting P around an axis parallel to LT), the case 2 is given by 2 or 3 strong vertical lines, whereas 1 and 3 consist of 10 or 20 lines, all of about the same width and distance apart. If the slits s, s' are finer (1 mm.), the fringes are throughout sharper. A single displacement, 1, 2, 3, corresponds to about 2 mm. When the edge of P' is approached the case 2 often shows vertical strands of fringes, a strong central strand, and two or three fainter ones either side of it. The cases 1 and 3 are not stranded.

A similar result (passage of case 2 into 3, fig. 16) may be produced by moving P forward, the case 3 appearing just before the pencils $b\,b'$ leave the edge of P'. Again, when M is moved rearward, when both b and b' are near the edge of P', the cases 2 and 3 are obtained. In general, the width of the diffraction pattern increases without changing the size of fringes, as the width of the available wave-front decreases. A similar result will be described in connection with figure 48, Chapter II. Naturally, if the displacement is considerable, it is accompanied by some rotation of fringes.

15. Displacement parallel to rays.—It now becomes of importance to test the range of displacement as modified by the angle of reflection, increasing from $\delta = 0$. It is therefore desirable to make a few direct measurements. The angle θ at P, figure 14, was found to be about 49° 45′, so that the total angle at M is $\delta = 40°\ 15'$. M and N are both on micrometers, with the screws normal

to their faces. P' is on a micrometer with its screw parallel to bb', so that this prism is shifted right and left. The range of displacement was found at

M, about 0.04 cm.; $x = 2 \times 0.04 \times 0.939 = 0.076$ cm.
P', about $y = 0.07$ cm.; $2y = 0.140$ cm.

where $x = 2e \cos (90—\theta)/2$ and $2y$ are the corresponding path-differences between the inception and evanescence of fringes. With a very fine slit, $2y$ was possibly smaller (see fig. 17).

The question at issue is thus, in the first place, how the value of $2y$ compares with x; for in the former case the angle δ is effectively zero. In other words, when M is displaced from M to M', over a distance e, the pencil b, figure 17, changes to b_1, and is soon lost at the edge of P', whereas, when P is displaced in the direction bb', over a distance y, the rays b and b' do not change their point of impact at the prismatic mirror P'. If PP represents the principal plane of the objective of the telescope and F its principal focus, there should be no accessory effect for the case y as compared with the case x.

Results bearing on this subject are given in table 9, in which the displacement e, observed at M and at N, as well as the displacement y at P', are recorded when a plate of glass of thickness E is inserted normally to the rays b, b'. The corresponding air-path difference computed from E, μ, B, and λ should be z, nearly. This is about the value ($2y$) observed, remembering that to set the micrometer, fringes of a particular pattern must be selected. The rotation of fringes being but 90° or less, there are no fiducial horizontal lines.

TABLE 9.—Reversed spectra. Refracting prism. $\theta = 49° 45'$. $B = 4.6 \times 10^{-11}$ (assumed). $x = 2e \cos (90° - \theta)/2$; $z = E(\mu - 1 + 2B/\lambda^2)$.

Detail.	E	μ	z	e	x	$2y$
	cm.	*cm.*	*cm.*	*cm.*	*cm.*	*cm.*
Mirror right, plate right...	0.736	1.526	0.3901 +.0195	0.204 .199 .206	0.381	0.400 .410
Mirror left, plate left.....	.736	1.526	= .4096	.208	.391	.410 .406
Mirror right, plate right...	.736	1.526	= .4096	.201 .205 .202	.381	.406 .402
Mirror left, plate left.....	.736	1.526	= .4096	.207 .207 .208	.389	.402 .400
Mirror right, plate right...	.736	1.526	= .4096	.205 .207	.387	.406
Mirror left, plate left.....	.736	1.526	= .4096	.206 .208	.389	.406
Mirror right, plate right...	.434	1.533	.2313 +.0115	.125 .124	.234	.248 .250 .248
Mirror left, plate left.....	.434	1.533	=.2428	.126 .125	.236	.255 .248 .246
Mirror left, plate right....	.434	1.533	=.2428	.127 .126	.237	

Furthermore, though μ was determined by the total reflectometer for each of the two plates used, B, the Cauchy dispersion coefficient, had to be assumed from similar results in my earlier work. Finally, the first plate ($E=0.736$ cm.) was slightly wedge-shaped and some adjustment for coincidence of spectra was needed. The second plate ($E=0.434$ cm.) was optically nearly plane parallel. One may therefore conclude from these details that $2y=z$ as nearly as could be expected.

The values of x, computed from θ and e, however, certainly fall below z, being about 6 per cent and 3 per cent short of it in the two cases, respectively; or, again, x is 0.019 cm. and 0.014 (about 5 per cent) smaller than the mean values observed for $2y$. This extra 5 per cent of path-difference can not be an error of observation or of adjustment, but must be interpreted as the path-difference added when the pencil shifts towards the edge of the prism (x) instead of being stationary as in y. In case of inverted spectra, moreover (next chapter), x is usually in excess of z, and the shift is the other way. The deficiency in x, though not equally marked, is present in observations both on the right and left sides of the prism P'.

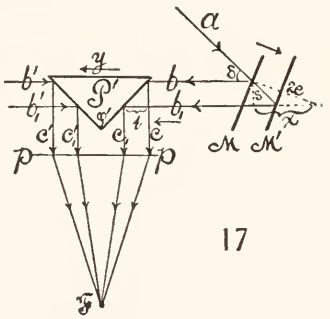
16. Breadth of efficient wave-fronts. Apparent uniformity of wave-trains. Rotation of fringes.—It follows from figure 17 that if M is displaced to M', over a distance e, the pencil b is displaced parallel to itself over

$$s=2e\sin\delta/2$$

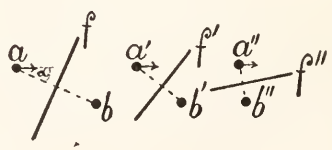
where $\delta=90°-\theta$. The pencil c is then displaced parallel to itself over a distance

$$t=s\tan\varphi'/2=s$$

since $\theta=49°\ 45'$, $\delta/2=20°\ 7'$, and therefore $s=2e\times 0.344=0.7e$, nearly. If the rotation of fringes is but 90°, either s (or $s/2$) is also the breadth of the strips, or patches of like origin, which, when sliding over each other more



17



18

or less, produce the fringes. This may be treated from a graphic point of view as follows, a theory not being aimed at:

In figure 18, let a and b be two patches of light of like color and origin at the objective pp, figure 17, producing interferences at the focus F. Hence the fringes will be arranged in the direction f, figure 18, at right angles to the

line joining a and b. Since a and b here correspond to c and c' in figure 17, let a be continually displaced to the right, as indicated by the arrows, figure 18. In proportion as the positions ab, $a'b'$, $a''b''$, are taken, the fringes must pass by rotation from f, into f', into f'', etc.—*i.e.*, over about 90°. In the present experiment, c, figure 17, can never pass across c', for they are essentially separated by the edge of the right-angled prism P'. Hence the rotation can not exceed 90°, for the vertical through a can not cross the vertical through b. This is not the case when a grating replaces P', as in figure 12; nor is it the case when, as in Chapter II, inverted spectra are treated, and the patches a and b slide *along* the edge of the prism. In such cases figure 18 may be continued symmetrically toward the right (mirror images), and the limit of rotation is therefore 180°. All these suggestions are borne out by experiment.

Moreover, if the first prism P, figure 14, is tilted slightly on an axis parallel to LT, a (fig. 18) will be lowered and b raised. If a and b are on the same level, the fringes are always vertical and pass through a *vertical* maximum, when ab is a minimum. On the other hand, if a and b are not in the same level, as in the figure, fore-and-aft motion brings the rays c and c' (fig. 17) to or from the edge of the prism P'. Hence the case ab passes into $a''b''$, or the reverse; in other words, the fringes pass through a *horizontal* maximum when ab is a minimum, etc. This is also shown by experiment.

Moreover, if α, figure 18, is the angle (in the observer's vertical plane) of ab to the horizontal, the horizontal distance between c and c' will be $ab \cos \alpha$, which is zero when $\alpha = 90°$, and both c and c' are at the edge. Suppose the full breadth of the strips are at the edge, so that the fringes present the strongest, coarsest, but narrowest field of case 2, figure 16. Then if either c or c' retreats until the fringes vanish, the width of the appreciably efficient strip cc' will be $ab \cos \alpha = t = s = 0.7e$, nearly. This is probably the best method of estimating the width in question. Usually, however, away from the edge, the succession 1, 2, 3, figure 16, is obtained. In such a case the breadth of efficient strip is $t/2 = 0.35e$.

The experiment made by moving screens with slits, forward or rearward, successively, by which the appearance and evanescence of fringes may be repeated through several cycles, is next to be explained. Here it is merely necessary to remember that the spectra c and c' are reversed, or that the colors of like origin and wave-length are successively farther apart. When the screens are alternately moved, therefore, the same phenomenon is in turn produced in slightly different colors. But as ab continually increases, whereas the efficient breadth of the strips does not, the fringes soon pass beyond appreciable smallness.

When, as in the earlier methods, but a single grating is used with two successive diffractions through it, the patches a and b are obviously in the same level when the longitudinal axes of spectra coincide. Hence the fringes are essentially vertical.

In the experiment with screens, s, s', figure 14, it is obvious that path-difference remains constant. The distance from the same wave-front in the

pencils b and b', figure 17, to the principal plane pp, is always the same; but pencils different in lateral position are successively selected. On the other hand, when the prism P' is moved in the direction y, parallel to bb', path-difference only is introduced, while the pencils selected remain the same. Supposing the ordinary conditions of visibility (magnification, etc.) to remain unaltered throughout, the wave-fronts are, as it were, explored in depth as to their uniformity—*i.e.*, the distance is apparently recorded throughout which a wave-train consists of identical wave-elements. Effectively, however, the rapidity with which fringes decrease in size beyond visibility is directly in question. Finally, when the opaque mirror M (or N) is moved from M to M', both effects occur together. Path-difference $x = 2e \cos \delta/2$ is introduced and the pencil is displaced from b to b'.

The x-effect is thus probably the same as if P' were displaced to the left and s were brought forward. Hence it is of great interest to determine the extent in which the values of y and x are different. It appears as if the distance within which the wave-trains are uniform is definitely limited and that it increases with the breadth of effective wave-front just instanced, while both increase with the amount of dispersion to which the incident white pencil has been subjected. Diffraction at the slit of the collimator may be regarded as the first dispersion. This seems to me to be a very important observation, and a systematic investigation of the lengths of uniform wave-trains, so understood, in their dependence on dispersion, is desirable, even if the geometry of the system should prove to be adequate to explain the phenomena.

17. Film grating.—The method of two gratings was now again resorted to, except that the first at G, figure 3, was a film grating. This attempt failed in my earlier work, when but a single film grating was used for the two diffractions, because of insufficient light.* In the present case, where two gratings (G' being reflecting) are employed, the method succeeded at once. The first grating constant was $D = 10^{-6} \times 167$ cm.; observations were therefore necessarily made in the second order of G', so that the spectra are not as intense as with prisms. But the fringes are perfect and may be made as large as desirable—with but two in the breadth of the spectrum, for instance. They come in and go out of range with inflation of form, and they are free from the awns seen in the preceding paragraph (with prism), probably because the light is less intense.

The phenomena in general are the same in character; but the range of displacement of either mirror is enhanced, conformably with the increased dispersion at G. This range was found to be about 6 mm. under the best conditions (arrows). If both M and N are successively displaced in the same direction, the total displacement available between the hair-like fringes at the extremes is about 1.5 cm. for each mirror.

* I have since obtained the fringes with a single film grating.

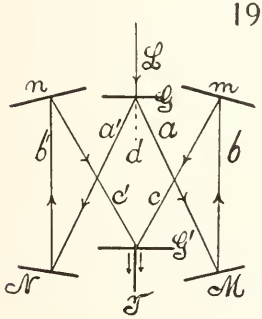
At these extremes the two patches of light on the grating G' may have been separated by several millimeters. The nature of the transformation from arrows to the oblique striations would be well reproduced if equidistant vertical wedges were moved from right to left, or the reverse, behind a vertical slit.

The distance between G and G' was about 10.2 cm., and between the spots of light on mirror M and gratings G and G', respectively, 22.2 and 12.6 cm. This corresponds to $\theta_1 = 20.5°$ and $\theta_2 = 36.2°$, so that $\delta = 15.7°$ and $\sigma = 56.7°$.

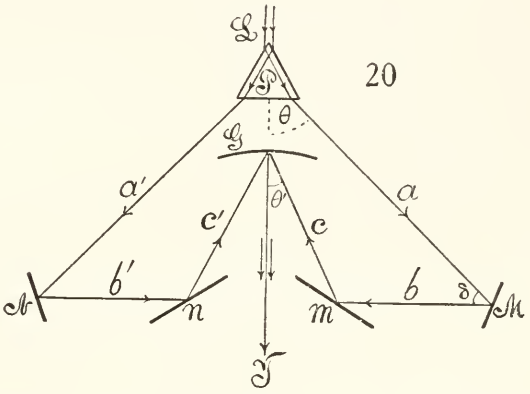
It is obvious that if the slit of the collimator is displaced right or left, the range of displacement, within which the interferences lie, will have different positions on the micrometer, because the path-differences are changed. A flickering arc may also introduce annoyances.

The present method has an advantage for ordinary practical purposes, as it does not require a ruled-glass grating at G.

19



20



The surprising success obtained with the film grating at short distances induced me to test similar methods at long distances. Figure 19 is an apparatus of this kind, in which L is the white beam incident from a collimator, G and G' are the transmitting gratings, M, N, m, n, pairs of opaque mirrors, T the telescope. The undeviated ray, d, is screened off. The component paths $a+b+c$, $a'+b'+c'$ were each about 4 meters long. The method of adjustment again consisted in bringing the shadow of the thin wire across the slit into the same position of the spectra seen in the telescope when the spectra coincide. For this purpose the adjustment screws for horizontal and vertical axes on M, N, m, n must be actuated together. To facilitate this tiresome work, with the observer at T, long levers brought from m and n, with their ends near his hands, as well as a lever from G' (fore-and-aft motion), were very useful. Since the adjustment screws at M and N are already within reach, it is thus easy to bring any Fraunhofer line to the middle of the field and to make these fields overlap, with the guide-wire central in both.

The attempt made with sunlight, to find the fringes when both G and G' are film gratings ($D = 167 \times 10^{-6}$ cm.), did not succeed. The light, moreover,

is not as bright as desirable, owing to the strong dispersion. When the grating G' was replaced by a ruled-glass grating ($D = 352 \times 10^{-6}$ cm.), the dispersion was not much reduced, but the light was better. The fringes were now found after some searching and seemed to be of D_1D_2 breadth, a strip of oblique lines of the usual character. But they were not brilliant and were hard to recover when lost. The Fraunhofer lines were still disagreeably blurred.

On exchanging the gratings (ruled-glass grating at G and film at G'), though the dispersion was smaller, the brilliancy of spectra was greatly improved. The fringes came out fairly sharp. However, on cutting down the incident beam at the collimator and near G to a breadth of not more than 0.5 cm., the fringes were acceptable and capable of high magnification. They remained visible for a displacement of 5 mm. at the micrometer at M. With fore-and-aft motion of G', the fringes rotated as usual from fine vertical hair-lines, through the horizontal (probably arrow-shaped forms of maximum size), back again to hair-lines. Here the excursion of G' was about 1.5 cm. On tilting the grating G' in its own plane and readjusting M, the rotation is through the vertical maximum (the linear phenomenon). With a slotted screen (0.5 cm.) at the collimator, the slit may be widened until the Fraunhofer lines just vanish. If the slit is but 0.2 cm., the fringes become bulky and the play at M is but 2 mm.

The film grating may be used by reflection, on adapting the apparatus in figure 12 for this purpose, by supplying a ruled grating or prism at P and the film grating (with its ruled side toward P) at G. If a ruled grating is put at P, the spectra and fringes are good; but naturally there is deficient illumination. Nevertheless a strong telescope may be used and a range of displacement of 4 mm. at M is available. This may be increased indefinitely by using a micrometer at M and N alternately. The chief difficulty was the (incidentally) unequal brightness of spectra.

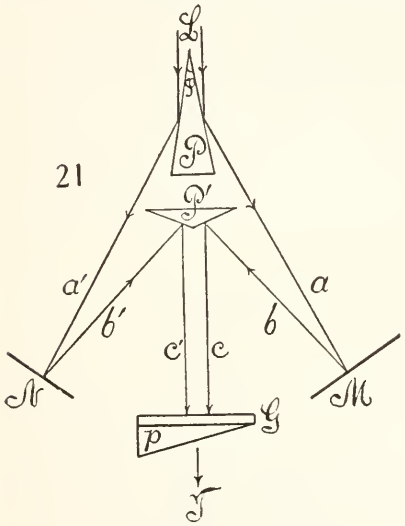
Again, the method of figure 14, apart from the drawbacks to which that method is incident, succeeds almost perfectly, both in the first- and second-order spectra. The fringes are strong and clear. An Ives grating of high dispersion ($D = 167 \times 10^{-6}$ cm.) was tested.

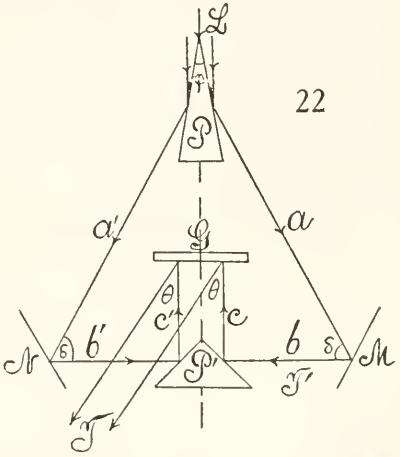
The method of figure 20, with auxiliary mirrors m and n to accommodate the dispersion of G, was also successfully tried. Here G was originally a concave *reflecting* grating. It was replaced by a film grating used as a reflecting grating, with entire success. The ruled side of the film should be free (without cover-glass), but the reversed side cemented on plate-glass as usual and the latter placed towards the telescope at T. The prism P, in other words, admits an abundance of light, so that even the loss in reflection from the film is not serious. Sunlight should be used without a condensing lens; or, if the latter is added, the light leaving the telescope is to be narrowed laterally.

18. Non-reversed spectra.—The prismatic method of cleaving the incident beam of white light is available for the superposition of non-reversed spectra,

under conditions where the paths of the component rays may have any length whatever. It is thus an essential extension to the method (fig. 21) given in the preceding report (PP', prisms; M, N, mirrors; Gp, Ives prism grating; T, telescope), where the path-differences were essentially small and the spectra reversed.

In figure 22, P is the first prism cleaving the white beam L, diffracted by the slit of the collimator. M and N are the opaque mirrors, the former on a micrometer. For greater ease in adjustment, the second prism P' is here right-angled, though this is otherwise inconvenient, since the angle $\delta = 90° - \varphi$ is too large. The rays reflected from P' impinge normally on the reflecting grating G ($D = 200 \times 10^{-6}$) and are observed by a telescope at T. P, P', M, and N are all provided with the usual three adjustment screws. P' must be capable of being raised and lowered and moved fore and aft. The field is





brilliantly illuminated. When the path-difference is sufficiently small, the fringes appear and cover the whole length of superposed spectra strongly. They are displaced with rotation if M is moved normally to itself.

As first obtained, the fringes were too closely packed for accurate measurement. But the following example of the displacement e of the mirror M, for successions of 40 fringes replacing each other at the sodium lines, shows the order of value of results: $10^3 e = 1.55$, 1.40, 1.60, 1.55 cm., so that per fringe

$$\delta e = 39 \times 10^{-6} \text{ cm.}$$

The computed value would be (φ, the prism angle)

$$\delta e = \frac{\lambda}{2 \cos \delta/2} = \frac{58.93}{2 \times .81} 10^{-6} = 36.4 \times 10^{-6} \text{ cm.}$$

assuming $\delta = 90° - \varphi$. The difference is due both to the small fringes, which are difficult to count, and to the rough value of δ. The range of measurement is small (if M only moves), not exceeding 1.6 mm. for a moderately strong

telescope. But one-half of this displacement is available, as the fringes increase in size (usually with rotation) from fine vertical hair-lines to a nearly horizontal maximum, and then abruptly vanish. This is one-half of the complete cycle.

If we regard the component beams, $a\,b\,c$ and $a'b'c'$, as being of the width of the pencil diffracted by the slit of the collimator, it is clear that the maximum size of fringes will occur when c and c' are as near together as possible; furthermore, that as M moves toward P', c continually approaches c', until b drops off (as it were) from the right-angled edge of the prism P'. To get the best conditions—*i.e.*, the largest fringes—c must therefore also be moved up to the edge of P and very sharp-angled prisms be used at both P and P'. The largest fringes (lines about 10 times the D_1D_2 distance) obtained with the right-angled prism were often not very strong, though otherwise satisfactory. Much of the light of both spectra does not therefore interfere, being different in origin.

Results very similar to the present were described long ago* and found with two identical half-gratings, coplanar and parallel as to rulings, etc., when one grating was displaced normally to its plane relative to the other. The edges of the two gratings must be close together, but even then the fringes remain small and the available paths also. Strong, large fringes, but with small paths, were obtained by the later method† of two identical transmitting gratings, superposed.

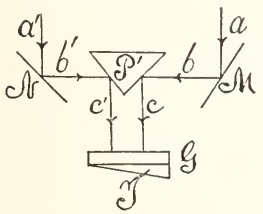
If the prism P' is right-angled (a special case of fig. 21), it may be rotated as in figure 23, so that the rays c and c' pass off towards the observer. They are then regarded through a prism-grating G and a telescope at T. This method admits of much easier adjustment. With the component beams $a\,b$, $a'b'$, coplanar, horizontal, and of about equal length in the absence of the prism P', the latter is now inserted with its edge vertical (rotation) and the white slit images in T (without G) superposed, horizontally and vertically. G is then added and the micrometer at M or N manipulated till the fringes appear. As above, they are largest when c and c' are as nearly as possible coincident and vanish as horizontal fringes at the maximum; for the effective parts of c and c' are component halves of the same diffracted beam from the slit. It is interesting to observe, seeing that interference also occurs when one of the superposed spectra is inverted on a line parallel to its length, that such diffraction is demonstrable in case of homogeneous light, even when a slit is absent. Both beams must be nearly at the edge of P' in order that strong, large fringes may be seen.

The case of figure 22 was subsequently again tried on the large interferometer, the distance P to $M-N$ being about 2 meters. G, in these experiments, was a concave grating and T a strong lens near the principal focus of G. The adjustment for long distances is not easy. The equilateral triangle of rays, a, a', b', b, should be first carefully leveled, the edges of P and P' being on

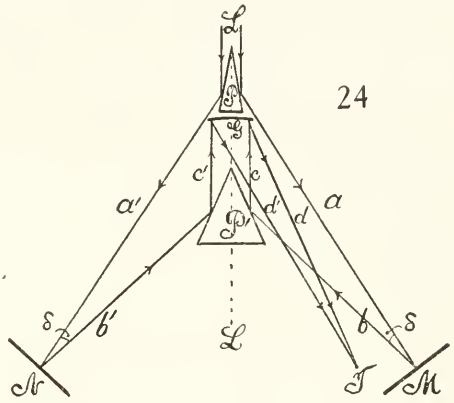
* Phil. Mag., XXII, pp. 118–129, 1911; Carnegie Inst. Wash. Pub. 149, chap. VI.
† Physical Review, VII, p. 587, 1916; Science, XLII, p. 841, 1915.

the median line. With G placed at the proper distance, the two spectra seen at T will usually be quite distinct in the field. They should show the shadow of the black line across the slit, at the same level in the spectra. The longitudinal axis of the spectra may then be made collinear by slightly tilting the edge of P' to the vertical, on a horizontal axis, with the adjusting screws. M and N are then rotated on a vertical axis till the D lines coincide. Small changes may be completed at M and N. The fringes when found are usually strong, but very fine, less than the D_1D_2 distance in width. I have been able to increase them to a width of $2D_1D_2$, but they are then faint. The two illuminated strips on the grating may even be an inch apart, but the fringes are as usual large when this distance is the smallest attainable (virtual

23



24



coincidence). The grating may be moved fore and aft without effect. As N is moved on its micrometer, the interferences are first seen as vertical hair-like striations, which gradually enlarge, rotate, and vanish just before reaching the horizontal and at maximum size. The range of displacement did not exceed 0.15 cm. for this rotation of 90°, so that the total displacement for 180° of rotation would be about 3 mm. Since N and T are close together, the manipulation is convenient here, but with another lens at T' the phenomenon could be traced further on the M side.

To secure a smaller angle of incidence and reflection, $\delta/2$, at M, figure 24, the combination of a silvered 20° prism P and a 30° prism P' was tested. M and N are the opaque mirrors, G the concave grating with its focus at T for inspection by a strong lens. L is the incident beam of white sunlight from the collimator, which is split into the component pencils $abcd$ and $a'b'c'd'$ and interfere at T. The results, however, were about the same as above, the range of displacement at M for 90° of rotation of fringes being about 0.15 cm. As a and b make angles φ and φ' with the line of symmetry LL',

$$\delta = \varphi' - \varphi$$

was about 10°.

At a subsequent opportunity I made further trials with the paired prisms of 20° and 30°, but failed to increase the fringes above about $D_1D_2/2$ width.

Two micrometers, one at M and the other at N, were installed, and moved forward in alternate steps, within a range of over 2 cm., naturally without modifying the fringes. These are now observed on both sides (N and M), each with the micrometer which is manipulated. One may note in passing that the two screws are being incidentally compared. To set the 30° prism properly it would have to be provided with a fine fore-and-aft, right-and-left slide adjustment, in order that its edge may be set sharply in the line where the two component rays intersect. An attempt was made to increase the dispersion by allowing a spectrum to fall on the first prism (20°), but without success.

It is noteworthy that the 30° prism at P' is no marked improvement as to range of displacement over the 90° prism at P', previously used. In other words, the effect of decreasing the angle of reflection δ at M is, unexpectedly, of small importance, in relation to the range of displacement at M. This result already treated in §16 will be accentuated in other ways below (Chapter II).

19. Non-reversed spectra. Restricted coincidence.—In figure 25, the white ray L from the collimator is diffracted by the grating G and the two spectra a and a', thereafter reflected by the parallel opaque mirrors M and N, to be again diffracted by the grating G'. The rays are observed by a telescope at T. If the gratings G, G' have the same constant, it is obvious that the field of the telescope will show a sharp white image of the slit, for each mirror. If $M\ N\ G\ G'$ are adjusted for symmetry by aid of the adjustment screws on each and the rulings are parallel, the two white slit images will coincide horizontally and vertically. If now a direct-vision spectroscopic prism or a direct-vision prism-grating G'' is placed in front of the telescope, the superposed white slit images will be drawn out into overlapping non-reversed spectra, which will usually show a broad strip of interference fringes.

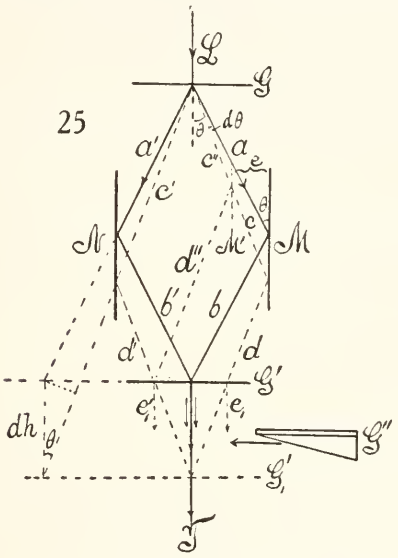
In my first experiments, G and G' were film gratings of high dispersion ($D = 167 \times 10^{-6}$). The field was therefore too dark and the fringes were obtained with difficulty because of the cumulative distortion of images from the gratings. When found, the fringes were very fine parallel lines, filling an irregular strip in the orange-yellow region, and it was already obvious that an enormous play of the micrometer-screw at M would be permissible.

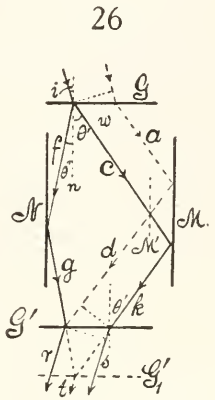
A number of film gratings were now tested and the best samples selected ($D = 175 \times 10^{-6}$), although the dispersion was still too large and the D lines not clear. To secure more light, a beam of sunlight 15 cm. in diameter was condensed to a focus on the slit by a large lens of about 2 meters in focal distance. The illumination was now adequate and the fringes were found at once, as they should be; for they are always present, though not in the same colored region. These fringes, found with more accurate adjustment, were also larger than before.

Figure 25 shows, if ab, $a'b'$ and cd, $c'd'$ are pairs of corresponding rays of the same order but different wave-lengths, λ and λ' respectively; that for the given position of G and G' only the rays $a\ a'$ issue coincidently at T. The rays cd, $c'd'$ issue at e_1, e'_1, and, though brought to the identical focus

by the telescope, the distance $e_1e'_1$ may be too large to admit of appreciable interference. Hence the colored strip within which interferences occur will comprise those wave-lengths which lie very near λ, whereas the colors lying near λ', etc., will be free from interference.

If, however, the mirror M is displaced parallel to itself to M' by the micrometer-screw, the rays $c''d''$ and $c'd'$ will now coincide at e'_1, whereas the rays from ab and $a'b'$ will no longer issue coincidently and may not interfere. Thus the interferences are transferred as a group from rays lying near λ to rays lying near λ'. It is obvious, therefore, that with the displacement of M the strip carrying interferences will shift through the spectrum and that an enormous play of the micrometer-slide at M will be available without the loss





of interferences. In fact, a displacement e of over 3 cm. of M normal to itself produced no appreciable change in the size or form of fringes, but they passed from the green region into the red. In consequence of the film gratings used, the strip in question was naturally sinuous and somewhat irregular, but the fringes themselves in the clear parts were straight, parallel, strong lines. They did not thin out to hair-lines at their ends, nor show curvature, as one would be inclined to anticipate. On the contrary, they terminated rather abruptly at the edges of a strip occupying about one-fourth of the visible length of the spectrum.

It follows, therefore, from figure 25, that the displacement of M does not change path-length or path-difference, for the rays are inclosed between parallel planes, as it were. Since the double angle of reflection is $\delta = 180° - 2\theta$, where θ is the angle of diffraction of G and G', the displacements of M over a normal distance e will shorten the path of M in accordance with the equation

(1) $$n\lambda = 2e \cos \delta/2 = 2e \sin \theta$$

where n is the number of fringes passing at wave-length λ. This equation is not obvious, since for constant λ, the distance between G and G', measured along a given ray (prolonged) for any position of M or N, is also constant. The equation may be corroborated by drawing the diffracted wave-front, which cuts off a length $2e \sin \theta$ from d''.

Since $\sin \theta = \lambda/D$ if D is the grating space, the last equation becomes

$$n = 2e/D$$

or per fringe

$$\delta e = D/2$$

a remarkable result, showing that the displacement of the mirror M per fringe is independent of wave-length and equal to half the grating space. An interferometer independent of λ and available throughout relatively enormous ranges of displacement is thus at hand. It will presently appear that it is also independent of the angle of incidence at G.

In case of the given grating and sodium light, $\theta = 19^\circ\ 37'$. Hence if δe is the displacement per fringe,

$$e = \lambda/2 \sin \theta = 10^{-6} \times 88 \text{ cm.}$$

Actuating the micrometer at M directly by hand (this to my surprise was quite possible without disturbing the fringes, except for the flexure of supports), the following rough data were successively obtained from displacements corresponding to 10 fringes:

$$10^6 \times \delta e = 65 \quad 95 \quad 90 \quad 80 \quad 60 \text{ cm.}$$

Without special precaution the fine fringes can not be counted closer than this, so that the data are corroborative.

If the incidence is at an angle i, as in figure 26, the rays entering at G obviously leave at the same angle i (symmetrically) at G'. In other words, rays enter and leave in pencils of parallel rays. The optic path of the component N ray, $f+g$, is

$$h/\cos \theta''$$

where h is the normal distance between G and G' and θ'' the angle of diffraction on the left. Similarly the optic path of the M' rays $c+d$ which meet $f+g$ in r is

$$h/\cos \theta'$$

where θ' is the angle of diffraction on the right. If now M' is displaced to M, $c+d$ is changed to $a+d$ of the same length; but if the wave-front w is drawn, it appears that the optic path of the M ray has been shortened to $2e \sin \theta'$, where e is the normal displacement of M' to M. Hence the path-difference is now

$$h/\cos \theta' - 2e \sin \theta' - h/\cos \theta'' = n\lambda$$

n being the ordinal number of fringes of wave-length λ. Furthermore, since h, i, θ', and θ'' do not change, the displacement per fringe is as above

$$\delta e = \lambda/2 \sin \theta'$$

For the angles in question the usual equations are given:

$$\sin\theta' - \sin i = \lambda/D \qquad \sin\theta'' + \sin i = \lambda/D$$

so that

$$\delta e = \lambda/2(\lambda/D + \sin i)$$

which is thus not quite independent of λ unless i is very small. It is obvious that the optic paths of $a+d$ and $c+k$ are identical. Hence the path-differences of the rays r, s are the same. If now the grating G' is shifted to G'_1, over the distance e', the same path-length is cut off from both r and s, and hence the fringes do not move. The locus or strip of fringes, however, is displaced in wave-length, bodily, as shown in figure 25.

The equation in $n\lambda$, which may be written (δ, a differential symbol)

$$n\lambda = h\delta(1/\cos\theta) - 2e\ (\lambda/D + \sin i)$$

suggests the phenomena to be expected both when λ is constant and i varies and when i is constant and λ varies. The former require a wide, the latter a narrow slit.

Some time after, with an improved micrometer, not directly manipulated by hand, I obtained the following data from a succession of 50 small fringes (arc lamp):

$e \times 10^3 =$ 3.7 3.9 4.0 4.1 4.2 cm
$\delta e \times 10^6 =$ 74 78 80 81 84 cm.

Again, from successions of 30 large fringes:

$e \times 10^{-3} =$ 2.6 2.6 2.4 cm.
$\delta e \times 10^{-6} =$ 87 87 79 cm.

All of these are below the value computed for sodium light, from imperfect adjustment. The march of values in the first series is probably incidental, for I was not able to eliminate the effects of flexure in my improvised apparatus. Again, the precise symmetry of the apparatus is not guaranteed.

Simple as the method appears in figure 25, it is in practice quite difficult to control. Fringes may be lost and thereafter hard to find again, and this in spite of the large range of displacement. The cause was eventually located in the circumstances under which the incident pencil L strikes the grating G. If L shifts to right or to left the symmetrical rhombus of figure 25 will be converted into a non-symmetric rectangle or into a figure as in figure 26. If G and G', M and N were rigorously parallel this should not produce any effect; but as they are not and as the surfaces are not optically flat (film gratings) the effect is very marked and probably of the same nature as a rotation of G' on an axis normal to its face. It requires but slight displacement of L to right or left to make fringes in the yellow change to hair-lines in the green or the red; or they may even be lost altogether. These fine fringes may sometimes be enlarged, at other times made smaller, by adding or thickening (rotation) the compensator. Naturally in all these cases the overlapping spectra are perfect. The only method of finding the fringes

after the parts are symmetrically placed relatively to the light is to move L successively and gradually toward one side or the other and to test each case with compensators 1 to 2 mm. thick, placed in the b or b' pencils. It would be advisable to place the slit on a right-and-left micrometer. When found, however, the fringes, if reasonably treated, are very persistent, strong, and easily enlarged.

Finally, the fore-and-aft motion of G' must produce a bodily shift of fringes, while the strip as a whole is displaced in mean wave-length; for figure 25 shows at once that if G' were displaced to G'_1, the λ rays bb' would lose their coincidence in T, while that property would now be possessed by the λ' rays, dd'. If G' is on a fore-and-aft micrometer, therefore, one might suppose a second method of interferometry to be available in which symmetry is retained throughout and (since the angle at which the rays bb' meet is $\delta = 2\theta$) subject to the equation

$$n\lambda = 2e' \cos \delta/2 = 2e' \cos \theta$$

where e' is the displacement corresponding to n fringes passing in wave-length λ.

This equation, however, is inapplicable, as already explained, because the pencils bb' are not reflected, but diffracted into T. In the symmetrical apparatus, therefore, no perceptible motion of fringes is produced by the fore-and-aft motion of G', because in all cases the rays bb' meet the grating with a constant phase-difference. If the phases are identical they remain so while G' is displaced. The strip of fringes as a whole, however, is slowly though imperceptibly displaced through the spectrum, without accentuated motion of the fringes within the strip. This inference was tested by placing G' on a fore-and-aft micrometer. Large displacements of the screw (fractions of a centimeter) shifted the strip from color to color as specified. A micrometric displacement of G', however, was unaccompanied by any appreciable displacement of fringes. On the other hand, any flexure of the supports of G' at once produced a marked displacement of fringes, while from mere micrometer displacement no measurement could be obtained.

Equation (1) is of interest in interferometry, in view of the very long ranges of displacement available. For such purposes gratings of lower dispersion (preferably ruled gratings or else prisms) should be used, to obtain greater luminous intensity in the spectrum. Of course, the gratings G and G' may have different constants, but in such a case $GNG'M$ will no longer be a rhombus. Since for constant λ the ray-lengths in figure 25 are constant for all positions of G parallel to G', M parallel to N, large path-difference may conveniently be introduced by compensators. If a thin sheet of mica is moved in either the b or b' pencils, there is a lively skirmish of fringes, but they do not change size appreciably. A glass plate 5 mm. or more thick placed in *both* rays b and b' and rotated produces the same results, but the fringes move more slowly. A plate 2.8 mm. thick, with strong fringes horizontal in the yellow, if placed in the b' pencil produces hair-lines inclined toward the left in the red; if placed in the b pencil, hair-lines inclined to the left in the green,

etc. In contrast with this, the shift from red to green, if produced without compensator by the displacement of M, shows scarcely any change of fringes, either as to size or inclination.

To change the size of fringes it is necessary to rotate the grating G' (relatively to G) on a horizontal axis normal to itself. They then both rotate and grow larger, attaining the maximum of size when the fringes are vertical. Fringes quite large and black, which are naturally much more sensitive to compensators, may be obtained in this way; but the fringes are still easily controlled by hand. Limitations of the incident light in breadth, or simultaneous rotation of M and N, produced no marked effects.

Fringes may also be enlarged on moving the collimator with slit micrometrically right or left, as already stated, though this must be done with caution, as the effects are often surprisingly abrupt; for when the system is not quite symmetric displacements on G will be equivalent to accentuated displacement on G', owing to the reflections. The reflected rays soon cease to intersect and the displacement on M and N is invariably large. Furthermore, by the insertion of compensators (glass plates 1 to 2 mm. thick) in the b or b' pencils, either directly or differentially, larger or smaller fringes may be obtained.

It is now of interest to return to the equation referring to the displacement of G', normal to itself, and to consider the resolving power of the system; for the latter bears a close analogy to the experiments made in a preceding paper (Carnegie Inst. Wash. Pub. 249, Chap. V, 1916) on the remarkable behavior of crossed rays. If G' is displaced to G'_1 over a distance $e'=dh$ (see fig. 25, where h is the distance apart of G and G'), the rays λ' meeting in T will now be in the same condition as were originally the rays λ. In other words, e_1 and e'_1 have become coincident at G'. If we assume that the same type of fringe results in these cases, and if $\lambda'-\lambda=d\lambda$, $\theta-\theta'=d\theta$ (for the passage of bb' into dd' is in the direction from red to violet),

$$d\theta=dh \sin\theta \cos\theta/h, \text{ nearly} \tag{2}$$

Since $\lambda=D \sin\theta$ and $d\lambda=-D \cos\theta\, d\theta$, this may be changed to

$$d\lambda/\lambda=dh(1-\lambda^2/D^2)/h \tag{3}$$

when D is the grating constant. This is the expression used heretofore.

In general it is to be noted that the present method, apart from any practical outcome, is of great interest as to the data it will furnish of the width of the strip of spectrum carrying interference fringes under any given conditions. For here the spectra are not reversed or inverted and the latitude of interference of diffraction throughout λ is much broader than in case of reversed spectra. But for this purpose films will not suffice and rigid refracting systems must be devised.

20. The same, continued. Homogeneous light. Dissimilar gratings.—To show the close relation of the present experiments with one reflection to the

earlier work with crossed rays and two reflections (*l.c.*), experiments may be made with homogeneous light. Accordingly, the sodium arc with a wide slit was installed and the fringes found without difficulty. Strands of fringes with nodules were obtained as before. These rotated in marked degree (180°) from vertical hair-lines, through coarse vertical strands with horizontal nodules, back to vertical hair-lines again, as either M or G' was suitably displaced normally to its plane. To shift the fringes of any form into the middle of the wide-slit image, a glass compensator in either b or b' may be resorted to, or both M and G' may be displaced together. Again, whereas the micrometric displacement of M produces a marked displacement of fringes within the strip in accordance with equation (1), the micrometric displacement of G' leaves the fringes stationary within the strip. While the strands and nodules were strong, the reticulation of fringes could not be clearly made out, in view of the use of film gratings in place of the ruled gratings used in the earlier report.

In equation (4), $D = 169 \times 10^{-6}$ cm., if $d\lambda/\lambda = 6 \times 10^{-8}/6 \times 10^{-5} = 10^{-3}$, $h =$ 60 cm., $D = 169 \times 10^{-6}$ cm.; whence $dh = 10^{-3} \times 60/(1 - (60/169)^2) = 0.07$ cm., nearly. Thus, if with ruled gratings the fringes due to the D_1 and D_2 lines could be separately recognized, it should be possible to distinguish between them here also, as the same phases require a differential displacement of G' of nearly a millimeter. The same result would be recognized at M by a displacement of $dh \tan \theta$, where $\theta = 21°$ nearly, being the mean angle of diffraction. The M displacement is thus $0.07 \times 0.36 = 0.025$ cm.

In case of homogeneous light the prism grating G'' is not needed and much more light is available if the telescope is used directly. The strands of interferences, being on a yellow ground, are not very strong. Nevertheless a few measurements of ranges of displacement were made by moving both M (displacement e) and G' (displacement h), alternately. The following values of e, h, and $h \tan \theta'$ were found, the film gratings having nearly the same constants:

$e = 0.5$ cm. $\quad h = 1.30$ cm. $\quad h \tan \theta' = 0.49$ cm. $\quad \theta = 19°\ 37' \quad \theta' = 20°\ 40'$

e and $h \tan \theta'$ coincide as closely as may be expected, seeing that the fringes in neither case can be quite brought to vanish.

Experiments were next made with a grating of less dispersive power ($D = 352 \times 10^{-6}$ cm.), ruled on glass and a stretched film grating of the same strength. It was found, however, that the long rhombus $GMG'N$ was very difficult to control, owing to the reflection at almost grazing incidence. The spectra also were not quite clear. The method was therefore eventually abandoned, as no fringes could be found.

The trial was then made with a weak grating at G ($D = 352 \times 10^{-6}$ cm.) and a strong grating at G' ($D = 167 \times 10^{-6}$ cm.). In adjustment the latter naturally overpowers the former and two reversed spectra are seen in the telescope (without prism grating) immediately behind G'. Both spectra were quite strong and sharp. With white light no fringes could be found even after long trial and a variety of adjustments.

The sodium arc was now used with a very wide slit and the fringes were found without difficulty. They consisted as usual of vertical hair-lines rotating through a usually horizontal maximum back to vertical hair-lines again, as either M, N, G' were displaced normal to their faces on their respective micrometers. These fringes are simply due to either one or the other sodium line separately and therefore seen on a yellow ground free from interference. Even after this, with the apparatus in adjustment for homogeneous light, white light was tried again in alternation, but no fringes appeared.

With sodium light a few measurements of the ranges of displacement were made. If θ and θ' are the angles of diffraction, $\delta = 180° - (\theta + \theta')$ and $x = 2e \cos \delta/2$, when x is the path-difference cut off at one end by the displacement e of the mirror M. The displacement of G' being y, it appears that, apart from sliding, e and $y \tan \theta'$ should be nearly equal. The results were

$e = 0.42$	0.42	0.45 cm.	$\theta = 9° 39'$
$x = 0.81$	0.81	0.87 cm.	$\theta' = 20° 40'$
$y = 1.74$		1.80 cm.	
$y \tan \theta = 0.66$		0.68 cm.	$\delta = 149° 41'$

It was not practicable to make the hair-lines quite disappear without a large excess of displacement in both cases. Even so the difference of e and $y \tan \theta'$ is too large to be explained by such an error. But the work with the present apparatus (screws not long enough) is not sufficiently accurate to make further discussion fruitful. The error will probably be associated with the oblique incidence of rays in case of a wide slit.

Very remarkable results were finally obtained with compensators of glass plate. Placed in one or both beams and rotated around a vertical axis, they rotate the fringes. This would be referable to the sliding of the ends of the two pencils on the grating G'. If, however, they are placed nearly normally in one beam, they produce no effect either of rotation or on the size of the fringes; but the pattern is displaced bodily across the wide yellow slit image. Glass plates 0.2 and 0.5 cm. were used. It is not until the thickness of plate reaches 2 cm. that appreciable thinning of the interference fringes occurs when the plate is placed in one beam. With optic plate this would be an excellent method for testing the lengths of uniform wave-trains. Finally, with a fine slit and coincident sodium lines, the fringes could be seen in the presence of a continuous spectrum as marked dots on the enhanced sodium lines. But nothing could be detected with non-coincident lines.*

21. The same, continued. Duplicate fringes.—The occurrence of strands and apparently duplicated fringes has already been suggested in the preceding paragraph. In further experiments definite results were eventually obtained *with sunlight.* These occur in very great variety, but two typical phases may be accentuated, given in figure 27. In the case *a* the two sets are more

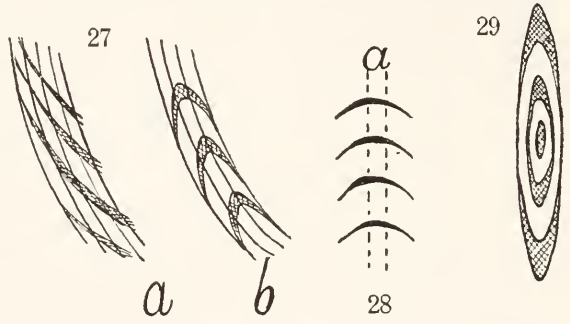
* Such fringes were since found, incidentally, in the white flash of a sodium arc. They were very clear, but could not be controlled.

nearly parallel, but one is always very large in comparison with the other. In case *b* the difference in size is even more marked and the fringes are nearly orthogonal. In intermediate cases fine large strands occur. These pass into each other continuously; the manner does not admit of description. They are seen best in the principal focal plane and both sets are about equally strong.

To obtain these fringes the adjustment was first carefully made with the sodium arc. Thereupon the arc was replaced by concentrated sunlight and fine fringes were recognized in the superposed spectra (longitudinal and transverse axes coinciding). These fine fringes were then enlarged both by rotating the grating G' (fig. 25) on its normal axis and readjusting M in each case, and by adding trial compensators in the M or N pencils. A glass plate 3 mm. thick gave the best results and they were very striking. The following are the chief characteristics:

When the mirror M is slowly rotated on a horizontal axis, moving one spectrum vertically, slightly over the other, the fringes pass through all their phases.

When M is slowly rotated on a vertical axis, which slides one spectrum horizontally over the other, the fringes are displaced, more or less, bodily in the spectrum. Thus in the case *b*, figure 27, the D doublets are many



times their own spacing (D_1D_2) apart. If the two D doublets approach each other, the fringes approach the D line from larger wave-lengths and *vice versa*. The fringes were lost when the doublets crossed over each other.

Rotation of the compensator in the first place moves the fringes as in interferometry, as does also the normal micrometric displacement of M. If this motion requires readjustment of M, the range of displacement is curtailed and the corresponding change of phase appears. In the second place, the compensator, on rotation, traces the contours of the curves by successively accentuating the vaguer parts, as will presently be explained.

The fore-and-aft motion of G' also moves the fringes bodily through the spectrum without marked change of phase. All fringes, whether produced with or without compensators, are ultimately curved lines.

The most remarkable results occurred on widening the slit. Supposing that large strands were visible in case of the fine slit, and that this was gradually widened until the slit width was 0.5 mm. or more, the strands were found

to have coalesced in a way which defies description. In their place appeared a wide strip of equidistant parallel crescents, as shown in figure 28. The Fraunhofer lines had long vanished and the appearance of the spectrum was whitish and intense. The fringes in question are thus in a measure achromatic. The strips appear quite regular through the breadth of the spectrum and its width may be one-third of the length of the spectrum. The fringes move with the normal displacement of M (interferometry) and the range is large (0.5 cm. without adjustment), provided M does not require readjustment by rotation. Simultaneously the strip is displaced longitudinally in the spectrum in the usual way.

On closing the slit the ellipses break up into sharp strands again without offering a systematic clue as to the manner in which this is done. The strands usually trend more or less vertically with two sharp, strong groups, flanked by one or more weak groups on each side.

On removing the condenser these crescents became more slender but much sharper, so that in spite of the diminished light they could be well seen. They were then found to be like the approximately confocal ellipses of displacement interferometry, though not subject to the same laws. They embraced over one-third of the visible overlapping (green-yellow through red) spectra, terminating in very fine hair-lines on one side but coarse lines on the other. On opening the slit to about 0.1 mm. the evolution was curious. With a very fine slit a relatively narrow strip of strong slanting lines was seen in the yellow. As the slit widened these developed curvature, adding the more slender complements of the ellipses on the red side, until this part of the spectrum was filled with confocal half-ellipses having a transverse major axis. The range of displacement of M is practically indefinite, depending simply on the degree to which the spectra overlap; 3 to 4 cm. were tried. A horizontally wide mirror at M is needed; for the ellipses travel through the spectrum and the pencil along the mirror, from end to end. Both sides of the ellipses may be traversed by rotating the plate compensator, which successively accentuates (in a transverse strip) a definite part of their contours. In this way the thick apices or either of the hair-like lateral ends may be clearly brought out. Thus the two lines a, in figure 28, limit the strong part of the ellipses. When a moves to right or left, the hair-lines appear more and more strongly until they terminate, showing that the inclusive strip is also limited.

To further study this result, the grating* G' was successively rotated in small amounts on a normal axis with adjustment at M. It was thus possible to find both the ends of the ellipses, as well as the central parts. As a result the form figure 29 was definitely brought out. The confocal ellipses are extremely eccentric, with very turgid apices, so that the central part, if in the spectrum, consists of transverse straight lines. Motion of M shifts the fringes to and from the center where they originate or evanesce.

* When nearly centered, rotation of M about a horizontal axis is also sufficient to complete the centering of the ellipses.

The ellipses move as a whole with M, without changing form appreciably, throughout the spectrum; but they move *very slowly*, quite differently in this respect from the round ellipses in displacement interferometry, which are extremely sensitive to displacement of M. In the present work it may take 5 or 10 cm. at M to pass the ellipses quite through the spectrum. They are strong and fine in spite of the film gratings used.

In the endeavor to explain these phenomena one may notice that the main features have already been accounted for. As to details, since the gratings are films which may act from both sides, explanations are hazardous. I do not believe, however, that the films (cemented with balsam on glass plate) had any other discrepant effect here than to make straight lines sinuous. The character of the phenomena, as a whole, is trustworthy.

In the case of the duplicated fringes (fig. 27, a, b, and the strands) seen with a fine slit, the danger is perhaps greatest. But it appears to me that the coarse lines in figure 27 are vestiges of the ellipses of figure 29, due to a wide slit. These are superimposed on special fringes resulting from the diffraction of the narrow slit. It is difficult to conjecture any other cause of duplication.

The shift of ellipses through the spectrum follows as before from figure 25. Their occurrence in case of a wide slit might be associated with the equation

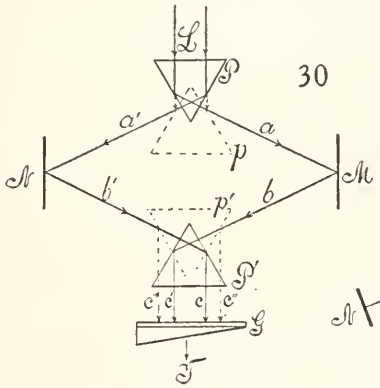
$$ne = D/2$$

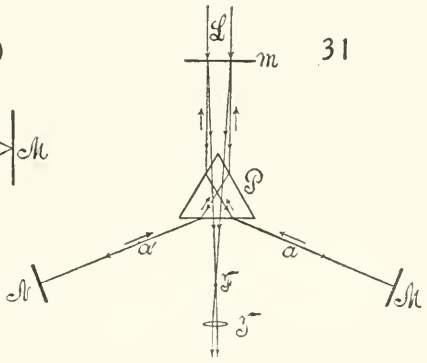
or with their independence of wave-length. They would therefore result merely from the obliquity introduced by dispersion. But the presence of the glass-plate compensator militates against this. In the peculiar behavior of the compensators when added or rotated around a vertical axis, the dispersion of the glass itself comes prominently into play, for the effect of introducing a corresponding air-path is negligible in its effect on form. Thus the removal of a 3 mm. compensating plate may leave the fringes almost too small to be seen, whereas the displacement of M over 3 cm. produces but little change of form.

Finally, the ellipses are developed in arc or contour from left to right, for instance, when the slit is widened; and they vanish from right to left as the slit is more and more nearly closed. The last lines for a closing slit make a narrow grid of fringes quite straight and strong.

22. The same. Prismatic adjustment.—The 60° prism has certain advantages in experiments like the present, particularly when non-reversed spectra are to be obtained. Figure 30 is a device of this kind, in which P is the separating prism and P' the collecting prism, the beam of white light L from a collimator entering the flat face normally on the front side and issuing normally on the rear side at c and c'. M and N are opaque mirrors parallel to each other, G a direct-vision prism-grating. The telescope is at T. The reflection may be either internal, as in the strong lines of figure 30, or it may be external on silvered faces of the prisms p and p', the appurtenances being shown in dotted lines. In this case the separated rays a, a', b, b' are collected

at c'', c''', to be joined in the telescope at T. The internal reflection being total, with the rays entering and leaving at right angles to the faces and requiring no silvering of the latter, I made use of it for the following experiments: M and N are on micrometers with the screw in the direction normal to their faces. P, M, N, P' must all be adjustable. After preliminary measurement for equal distances, the fringes were found without trouble. They were strong but fine, beginning with vertical hair-lines and gradually rotating as they grew coarser, till they rather abruptly vanished. The displacement of the M mirror did not exceed 0.6 mm., nor the rotation 30°. The spectra being non-reversed, the fringes covered the whole field. Nevertheless these lines must probably be regarded as arcs of circles or ellipses with enormously distant centers. In fact, the appearance of the whole of the elliptic symmetry, in the preceding experiments (§ 21) with gratings, is also to be associated with a slight difference of length of two overlapping spectra. This is necessarily the case, since the two gratings G and G', figure 25, have never quite the same constant. The third grating must therefore produce two spectra, the one slightly incremented and the other decremented in length, respectively, as compared with the case for white light.





One would naturally suppose that the abrupt evanescence of fringes was due to the escape of the b beam at the edge of the prism P'; but this is not possible, as the mirror M was traveling toward the rear. Furthermore, the fore-and-aft motion of the prism P' over several millimeters had scarcely any effect on the fringes. This is unexpected; for the rays, c, c', are compelled to approach or recede from each other by this motion. Finally, the sodium doublets may be moved at some distance (many times their breadth) apart without destroying the fringes. They are often most distinct when the D lines are not superposed. The same is also true for the longitudinal axes, though to a less degree.

These features are therefore peculiar. The rays c c' were about 5 mm. apart. Unfortunately the faces of the prisms were optically inadequate, so that the sodium lines were not sharp. For this reason no results were obtained with homogeneous light and a wide slit.

To enlarge the fringes, the prism P' may be rotated around a horizontal axis parallel to LT. The fringes then also rotate, but the increase of size so obtained is usually not striking. Moreover, no observable effect, either on the size of fringes or on the range of displacement, is produced by inserting compensators in one beam or both. If M and N are moved together toward the right or left, the result is not appreciable. A great variety of different adjustments showed a range of displacement, at M, about the same (0.06 cm.), whether the patch of light on the prism was wide or narrow. The range of fore-and-aft motion of P' within which fringes are visible was 0.52 cm. They vanish quite abruptly when the light is near the edge of the prism, although *both spectra* are still strongly visible. When the light is nearer the base of the prism they vanish more gradually. Definite strips of white light on both sides of the prism, therefore, coöperate to produce the fringes. The remainder of the illumination is ineffective. The distance apart of c and c', as modified by fore-and-aft motion, curiously enough, is here without marked influence. It is true, however, that the largest fringes were obtained when the two pencils of light from M and N coincided at the objective of the telescope, although the D lines were in this case far apart. The attempt to find a systematic method for enlarging the fringes failed, possibly because the prism angles were not quite identical. The striking contrast in the results obtained here in comparison with those of the preceding paragraph, although both methods are essentially the same, is noteworthy.

It is for this reason that I thought it desirable to test the method in figure 31, which accomplishes with a prism what was done in my original experiments with reversed spectra, by the aid of a grating. In the figure the incident beam of white light L from a collimator strikes the 60° prism at its edge, and is then refracted into the paired pencils a, a'. These are reflected normally by the opaque mirrors M and N, again refracted by P as each pencil nearly retraces its path. The return beams, however, are given a slightly upward trend, so as to impinge on the opaque mirror m (curved or plane). The rays reflected from m, in such a way as to avoid the prism P, may be reunited in the focus F observed by the lens T, or (if parallel) collected by a telescope at T. In view of the prism, the spectra are small and reversed, but may be brought to overlap at the red ends, which are towards each other.

The small dispersion makes it necessary to use a strong telescope if the Fraunhofer lines are to be visible and the D lines separated. Usually the two doublets will be at a small angle to each other, but this does not mar the interferences. When the adjustment has been made symmetrically, a strong linear phenomenon may be found not differing in appearance from the results obtained when a grating was used at P, figure 31. When the mirror M is displaced, however, the fringes appear in the form of multiple vertical hair-lines, which grow coarser until but a single dark line flanked by a bright line is visible. With further displacement the phenomenon again vanishes in passing through multiple hair-lines. This appearance of hair-lines is one distinguishing feature; but a much more important result is the small range

of displacement. It was found to be, between appearance and evanescence of fringes,

$$\delta e = 0.112 \quad 0.119, \quad \text{etc., cm.}$$

thus scarcely larger than a millimeter, whereas in the case where a grating ($D = 352 \times 10^{-6}$ cm.) was used in place of P the range of displacement was of the order of 5 mm.

If the spectra be regarded with a prism grating, they become relatively long and short, respectively; but the phenomenon is none the less strong, although it is apt to lie outside of the two sodium doublets and not midway between them, as with the telescope. It seeks out the line of coincident wave-lengths. Now, inasmuch as the refraction from M is normal and the rays virtually retrace their paths both in the case of the prism and the grating (in the original adjustment), it seems at first difficult to avoid the conclusion that wave-trains are more uniform in proportion as they have been more highly dispersed. The only misgiving would be the fact that the phenomenon with prism appears and vanishes in hair-lines, whereas with gratings it goes out rather abruptly. Otherwise one would regard white light as consisting of irregular pulses incapable of prolonged interference, whereas the dispersed wave consists of wave-trains in each color, which throughout a considerable number of wave-lengths are plane polarized. True, if there is sliding, the sections of the two light-pencils, the points of which are capable of interfering in pairs, increase in area proportionately to the dispersion.

Suppose that for low dispersion the fringes may be regarded as extremely eccentric, virtually linear ellipses, the lateral distance between which very rapidly diminishes, so that, since $\delta e = 0.12$, but

$$\frac{1}{2}\frac{0.12}{3 \times 10^{-5}} = 2000$$

can be seen by the given telescope. These lines would move behind the strip carrying interference fringes as M is displaced. If now the dispersion were much increased, say from $\frac{d\theta}{d\lambda} = 2 \times 760$ for the prism to 2×2880 for the grating, the ellipses would be much less eccentric as a whole and their lines would have grown coarser, so that many more would be visible by the given optical system. As the dispersion is increased $2880/760 = 3.8$ times, the range of displacement should increase similarly to $0.12 \times 3.8 = 4.6$ cm. The plane ruled grating ($D = 352 \times 10^{-6}$ cm.) in question was now again mounted in place of P and under good illumination the range 0.48 cm. was found experimentally. This agrees very well with the estimated value. Moreover, on close inspection it is discernible that the linear phenomenon really consists of extremely eccentric ellipses, which in case of the best adjustments manifest the very sharp arrow-like forms. It also enters and vanishes in multilinear form, though the lines are not hair-lines. Thus the assertion that increased uniformity of wave-train accounts for the long range of displacement and

visibility in case of the grating is not warranted. In the second order of the ruled grating or with a grating of higher dispersion ($D = 175 \times 10^{-6}$ cm.) the field was too dark for experiments of this kind. In this work, however, I obtained the linear phenomenon for the first time, from the double diffraction of a film grating.

In conclusion, it is interesting to refer to a relation of the reversed and the inverted spectra and their interferences. If in case of reversed spectra one of the superposed pair is rotated 180° in its own plane, around an axis normal to that plane and through the line of symmetry, the new pair of superposed spectra is an inverted system. At the same time the interferences which are ellipses in both experiments probably rotate their major axes 90°. In the case of reversed spectra this major axis is transverse, coinciding with the line of symmetry in a given wave-length, and the ellipses are *extremely* eccentric, whereas in the case of inverted spectra the major axis is probably longitudinal. It is not unusual to obtain a single line running all the way from red to violet; but arrow-shaped forms never occur, so that the ellipses are rounded forms and belong to distant centers. An adequate reason for the highly eccentric, closely packed elliptic fringes of reversed spectra on their evolution from the round ellipses of inverted spectra by rotation is yet to be given.

23. Apparent lengths of uniform wave-trains.—In § 16 certain results were given which made it seem plausible that the path-differences within which interferences are producible (*i.e.*, the apparent lengths of uniform wave-trains) increase, as the dispersion to which the incident collimated white light is subjected is made continually greater. Work with this quest in view is reported in table 10, the plan being to produce the interferences by one and the same method, but with a successive variation of the dispersion of spectra. The method, figure 14, was first selected for this purpose, inasmuch as the use of prisms and gratings of different dispersive power at P meets the requirements, while spectra of the first and second order are equally available.

It is obvious that in work of this kind the spectra must be bright, otherwise the fine lines will escape detection. Deficient values will thus be attained if the spectra are too dark. Moreover, the results can not furnish data of precision, since the exact instant at which fringes, continually decreasing in size, have actually vanished, can not be fixed; and it is the fine fringes which furnish a considerable amount of the displacement. The differences, however, are so large that not only orders of values are clearly apparent, but the ranges more than sufficiently so to substantiate the argument.

It is possible that the method, figure 14, gives the half-ranges only, since the efficient patches of light, figure 8, can not cross each other. The methods applied will nevertheless be trustworthy, since they are identical, the same telescope and other appurtenances being used throughout. Later the grating method (fig. 3), suitably modified, will be used. Path-lengths of a meter or more were usually admissible.

In table 10 the first series of measurements is obtained with a 60° prism,

the dispersive power $d\theta/d\lambda$ being computed (approximately) from Cauchy's equation, so that

$$\mu = A + B/\lambda^2 = \sin(\varphi+\delta)/2/\sin\varphi/2$$

nearly, and therefore

$$d\delta/d\lambda = 4B \sin\varphi/2/\lambda^3 \cos(\varphi+\delta)/2$$

φ being the prism angle (60°) and δ the angle of minimum deviation. The constant B was put 4.6×10^{-11}.

TABLE 10.—Ranges of displacement, e, y, for different dispersions. Method of figure 14. $B=4.6\times10^{-11}$. $\mu=1.6$.

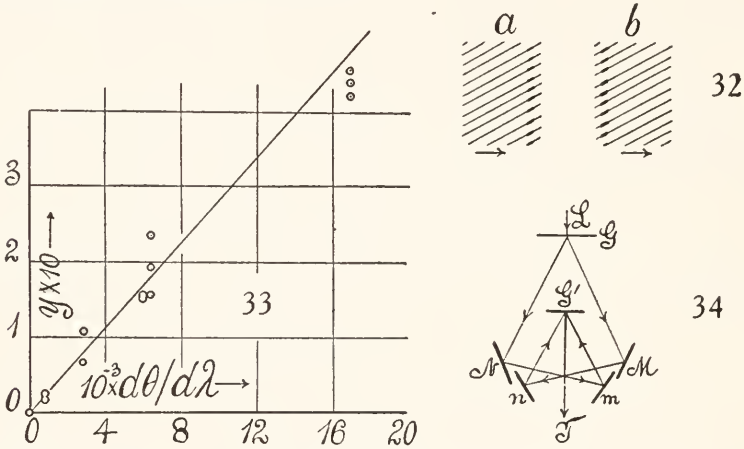
Disposition.	$e_M\times10^3$	$e_N\times10^3$	$y\times10^3$ at P	$d\theta/d\lambda$	θ	Remarks.
	cm.	*cm.*	*cm.*			
60° prism P, 90° prism P'	26	19	16	760	49° 45′	
	25	18	17			
	24	17	19			
Mean.....	25	18	17			
Same. P' brought forward	28	29	27	760	49° 45′	
	32	30	23			
	...	...	26			
Mean.....	30	30	25			
Ruled grating P, 90° prism P'	100	81	65	2,880	9° 39′	
	100	89	76			
	117	...	56			
Mean.....	106	85	66			Too dark.
Same, mean.....	161	136	108			Very bright.
Same, second order from P	250	229	155	6,030	19° 34′	
Same, second order near edge.....	227	...	150			Bright spectra.
Film grating P, 90° prism P'	173	184	155	6,400	20° 40′	Too dark.
Same.....	301	247	183			
	303	226	200			Very bright.
Mean.....	302	236	191			
Same, vertical fringes.....	325	...	234	6,400	20° 40′	Very bright.
Same, second order from P	482	422	450	16,910	44° 56′	
	461	...	427			
Mean.....	472	422	438			Bright.
Same, second order, vertical fringes.....	500	...	...			Strong fringes.

In the remaining series $d\theta/d\lambda = 1/D \cos\theta$, the usual expression for the grating, θ being the angle of diffraction and D the grating space. The dispersive power thus increases from about 800 to 17,000, over 20 times. Throughout this whole enormous range good fringes were obtained.

The values e show the displacement of the opaque mirror M during the

presence of fringes, and of the opaque mirror N as specified. Of these, e_M is systematically larger than e_N for reasons which do not appear. The screws were of American and foreign make, but they could not be so different. It is due very probably to residual curvature in the mirrors and surfaces, whereby fringes on the left (N) vanish sooner than those on the right (M). The datum y is the displacement of the right-angled reflecting prism P', parallel to the component rays bb'. This value is smaller than e for reasons already discussed in § 16. All measurements were frequently repeated and the means finally taken for comparison with $d\theta/d\lambda$.

In the third series (ruled grating and concave grating) with specially brilliant spectra, the phenomenon of figure 32 was observed. A wide field of faint fringes was visible, enormously accentuated and clear in the narrow strip of the linear phenomenon. As the micrometer mirror at M moves forward, these faint fringes shift bodily across the stationary bright linear strip, beginning therefore with the pattern a and ending with b. The faint fringes follow the rules of displacement interferometry.



In addition to the data of the table, a large number of miscellaneous tests were made with the reflecting prism in different positions. Unless brought too far to the rear, when the beams are lost at the edge and e too small, the results for fine and coarser fringes were of the same order.

The values of y have been graphically given in figure 33; those for e are not sufficiently regular in the dispersive powers above 1,000 for this treament. It is probable, for instance, that at 16,900 the sliding along the prism surface is interfered with. All the data, in consideration of their limitations, bear out the inference that the range of displacement within which fringes are seen increases in marked degree with the dispersion. The average initial ratio $2\lambda/(d\theta/d\lambda)$ is about 60×10^{-6} cm.

A very surprising result in these experiments is the efficiency of the film grating in series IV and V, not only in the first but in the second order of spectra.

After these experiments an attempt was made to obtain similar results with the more comprehensive method of two gratings (transmitting G and reflecting G') of figure 3, above. But here the choice of gratings with appropriate constants was limited and with high double dispersion the fields were apt to be too dark. Good results were obtained with the 60° prism and concave grating and with the ruled grating together with the latter. In the method of figure 3, the second angle of diffraction is necessarily greater than the first, $\theta' > \theta$. To obviate this difficulty the method was modified for prisms as in figure 20, where G is the concave grating, T a strong lens near its focus, and m and n auxiliary mirrors. If this method is used for highly dispersive gratings (G replacing P), the rays must be crossed as shown in figure 34. The fringes were found in this case when G was a film grating, but the work had to be abandoned, as the spectra were dull.

The data given in table 11 again show marked increase of displacement with the dispersion $d\theta/d\lambda$, though it is not proportional here. The method with two gratings lacks the brilliancy of the prism method.

TABLE 11.—Range of displacement for different dispersive powers. Method of figure 20, full displacement.

Details.	e_M	e_N	$\frac{d\theta}{d\lambda}$	θ	Remarks.
	cm.	*cm.*			
60° prism and concave grating.....	0.357	0.315	760	49° 45′	Bright.
	.300	.282	760	49 45	Too dark.
Ruled and concave grating.....	.514	.520	2,880	9 39	Bright arrows.
	.509		2,880	9 39	Dark.
Film and concave grating.....			6,400	20 40	Too dark.

24. Normal displacement of mirrors ($\delta = 0$).—This desideratum was secured in the original methods, in which a single grating was used for both diffractions. Rays in such a case have to cross the grating somewhat obliquely to the horizontal. The method, furthermore, is restricted to the linear vertical fringes, which are not useful if practical measurement is aimed at.

In the methods with a right-angled reflecting prism (fig. 14), this result is easily secured by displacing the prism. In all other methods ($\delta > 0$), the displacement of mirror is accompanied by sliding of the pencil along it. The effect, as has been shown, is not negligible. It therefore seemed desirable to devise other methods in which $\delta = 0$, and figure 35 is a device of this kind.

Here G and G' are two identical gratings, the first, G, receiving the light L from a collimator. The component pencils a, a' pass through the half-silvered plate H, and thence (b, b') to the opaque mirrors M and N, one or both on a micrometer. The pencils b and b', impinging normally, retrace their paths and are thereafter reflected at the plate H into c and c'. These strike the second grating G' at the proper angle of diffraction and thereafter enter the telescope T together. The path of rays is symmetrical throughout. White light is screened off at d. Reversed spectra are seen at T. Unfortunately the only identical gratings at my disposal were film gratings of high dispersion

($D = 162 \times 10^{-6}$). As a result of the two diffractions and the half-silver reflection, the spectra were too dull to make it worth while to look for fringes, at length. None was discernible after some searching, to my regret, for the method itself has many points of interest and with gratings of low dispersion it succeeds.

Later I stripped a celluloid film from the ruled grating ($D = 352 \times 10^{-6}$) and mounted it by simple stretching. Using the original grating at G and the film at G', the fringes were found with some patience. The spectra were fairly bright (arc lamp) and the fringes reasonably strong; but they admitted of a displacement of only 1.8 mm., in spite of the vanishing angle $\delta = 0$. Possibly this small displacement is due to the imperfect film grating.

In further experiments I half-silvered plates of glass to different density. In this work I obtained adequately bright spectra and practically perfect fringes, but the range of displacement ($\delta = 0$) could not be increased above 1.8 mm. Within this interval the fringes seem to change form but little, thinning only being evident. Then they become dull and vanish.

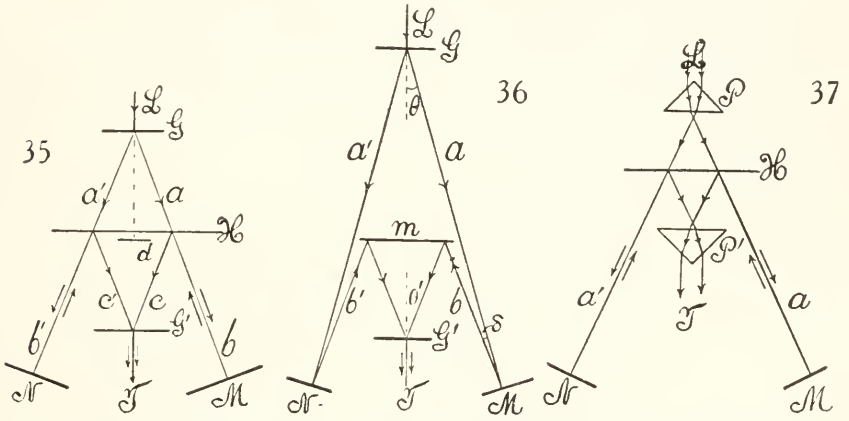
The method was temporarily modified, as shown in figure 36, where G is a ruled grating ($D = 352 \times 10^{-6}$ cm.), G' a film grating ($D = 176 \times 10^{-6}$ cm.), and m an opaque mirror. This naturally introduces an angle $\delta = \theta' - \theta$, which is negative when $\theta' > \theta$, or the grating G shows greater dispersion. The mirror is limited in breadth, so that the rays a, a' have free access to M and N. The fringes were found after some trouble, for the transmitting grating G' also acts as a reflecting grating if the rays b, b' fall upon it, and it is not always easy to separate these two cases, each of which will give fringes on proper adjustment. The spectra are very bright and the range was about 2 mm.

The same method was now carried out with prisms, as shown in figure 37, where L is the incident pencil from a collimator, P and P' right-angled prisms, I the half-silvered plate, N and M opaque mirrors on micrometers, T the telescope. The spectra seen at T have each been four times refracted and twice reflected, at M and H. They are very bright, so that a very fine slit (here specially desirable) is available. The sodium lines are not separated. On bringing the spectra to overlap at their corresponding edges, the fringes were found. They are peculiar, inasmuch as they show the phenomenon of figure 32, but with the faint fringes curved and more prominent than heretofore. In other words, the faint phenomenon shifts across the field from side to side, but is enormously accentuated at the transverse strip of the linear phenomenon. Narrowing the incident pencil broadens and blackens the fringes. They may be obtained in the gap between two spectra just separated. The range of displacement within which fringes are seen was, however, very small, not exceeding 0.2 mm. This is a characteristic of these fringes and in keeping with the low dispersion.

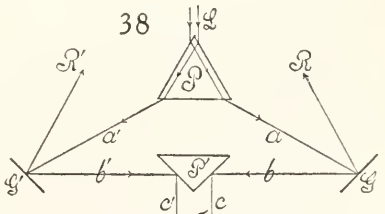
It is interesting to note that the systems figures 35, 36, 37 constitute an element of a direct-vision spectroscope. It has been shown that it can be made quite powerful.

The same method, figure 37, was now used with two 60° prisms of highly

refracting glass. In contrast with the ease in which the adjustments were made with the symmetrical 45° prisms, the corresponding work with 60° prisms proved to be exceedingly difficult. True, the prisms were large, including long glass-paths. The sodium lines, now clearly separated, were markedly curved, so that on placing them near together they either assumed an O-shape or an X-shape. But the spectra were brilliant and nothing appeared to militate against a successful result. But it was not until after days of searching that the fringes were found, and then only with two prisms of different, highly refracting glass. They were not quite uniform, but it seemed impossible to improve them. The ranges of displacement were found to be 0.088 to 0.093 cm. with the electric arc, 0.103 cm. with (condensed) sunlight. This is again in accord with the large increase of dispersion, the range of displacement being about five times greater than was the case with 45° prism of less refracting glass.



25. Diffraction at M, N, replacing reflection.—The present method of observing interferences in the zero, first, second, third, and even fourth order, successively, without essential change of the parts of the apparatus, is noteworthy. I happened to possess a plane reflecting grating ($D \times 10^{-6} = 200$), cut into two equal parts by a section parallel to the rulings, and it was therefore easy to devise the method. In figure 38, the incident light L from the collimator is separated into two component beams a and a' by the 60° prism P. This is essential here, as an abundance of light is needed (sunlight should be focused by a large lens of long focus (5 feet) on the slit). The rays a, a' are then either reflected or diffracted in any order by the plane reflecting gratings G, G' into the collinear rays b, b'. They are then reflected by the silvered right-angled prism P' and observed in a telescope at T. G and G' and if possible also P' should be on micrometers, so that



corresponding displacements e, e', normal to G and G' and y in the direction bb', may be registered.

The adjustments, if symmetry were demanded, would be cumbersome; for, in addition to precise modification of the position and orientation of the prisms P, P', the grating requires fine adjustment and a means of securing parallelism of the rulings. But an approximate adjustment does very well and no pains were taken in the first experiments to secure symmetry. The spectra were intensely brilliant in the low-order work; but even in the fourth order the light was adequate. One may note that here the gratings do not reverse the dispersion of the prism P, though this is relatively small. Table 12 is an example of results:

TABLE 12.—Ranges of displacement varying with dispersion. Paired gratings and 60° prism. $\theta = 46°$. $\delta = 44°$. $x = 2e \cos \delta/2$.

Order	Observed $e \times 10^3$	$x \times 10^3$	$\frac{i}{\theta}$	$d\theta/d\lambda$	Remarks.
	cm.	*cm.*			
0	38	70	22°	760	
1	180	351	12.8°	3,490	
	200		31.2°		
	180	351			
	200				
2	420	777			
	420		3.5°	6,440	
	400	721	40.5°		
	380				
3	320	573	−6.4°	9,930	Fringes lost at edge?
	300		50.4°		
	520	962			
	520				
4	580	1070	−17.6°	14.800	Fringes faint.
	580		61.6°		
	520	910			Fringes faint.
	450				

The fringes in the zero order were good and strong, not inferior to any of the others, but unfortunately too short-lived. In the fourth order the fringes are weak (although the enormous sodium doublets stand out clearly), doubtless from excess of extraneous light. Here also it is difficult to prevent the beam from vanishing at the edge of the prism P'. Hence the anomalously small displacement, a discrepancy which is already quite manifest in the third order.

The present experiments furnish a striking example of the uniform breadth of the strip of spectrum carrying the fringes, quite apart from the dispersion of the spectra. In the prism spectrum, where the sodium doublets are indicated by a hair-line just visible, to the fourth-order spectra, where they stand apart like ropes, the linear phenomenon has the same width.

The computation of the dispersive power in these cases is peculiar. It will be seen from figure 38 that the angle $\delta = 44°$ between the incident ray a and

the diffracted ray b is constant and is $\delta=\theta+i$ in the first and second and $\delta=\theta-i$ in the third and fourth orders. Hence in succession

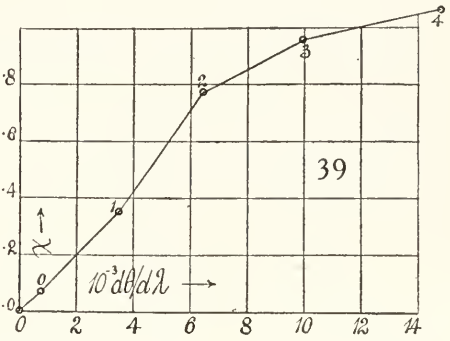
$$\sin(\delta-i)-\sin i=\lambda/D \qquad \sin(\delta-i)-\sin i=2\lambda/D$$
$$\sin(\delta+i)+\sin i=3\lambda/D \qquad \sin(\delta+i)+\sin i=4\lambda/D$$

from which equations the angle i may be computed. I did this with sufficient accuracy graphically, and the values of i and θ so found are given in table 12.

Since $d\theta=di$, apart from sign, it follows that the dispersing power is

$$-d\theta/d\lambda=n/D\,(\cos i+\cos(\delta-i))$$

where n is the order of the spectrum and i changes sign in the third and fourth orders. With the values of i given, the data for $d\theta/d\lambda$ in the table were finally computed. The dispersive power of the prism was computed as above and is to be added to all the succeeding dispersive powers. Figure 39 shows the relation between the dispersive powers and the path-difference $x=2e\cos\delta/2$ computed from the observed range of displacement e of the grating G. The largest values of x are taken, as they are the most probable. The effect of dispersion here breaks down in the third and fourth orders, as already stated, probably from incidental causes. For the spectra themselves were still adequately bright, but the fringes were faint for some reason and I failed to make them stronger. The rate $x/(d\theta/d\lambda)$ is here about 120×10^{-6} initially. This is larger than above, owing to the differences of apparatus used, etc.



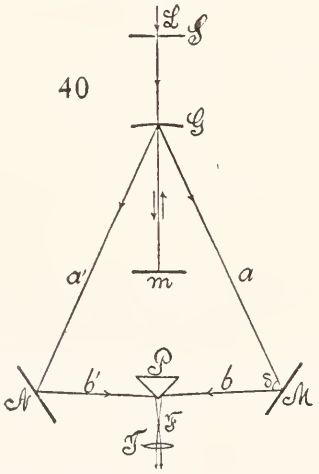
26. Experiments with the concave grating.—As there was an excellent Rowland grating in the laboratory with a 6-foot radius and a grating space $D=177\times10^{-6}$ cm., it seemed worth while to obtain the interferences with it. I had hoped to doubly diffract the rays at the same grating, but there is not light enough to make this method fruitful. Accordingly the device, figure 40, promised the best results, where L is a convergent pencil of sunlight, S the slit. The pencil L is carried above the grating G to the opaque mirror m, whence it is reflected to the grating and diffracted into the component beams a and a'. These are in turn reflected by the opaque mirrors M and N (on micrometers) into the pencils b and b', nearly collinear. The latter are then reflected by the silvered right-angled prism P to the common focus F, to be observed with the lens T. The spectra are very bright and highly dispersed and are easily made to overlap on their contiguous edges (parallel to a Fraunhofer line D, for instance) sufficiently to show the linear phenomenon of reversed spectra.

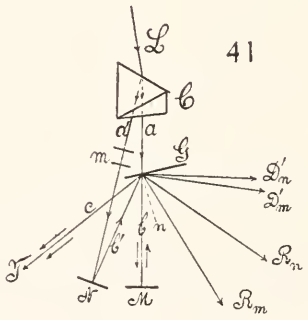
The fringes are easily found and splendid, though they are not superior in this respect to the fringes obtained by other methods. P is also on a micrometer with the screw in the mean direction $b\,b'$. The range of displacement of P was about $y=0.55$ cm., so that the available path-difference is considerably above a centimeter. Within this the fringes pass from fine hair-lines through a maximum and back again, apparently without rotation. To enlarge the fringes the grating G may be tilted in its own plane or a similar adjustment made at P.

The longitudinal axes of the spectra (wire across the slit) are not in focus with the D line; but though hazy they suffice for adjustment. Naturally the distance $FbaG$ is the radius of the grating R (6 feet) and the distance $Sm+mG$ is $R\cos\theta$. The distances are approximately laid off and the observer at T may then push the mirror M fore and aft by the aid of a lever till the Fraunhofer lines are sharp.

Unfortunately the spectra as a whole are shifted by the micrometers, together when P moves and separately when M or N moves.

27. Polarization.—The two rays obtained from calc spar, if corrected for polarization, should be available for interferences of the present kind. Naturally an achromatized calc-spar prism (C, fig. 41) is most convenient for the





purpose. White light from a collimator, L, is doubly refracted by this prism C, and the extraordinary ray a, just missing the grating G (above or on the sides), impinges on the opaque mirror M and is thence reflected to the grating G. The ordinary ray a' is reflected from the opaque mirror N and thence also reaches the grating. These two pencils, b, b', are directly reflected by the grating ($D\times 10^6=200$ cm.) into R_m and R_n and diffracted into D'_m and D'_n. By suitably adjusting the grating between C and M and inclining it as shown, two coincident spectra may be made to pass along the common direction c to the telescope at T. These spectra are quite intense. One is somewhat

more dispersed than the other, owing to the difference of angles of incidence i, i' and to the residual or differential dispersion at the calc-spar prism, for only the a pencil has been adequately achromatized. In my apparatus the distances CM and GM were about 130 and 100 cm. and the distance NM roughly 30 cm. N is on a micrometer, as it is nearer to the observer at T, though it would be preferable to put M on a micrometer.

To obtain interferences of the present kind, the plane of polarization of either a or a' must be rotated 90°. This may be done by two quarter-wave-length micas M, in a', the first of which (set at 45° as usual) produces circularly polarized light and the second then erects the vibration into parallelism with the vibration of the pencil a. Other methods will presently be resorted to.

With this adjustment fringes were found at T after some searching. They were large, but occurred in a transverse strip of spectrum about $D_1D_2/2$ in width. True, the spectra are without reversion; but, as stated before, one was about one-fifth longer than the other. This is probably the reason for the narrowness of the strip, for the fringes should otherwise fill the spectrum.

The fringes as first found admitted a displacement of N of about 0.3 cm. only. They were hard to control, needed sharp longitudinal adjustment, and when lost were difficult to find again. They rotate from and to vertical hair-lines, through a horizontal maximum. They are always found in the line of symmetry, which for unequal spectra moves more rapidly than the Fraunhofer lines if they are separated. The nearer quarter-undulation plate at W may be considerably rotated without quite destroying the fringes.

If the double quarter-wave-length plate is suitably put in the a beam, results of the same kind are naturally obtained. If a single quarter-wave-length plate is placed in each beam, at 45°, both will be circularly polarized, the position of the micrometer being intermediate. I tested this case at some length, but found no interferences, as was to be expected. Circularly polarized rays of the same sense do not interfere.

In place of the achromatized calc-spar prism, a double-image Wollaston prism or a double-image Fresnel prism (rotary polarization) could be used. Unfortunately I had neither of these, but the latter in connection with an analyzing nicol would have been worth testing.

CHAPTER II.

THE INTERFERENCES OF INVERTED SPECTRA.

28. Introductory.—If two identical spectra are superposed in such a way that one is rotated 180°, on a transverse axis (parallel to the Fraunhofer lines), with respect to the other, it will be convenient to refer to the phenomena resulting and described in Chapter I as the interferences of reversed spectra. On the other hand, if one of the superposed spectra has been rotated 180° with respect to the other on a longitudinal axis (parallel to the length of the spectrum), we may refer to the interferences as those of inverted spectra. The absence of either of these adjustments would then be accentuated as non-reversed or non-inverted.

In the case of inverted spectra, therefore, we are dealing with phenomena of virtually homogeneous light, exhibited throughout the length of the spectrum. Such experiments were made cursorily in my first paper on the subject,* but the phenomenon is very peculiar, apparently anomalous, and further treatment is therefore desirable.

29. Apparatus. Non-inverted spectra.—The apparatus formerly used for long optical paths is difficult to manipulate. It has therefore been simplified in the present method and used for short distances, so as to be wholly in the observer's control. The parts of the apparatus are conveniently assembled as in a preceding experiment, except that the slit which furnishes the collimated light L, figure 42, is now horizontal—*i.e.*, at right angles to the edge of the sharp prism P (about 20° at apex). The rays a and a' (horizontal blades), after leaving the opaque mirrors M and N, are then reflected from the sides of the right-angled prism P' into c and c'. Thus far the light is white; but c and c' are now diffracted by the grating G with its rulings horizontal (parallel to slit) and with the interposition of an auxiliary prism p (edge horizontal), the two spectra due to c and c' are observed by a telescope at T.

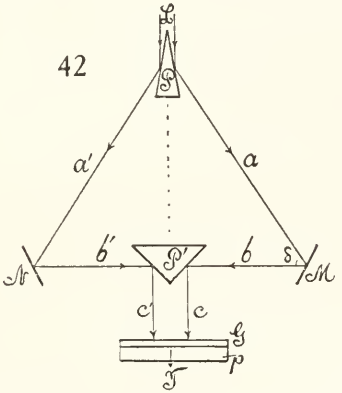
The experiment succeeds best with sunlight. The triangle of rays, a, a', b', b, is first made isosceles and horizontal by adjusting P, P', being set midway and symmetrically between M and N. The two spectra in the telescope (vertical ribands) are now made to overlap at their inner edges and the two sodium doublets placed accurately in contact, by aid of the adjustment screws on the mirrors M and N. The latter are then to be moved micrometrically (Fraunhofer slide) until the fringes appear. The experiment is not an easy one.

It is obvious from figure 42 that the two superimposed spectra are non-

* Am. Journal, XL, pp. 486 to 498, 1915, § 4; Carnegie Inst. Wash. Pub. 249, Chap. I.

inverted or direct. Hence with a wide slit, or insufficiently homogeneous light in the direction of a given Fraunhofer line, no fringes will appear. Such fringes as may in any case be found will not, therefore, much outlast the Fraunhofer lines, so far as width of slit is concerned. Furthermore, even if the slit is narrow and the spectra coördinated, there will be no fringes obtainable if the superimposed solar spectra are quite unbroken—*i.e.*, without incidental furrows in the direction of their length (normal to the Fraunhofer lines). For it is to be noticed that the slit is horizontal, and therefore there is no observable diffraction—*i.e.*, virtually no slit in the horizontal direction.

If, however, the spectrum field is interrupted longitudinally by a thin (0.1 mm.) wire drawn across the slit (or, much better, by very fine specks of dust lying incidentally within the slit), then these fine opaque objects will effectively replace the slit, or act analogously to a slit in the horizontal direction. Hence fringes will appear when the path-difference is sufficiently small, associated with the geometric shadow of the opaque objects, throughout the length of the spectrum.



We have here, therefore, a peculiar case of the diffraction of a rod, from two separately controlled half-wave-fronts. The fringes at one extreme of adjustment of mirror M begin with fine horizontal lines, which on moving M incline and enlarge until they gain the maximum of size in the vertical direction. After this, on further motion of M in the same direction, they incline further, diminish in size, and finally become horizontal and hair-like again. They move along the horizontal axis with M, subject to the equation

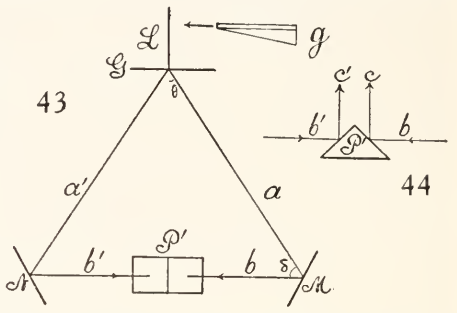
$$\frac{de}{dn} = \frac{\lambda}{2\cos\delta/2}$$

where $\delta/2$ is the angle of incidence at M, λ the wave-length, and de/dn the normal displacement of M per fringe.

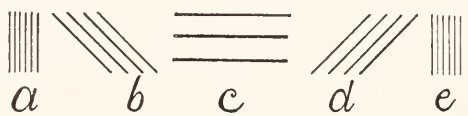
Within the region of overlapping spectra each longitudinal black line is covered from end to end with fringes, the strip being about of D_1D_2 width or more if the line is thinner. A broad black line (thicker wire across slit)

shows the fringes at its edges only. While the spectrum may thus be covered with independent strands of fringes, they all move or change phase together. The range of displacement of the micrometer-screw is about 2 mm. When the spectra are about to separate—*i.e.*, when overlapping ceases—the fringes are apt to be particularly wide, say even $4D_1D_2$, and they may be seen in the gap between spectra. In general, the degree of coarseness of fringes depends on the adjustment for parallelism of spectra.

30. Apparatus and results for inverted spectra.—The preceding apparatus may be modified as shown in figure 43. Here L is a collimated beam of white sunlight from the vertical slit, G a transmitting grating. The component pencils a and a' of spectrum light impinge on the opaque mirrors M and N, and are then reflected in b and b' to reach the silvered sides of the right-angled prism P'. This is now placed with its sides at 45° to the horizontal and its edge in the direction of the incident beam L prolonged. Hence the two pencils b and b' are reflected vertically upward (fig. 44) and appear as two identical and parallel spectra in the field of a telescope, vertically above P'. Observation is conveniently made downward to obviate additional reflection. If the triangle a, a', b', b is horizontal and isosceles there is no difficulty. On slightly moving the adjustment screen on M, N, P' (which must be revolvable on a vertical axis, and P', or the beam L, movable up or down), to bring the two spectra into coincidence along a given longitudinal axis, and a transverse axis like the D lines, the two spectra are symmetrical—*i.e.*, mirror images one of another with respect to the longitudinal axis. If, now, the mirror M is moved on a micrometer, the fringes of inverted spectra appear when the path-differences are nearly the same.



45



Obtained at short distances (of the order of a foot) on the cast-iron block (Chap. I, fig. 3), these fringes are quiet and better circumstanced for observation; but their characteristics are the same as found for them before (Chap. I, § 4, Carnegie Inst. Wash. Pub. 249). They lie within a narrow strip at the line of symmetry of the two superposed spectra, running from end to end and in breadth about three times the distance apart of the sodium lines ($3D_1D_2$). When the mirror M is moved micrometrically in one direction, the fringes begin to appear as fine hair-lines (a, fig. 45) parallel to the D lines. These fine fringes gradually coarsen and rotate until they reach their max-

imum size c, when they are perpendicular to the D lines. A single black or bright line may here extend from end to end of the spectrum. Thereafter they grow finer (rotating again) in the same way until they vanish, e, as they began. The total angle of rotation is thus 180°.

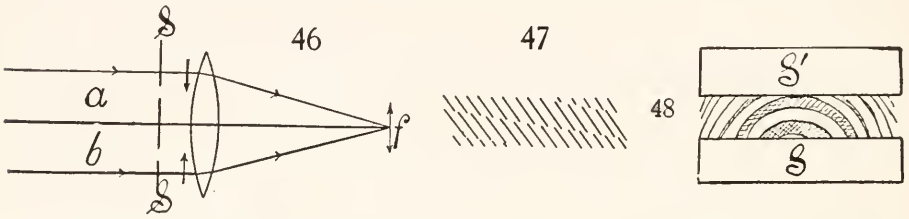
If the two beams b and b', figure 43, are moved nearer the edge of the prism, the fringes become larger, but usually not much. At least I did not, at first, succeed in separating the fringes much beyond the D_1D_2 distance. The width of the longitudinal interference strip remains unchanged. If the light is removed at the line of symmetry (wire across slit), the fringes are sharply outlined across the black line. Being so small, they are naturally always sharp and vivid. The range of displacement of M within which fringes are visible was about 0.2 cm. for the given grating ($D = 352 \times 10^{-6}$), corresponding to the complete rotation 180°, instanced above. If the slit is widened, the fringes slightly outlast the Fraunhofer lines. They also lie in the principal focal plane.

The remarkable feature of these fringes is the definite breadth of strip, from red to violet, within which they lie. With full wave-fronts the striations look as though they were cut between two parallel lines, $3D_1D_2$ apart, In some adjustments, however, suggestions of concealed fringes, very faint prolongations of the strongly marked striations, are unmistakable.

31. Wave-fronts narrowed.—The longitudinal strip within which the interferences lie is very sharply limited in breadth, as has been stated. It may, however, be broadened by screening off the white beam, as it leaves the collimator, *from below*. When the whole length of slit is utilized, the strip may not be more than D_1D_2 in width. As the vertical blade or beam of white light is cut off, more and more from below, the strip increases to a width of $4D_1D_2$, and when the two inverted spectra in the field of the telescope begin to separate at the line of symmetry, the strip may be over $10D_1D_2$ in width. It is obvious that in such a case the light comes from near the horizontal top edge of the prism. The wave-fronts are slit-like. The field within which diffraction is perceptible in the telescope increases in breadth as the colored wave-front, incident at the objective of the telescope and parallel to the spectrum, decreases in breadth in the same direction. In figure 46, a and b are the two component beams from the two faces of the prism, respectively. The focus is at f. The arrows show the effect of narrowing. The oblique rays (omitted) are similarly affected and in step with the axial rays shown. But the fringes are not changed in size. They may, however, be definitely changed in inclination. Size results from the anterior relations of the spectra (distance between paired pencils), and not from the width of wave-front.

These inverted fringes admit of much magnification. With a strong telescope (magnification about 15) they are quite sharp only in a part of the magnified spectrum and grow vague beyond, showing that the component spectra are not quite identical after the two reflections. When not quite in adjustment, the strip is liable to exhibit separate oblique strands, lying within

the same strip or region (fig. 47). They may become sharp by changing the focal plane of the eye-piece. When parallel to the length of the spectrum and seen in a strong telescope, about 7 lines alternately black and white may be counted. The whole lie within a strip of not much above D_1D_2 width. The range of displacement of M for a rotation of 180° of fringes is about 0.25 cm. Change of size of fringes from red to violet is hardly appreciable.



The same results may be obtained by placing a screen SS, figure 46, with two parallel slits, under the vertical telescope, to admit and limit the two rays c and c' in figure 44. It was found that slits 3 or even 6 mm. apart may still show fringes, though they are obviously smaller as the distance apart is greater. The most interesting results were obtained by bringing the rays a little beyond the edge of the prism, so that the spectra in the telescope SS', figure 48, are separated at some distance. A long collimator (1 meter) is advantageous. In this way the character of these fringes was definitely established. They are of the elliptic type, as suggested in the figure, characteristic of the displacement interferometer, and the cases, figure 45, a, b, c, d, e, are thus merely the intercepts of ellipses with the distant centers, between parallels. Very coarse central fringes were obtained in the dark gap, and the displacement at mirror M, between the extreme hair-line types, was now only about 0.08 cm., all fringes filing by the coincident D lines while the micrometer shifted.

Hence this method is available for displacement interferometry, the horizontal type c, figure 45, normal to the D lines, being used for setting the micrometer at M. If a plate of glass of thickness E and index of refraction μ is inserted normally into one beam, the corresponding air-path is

$$z=E\left(\mu-1-\lambda\frac{d\mu}{d\lambda}\right)=E\left(\mu-1+\frac{2B}{\lambda^2}\right)$$

when B is Cauchy's constant and the wave-length λ. I assumed $B=4.6\times10^{-11}$ and $B/\lambda^2=0.0265$. On the other hand, the same air-path for a normal displacement, e, of the mirror as given by the micrometer-screw is

$$X=2e\cos(90°-\theta)/2=2e\cos\delta/2$$

where θ is the angle of diffraction of the grating G, figure 43, and $b\,b'$ is normal to the direction of incident light. Hence

$$E(\mu-1+2B/\lambda^2)=2e\cos(90°-\theta)/2$$

A rough experiment was made with a plate $E=2.2$ cm. thick, $\mu=1.53$.

The corresponding displacement found was $e=0.92$ cm. The computed displacement should be $e=0.80$ cm. The low value was supposed to be due to the need of readjustment (wedge-shape) and insufficient normality of plate. Further data (table 13) were therefore investigated for thinner plates, but they do not clear away the difficulties.

TABLE 13.—Inverted spectra. $\theta=9°\ 39'$. $x=2e\cos(90°-\theta)/2$. $\mu=1.526$; $B=4.6\times10^{-11}$; $2B/\lambda^2=0.0265$; $z=E(\mu-1)+2EB/\lambda^2$.

E Observed.	e Observed.	x	e Computed from $x=z$	z	E Computed from e (observed) and $x=z$
0.736	0.298	0.455	0.268	0.3901 +0.0195	0.817
	0.282	0.431	0.268	=0.4096	0.774
	0.295	0.451	0.268		0.809
	0.314	0.480	0.268		0.861
	0.311	0.475	0.268		0.853

In table 13, e is the observed normal displacement of the mirror M, x the corresponding computed path-difference, z the path-difference computed for the glass of thickness E and the index of refraction μ. From z the displacement e or from x the glass thickness E may be computed. These are given in the table. In the second and third parts of the table, the edge of the prism P' was inclined at an angle to the line of symmetry, in opposite directions. The effect of this is manifest, but it does not explain the very large values of x for the symmetrical adjustment (rays from grating to mirror making an isosceles triangle) of the next observations. These were made with care. P', figure 43, lay at the middle of the base of the isosceles triangle of rays from G. The long collimator was used, giving two splendid spectra, and rays were raised until magnificent large, cord-like fringes appeared. The longitudinal fringe, a single line normal to the sodium lines extending throughout the spectrum, made it possible to set the micrometer to about 0.0003 cm., or 5 wave-lengths. The motion of fringes with the rotation of plate being very striking, the plate was placed in the normal position to the rays by noting the retrogression of fringes at this point. The total range of displacement between extreme hair-like striations was 0.25 to 0.30 cm. One circumstance was noticed for the first time—that on limiting the blade-like beam from below (as above described) the fringes not only enlarge, but rotate—*i.e.*, path-difference is modified.

It is thus difficult to ascertain the discrepancies in x in table 13, as these values should be nearly 0.41 cm. throughout, or in e, which should be about 0.27 cm. when the prism is symmetrically placed.

32. Inverted spectra. Further measurements.—The curious results shown in table 13 induced me to endeavor to detect the nature of the discrepancy by displacing the prism in the direction of the beams incident upon it. To

do this effectively it was necessary to do the work at long distances (meters), in order that adequate space might be available between opaque mirrors and prism. Accordingly M, N, P', figure 43, were all placed on micrometers, with the screws normal to the faces of the mirrors and the right edge of the prism, respectively. The fringes were found without difficulty and they were large and perfect near the edge of contact of the spectra. Though the sunlight was waning, a few measurements of ranges of displacement were made. They were on the average (e at M and N, y at P):

$$e_M = 0.095 \text{ cm.} \qquad e_N = 0.097 \text{ cm.} \qquad y = 0.062 \text{ cm.}$$

and since $x = 2e \cos \delta/2$ should correspond to $2y$,

$$x_M = 0.145 \text{ cm.} \qquad x_N = 0.148 \text{ cm.} \qquad 2y = 0.124 \text{ cm.}$$

Here, as above, $x > 2y$, or the sliding along the edge of P which accompanies e is distinctly effective, being nearly 16 per cent of $2y$.

Next day, with a bright sun, so that much finer fringes could still be detected, the range could be increased to $e_M = 0.2$ cm. or $x_M = 0.3$ cm. when the spectra were all but separated on their near edges and fringes very large. For the case of much overlapping of spectra, $e_M = 0.15$ cm., $x_M = 0.22$ cm., were obtained. Finally, when the spectra were all but separated on the far edges (implying reflection at some distance from the edge of the prism P), the fringes were glittering, but too small to be distinctly seen.

TABLE 14.—Inverted spectra. Long distances. Plate. $E = 0.434$ cm.; $\mu = 1.533$; $B = 4.6 \times 10^{-11}$; $z = 0.2313 + .0115 = 0.2428$.

Series, etc.	Observed e	Observed e	Observed $2y$	x	x
	cm.	*cm.*	*cm.*	*cm.*	*cm.*
I. Ruled grating. $10^6 D = 352$	0.184	0.186	0.253		
	0.184	0.185	0.253		
Mean.....	0.184	0.185	0.253	0.281	0.283
II. Do., another adjustment..	0.185	0.184	0.246		
	0.185	0.184	0.246		
	0.186		0.248		..
	0.186		0.248		
Mean.....	0.185	0.184	0.247	0.283	0.281
III. Do., another adjustment..			0.244		
			0.244		
IV. Film grating. $10^6 D = 167$.			0.234		
			0.240		
V. Prism 60°.....			0.244		

In table 14 the results for e_M, e_N, and y are given, when these displacements are produced by a glass plate $E = 0.434$ cm. thick. If the coefficient of dispersion B is assumed, the displacement computed from λ, μ, E would be $z = 0.243$ cm. Although the values of $2y$ are larger than this, the difference

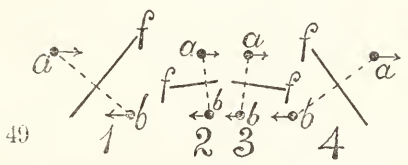
must be ascribed to the assumed value of B and to the difficulty of placing the plate normal to the rays. The method of reversion of fringes, used elsewhere, is not sufficiently sensitive here. The data for x are again in excess of y by about 13 per cent.

Finally, a series of consecutive measurements were made of the ranges of displacement, $2y$, for different dispersive powers at G, figure 43, all under (otherwise) like circumstances. The mean results were for

60° prism.....	$d\theta/d\lambda =$ 760.	$2y = 0.060$ cm.
Ruled grating.....	2,880.	.117
Film grating.....	6,400.	.208

Three or more measurements, completed in each case, were in good agreement. The attempt was also made to use a 45° prism here, but the spectra were too small and the fringes could not be found. In each of these cases the value of $2y$ for the plate $E = 0.434$ cm., as shown in table 14, series III, IV, V, are virtually the same. The rapid increase of range of displacement with the dispersion of the system is thus again encountered.

33. Rotation of fringes.—A word must now be given relative to the rotation of fringes, which is here throughout 180°, whereas in the similar case above (Chapter I, §§ 25, 26) the rotation was but 90°. It will be seen on consulting figure 43 that if M moves micrometrically, normal to itself, the pencil b will slide fore and aft, along the edge of the reflecting prism P'. Thus b may be either in front of or behind b' or coplanar with it in a vertical plane. It will not generally be collinear. This is an essential part of the explanation.



49

In figure 49, let a and b be the two patches of light of like color and origin, which produce interferences. The fringes will therefore be arranged in the direction f, normal to the line ab. Now suppose a is moved toward the right or b toward the left, or both, parallel to the edge of the prism, as the arrows in the figure suggest. Then the fringes will successively take the trends of which cases 1, 2, 3, 4 are typical examples. In other words, they will be markedly accelerated and retarded in passing through the cases 2 and 3 respectively. This is precisely what takes place and suggests why the case between 2 and 3 may be used as a fiducial mark in interferometry. If a and b also move vertically, in figure 49 there will be no essential difference, unless the latter motion is large. In such a case the rotation may become 1, 2, 2, 1.

The displacement of b parallel to itself, for a normal displacement e of the mirror M, will be, as above, figure 17, if $\delta = \theta' - \theta = 90° - \theta$

$$s = 2e \sin \delta/2$$

and the corresponding displacement of c parallel to itself, since $\varphi' = 90°$, $t = s \tan \varphi'/2 = s = 2e \sin \delta/2$.

If $\theta = 9°39'$, $t = s = 2e \times 0.81 = 1.62e$. Thus if $e = 0.25$ cm., $t = 0.4$ cm., and since t is twice the width of the patches or strips sliding over each other, the width of this strip would be 0.2 cm.

It is the sliding of the pencil b along the edge of P' which introduces additional path-differences whenever P' is not symmetrical and its edge not parallel to the plane $a\,a'$. It is probable also that the same restrictions as to the breadth and depth of efficient wave-fronts will apply here as before; but this should be specially investigated. The nearly circular outline of the locus of fringes, when spectra are both reversed and inverted in §36, even though homogeneous light is in question in the last case, clearly points in this direction.

34. Range of displacement varying with orientation of reflector P'.—The displacement e of the mirrors M and N slides the corresponding pencil b or b', figure 43, along the edge of the reflecting prism P', and a reason for the rotation of fringes is thus easily at hand. It does not at once appear why the right or the left displacement (y) of P' should also produce a rotation of fringes; for here the pencils b and b' remain collinear and there is no sliding. It must thus be remembered, however, that the fringes are ultimately elliptic; for the axis parallel to the Fraunhofer lines is conditioned by the obliquity of rays in this plane only, whereas the axis in the direction of the length of spectrum depends on dispersion. The motion y of P' displaces these ellipses bodily through the spectrum. Hence the fringes first appear at any given Fraunhofer line in the form of hair-like striations parallel to it. These enlarge and rotate to a maximum normal to the Fraunhofer line. In fact, a single interference line may now run from end to end of the spectrum. Thereafter the fringes vanish in symmetrically the same manner and are last seen as fine striations parallel to the Fraunhofer line. It is possible, therefore, that the sliding of pencils which accompanies the e displacement accounts for the difference of values of $x = 2e \cos \delta/2$ and $2y$.

Before discussing this question further it seemed necessary to study the effect of different orientations of P' relative to the $b\,b'$ rays. One may note, preliminarily, that a rotation of M and N on a horizontal axis parallel to their faces, or of P' on a horizontal axis parallel to its edge, also rotates the fringes; but it seems probable that these motions are virtually equivalent to a displacement, y, of the edge of the prism.

The fringes may be seen in all focal planes, at least the long line parallel to the length of spectrum. The others may often be restored by rotating the grating. The marked occurrence of fringes in the narrow longitudinal gap between two spectra (overlapping just removed by the rotation of M and N on a horizontal axis) can possibly be explained in this way. These fringes in the dark space are very sharp and luminous and seen in the principal focal plane with the Fraunhofer lines. But it will usually be found that on drawing the ocular out the separated spectra will overlap at their edges again,

whereas on pushing the ocular in from the principal position the separation is increased. Hence, to account for the disturbance in the ether gap, as it were, it seems most reasonable to assume that the rays cross and interference occurs after the rays have passed the principal focal plane (*i.e.*, nearer the eye of the observer), and that the interferences occurring here are projected into the principal focal plane. Nevertheless, the fringes are so strong and sharp that the two clearly focused spectra seem to react on each other across the gap at their edges. I have pointed out similar phenomena in the preceding report (Carnegie Inst. Wash. Pub. 249). The case is just as if a telescope or lens focused on a single or a Young's double slit (with the images sharply delineated) should show fringes.

In adjusting the interferometer, figure 43, for these experiments, the following systematic plan was pursued. By a rough adjustment with sunlight and measurement, all parts of the apparatus are first placed symmetrically to each other (as in figure). The direct beam should just graze the edge of the prism P' and the naked eye, viewing the edge from above, should see the two bright rays of the same color (reflected from M and N) contiguously near the edge. In the spectra of the same length on the two sides of the prism P', the same colors are opposite each other. On looking down on the edge of the prism with a telescope (fine slit), two sharp and clear spectra should be seen, which can be made to overlap at their edges in any amount by rotating M and N on a horizontal axis. Finally, the D lines are brought into coincidence by rotating the grating G on a vertical axis. The largest fringes are obtained by slightly raising and lowering the incident beam L to the grazing position in question. By displacing P on the micrometer, right and left, the fringes are soon found.

The first experiments were made with the object of testing the effect of a slant, to the right or left, of the edge of the prism on the range of displacement y. With a 60° prism at P, the search was found to be too difficult and therefore soon was given up. The few data obtained were: Edge of P' symmetrical—range, $y=0.061$, 0.050, 0.062 cm.; edge of P' toward left—range, $y=0.63$ cm.; showing no certain difference.

P was therefore replaced by a ruled grating ($D=352\times10^{-6}$ cm.) to obtain greater dispersion. The ranges of displacement, y, now found were: edge of P' to left, $y=0.120$, 0.130 cm.; edge of P' symmetrical, $y=0.128$, 0.127 cm.; edge of P' to right—$y=0.110$, 0.113 cm.; readjusted, 0.130, 0.132 cm. These differences are apparently incidental, as much depends on the light. In a darker field fringes vanish sooner. One may assume that slight inclinations of the edge of the reflecting prism P' are without consequence.

The next experiment was to determine the effect of a lack of collinearity of the rays $b\,b'$. This shows itself to the naked eye looking down upon the edge of the prism from above, since by rotating M and N in contrary directions around a vertical axis the bright spots of light move along the edge of the prism from front to rear, or the reverse. If regarded by a telescope, the axis of the instrument will be correspondingly inclined toward the front

or to the rear. The data obtained for the range of displacement were now: Images and telescope toward rear, $y=0.124$, 0.140 cm.; $y=0.150$, 0.142 cm.; images and telescope toward front, $y=0.146$ cm., $y=0.154$ cm.

These differences are again incidental. The following data were subsequently found: Telescope inclined rearward, $y=0.100$, 0.110 cm.; 0.143, 0.140 cm.; telescope vertical, $y=0.150$, 0.150 cm.; 0.162, 0.151 cm.; telescope inclined forward, $y=0.150$, 0.133 cm.; 0.145, 0.162 cm.

In the first experiment the illumination was insufficient, so that the finer fringes escaped detection. Hence, it is here also probable that slight departure from collinearity in the rays $b\,b'$, normal to the edge of the prism P', is without consequence. Discrepancies are introduced by changes in the intensity of light—conditions which are often hard to control.

As the range of displacement is not a quantity which can be accurately ascertained, the effect of the insertion of a glass-plate compensator, 0.434 cm. thick, was determined, with a similar end in view, for different angles of the rays $b\,b'$ (nearly normal) to the edge of the prism P'. The results were: Telescope inclined toward front, $y=0.122$, 0.123 cm.; telescope vertical, $y=0.122$, 0.122, 0.122 cm.; telescope inclined toward the rear, $y=0.120$, 0.121 cm. These are the differences of the displacement corresponding to the linear central fringes normal to the sodium lines, obtained in the presence and absence of the plate. The path-difference computed above was $z=0.2428$ cm. This is as near $2y$ as the observations warrant.

It follows, therefore, even if the observations are in their nature not very precise, that if the rays b and b' meet at such small angles as any reasonable adjustment may introduce, the effect may be disregarded. Furthermore, that the difference between $x=2e\cos\delta/2$ (where e is obtained by moving the mirrors M and N parallel to themselves) and $2y$ (obtained by moving P' at right angles to its edge) is to be ascribed to the sliding along or across the edge. The rotation of fringes which necessarily occurs in displacement interferometry by the shifting of the ellipses is augmented or decreased in the former case (x) by the equivalent of the sliding in question. The reason for this has clearly been suggested in connection with figure 18, Chapter I, and figure 49, Chapter II.

35. Range of displacement varying with dispersion.—The interesting method in Chapter I, § 25, where the opaque mirrors are replaced by two identical gratings (halves of the same grating) with the object of obtaining successive orders of dispersion, may be used in connection with figure 43 of the present chapter. It is therefore the object to find the range of displacement y of the prism P' when the fringes pass from the initial transverse hair-lines to the final transverse hair-lines (fig. 45), through the longitudinal maximum of size. The same difficulty inheres in this method as in the above, viz, it is not possible to state precisely when the hair-lines have vanished; but the successive orders of range of displacement are so different that interpretable results are obtained. The experiments in the large interferometer

proved very trying, however, because the ruled faces of the available gratings at M and N were but 0.5 inch square. There is thus, without refined and special instrumental equipment, considerable difficulty in adjusting the rays to this small surface. This was particularly true in the higher orders of spectra.

To obtain sufficient light the resolving grating G was replaced by a 60° prism. The dispersive powers are thus the same as in § 25, Chapter I. The work proceeded smoothly in the orders of 0 (reflection from grating face) and 1. In the third, the fringes were hard to find and hard to retain, for reasons which I do not understand. There was abundance of light, except in the fourth order, which was abandoned for that reason. The best results were:

Order 0,	$y=0.066$ cm.	$d\theta/d\lambda=$ 760
1,	.230	3,500
2,	.450	6,400
3,	.650	9,900

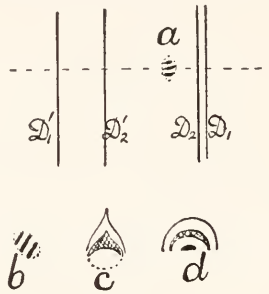
Though much time was spent on this work, the results (excepting the first) are doubtless still too low. Since the path-difference $2y$ corresponds to $x=2e\cos\delta/2$, *cæteris paribus*, and since the data in x, table 12, are essentially half the total range (rotation but 90°, while it is 180° here), y corresponds to x. Thus the results in table 12 are larger throughout, but the present data make a smoother series even through the third order.

36. Spectra both reversed and inverted.—This is an interesting combination of the two methods of investigation and not very difficult to produce. Retaining the adjustment for inverted spectra as in § 30, figure 43, the light impinging on the grating G is dispersed, preferably by a direct-vision grating (with auxiliary prism). The rulings of both gratings (the prism grating g inserted as shown being between the collimator at some distance and the grating of the interferometer G, figure 43) must be parallel. If the grating constants are different ($D=167\times10^{-6}$ cm. film and $D=352\times10^{-6}$ ruled grating were employed), the spectra in the telescope are naturally of different lengths; for the dispersion of the prism grating g is increased on one side and decreased on the other side by the second grating G. Moreover, this decrease from the larger dispersion of the first grating g is beyond zero (achromatism) into negative values. Hence, the corresponding duplicate spectrum in the telescope is a small and a large spectrum reversed, while the inversion remains intact. In the experiment made, the larger $D'_1D'_2$ distance was somewhat more than twice the smaller D_1D_2.

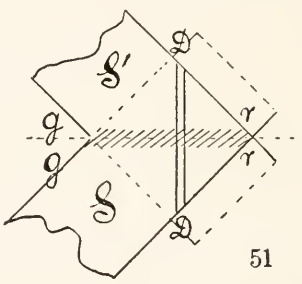
It is now merely necessary to place any longitudinal axis (line of symmetry) of the spectra in contact, or it is but necessary that the spectra are longitudinally parallel and overlap. The phenomenon a, figure 50, then appears at the intersection of the lines of longitudinal and of transverse symmetry. It is thus proportionately nearer the smaller D_1D_2 and farther from the larger $D'_1D'_2$ doublets, but always between them. If the D_1D_2 lie within the $D'_1D'_2$ lines, the fringes lie within the D_1D_2 pair.

The phenomenon, which should be observed with a powerful telescope, usually consists of three small elongated dots, lying within an elliptic locus, the locus usually having a transverse axis (parallel to the Fraunhofer lines) about two or three times as long as the longitudinal axis (parallel to lengths of spectra). As a rule, the width was D_1D_2 and the length larger than $D'_1D'_2$, but this ratio may be changed, as above, by screening off the wave-front. The fringes are not more than one-half of D_1D_2 apart and are frequently horizontal (longitudinal), however the micrometer at M is shifted.

The interesting result is here again met, incidentally, that spectra, though of different lengths, are nevertheless quite capable of producing strong interferences.



50



51

In further experiments with the long collimator and very bright spectra, a variety of other forms were obtained, shown at b, c, d, figure 50. In the patterns a and b, the elliptic outline, sometimes circular, is always evident from the enhanced brightness of the bright fringes of the spot. The arrow-shaped form, c, inclosed a bright egg, whereas d was usually sharply semicircular. As any adjustment of overlapping spectra suffices, the D lines may be quite out of the field, or the spectra may be slightly separated with the interference spot in the gap.

The experiment was also made of crossing the spectra at some other angle than 0° or 180°. To do this the rulings of the prism grating were placed at right angles to those of the interferometer grating, as in Newton's method of crossed prisms. Seen in the telescope (adjusted for inverted spectra, as above, § 30) the two spectra now made an elbow with each other, figure 51, while the D_1D_2 lines are still parallel and can be put in coincidence. At first no interferences could be detected in any adjustment. Later, however, on using the large collimator, strong interferences were obtained in the line of symmetry of the elbow and normal to the D lines, as shown. They have the same characteristics as the preceding and persist during a displacement of M of about 0.3 cm.

37. Experiments with the concave grating.—If in the device figure 40, Chapter I, the prism P is rotated 90° on an axis parallel to $b\,b'$, so that the rays move upward, the phenomenon of inverted spectra may be realized. The fringes are observed with a lens from above or reflected forward. They

were found without much difficulty and showed a range of displacement (y) of the prism P, right or left, in various adjustments, of at least $y=0.71$, 0.61, 0.67 cm. larger, therefore, than with the forward prism, as was inferred. Of course, much depends upon how far the extremely fine fringes at the beginning and end are pursued.

This method is not very convenient for the present purposes. In the first place, the distance $GMPF$ is given, an unnecessary restriction on the adjustment, unless the lens T is replaced by a short-distance telescope, which has other disadvantages. In the second place, the mirrors M and N can not be used for displacement, as they move the Fraunhofer lines of the corresponding spectrum. In fact, M or N affords a method for the adjustment of these lines to coincidence. Finally, the amount of overlapping which is usually secured is always very partial, and if the edge of the prism P is not quite sharp and well silvered, the edges are ragged. Even in the right-and-left displacement (y) of P, the spectra are carried bodily with it in front of T. Although this is no serious objection, it is an unnecessary complication. In spite of the brilliant spectra and large ranges, I did not spend much time in developing the method.

38. Conclusion. General methods.—The origin of the phenomenon of reversed spectra seems to be the slit of the collimator, the diffraction of which furnishes a patch of light, effectively 1 or 2 mm. in breadth, out of which the component rays are to be separated. Spectroscopically the slit furnishes the degree of homogeneous light within which the phenomenon may be developed.

In the case of inverted spectra, the slit is not primarily necessary, for here the interferences occur in the direction of (or the fringes lie normally to) the Fraunhofer lines and therefore virtually in homogeneous light. The fringes are due to the continuous changes of the obliquity of rays in each separate color and thus belong to the phenomenon of a wide slit with homogeneous light. The fringes of reversed spectra owe their occurrence to the continuous change of the obliquity of rays produced by dispersion and require a spectroscopic slit. In the case of combined inversion and reversion, the locus of fringes is not far from circular, though the major axis of the ellipse corresponds to the inversion. Obliquity and dispersion are thus about equally effective.

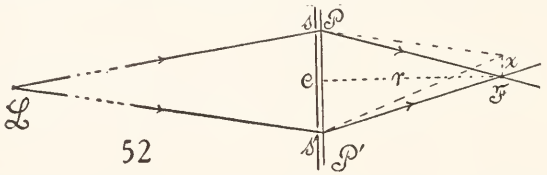
The patch of light rays of identical origin may now be separated into two component rays by a variety of methods. The white pencil may simply be cleaved by the edge of a sharp silvered prism, or the pencil may be refracted into two beams at a blunt-edged prism, or the separation may be produced by the diffraction of a grating, by polarization, etc.

Two entirely distinct pencils are thus obtained, subject to independent control, by which the phenomenon of diffraction may be generalized. In other words, in the classical experiments in diffraction, the diffracting system is rigid. Take, for instance, the following experiment, which has a close bearing on the phenomenon of this paper. In figure 52, L is a distant slit or a fine Nernst filament, P the principal plane of the objective of a telescope

with the principal focus at F, to be observed with the eye-piece. The screen $s\,s'$ with a double slit parallel to the linear source L is placed in front of the objective. Brilliant interferences are then seen at F, which are coarser as the distance e between the slits $s\,s'$ is smaller, and if the distance PF is r and the distance between fringes is x, the usual equation

$$\lambda/e = x/r$$

is applicable. Owing to the direct application of this experiment to the above investigations, its very fundamental importance in the theory of resolution of optical instruments, etc., it seemed worth while to give it experimental treatment here. The screen $s\,s'$ is conveniently made by cutting parallel lines with a sharp triangular cutting stylus and a steel T-square, on a blackened gelatine dry plate. A number of such doublets 0.05 to 0.5 cm. apart may be ruled at a distance of about 0.5 inch apart. When the parts are assembled, the fringes may be seen in all focal planes F, and the fringes are in fact much more brilliant with the ocular out of focus. The enormously large diffraction of each single slit is simultaneously visible, and if two doublets are close enough together, their systems may be seen superposed. If c is small (less than 0.1 cm.) the fringes are in fact visible to the naked eye without a telescope. With two identical doublets close together, the fringes may be seen to be alternately in step and out, as the ocular of the telescope moves outward, until finally the diffractions of the "rod" between the doublets is strikingly manifest. This has also been generalized in the present work.



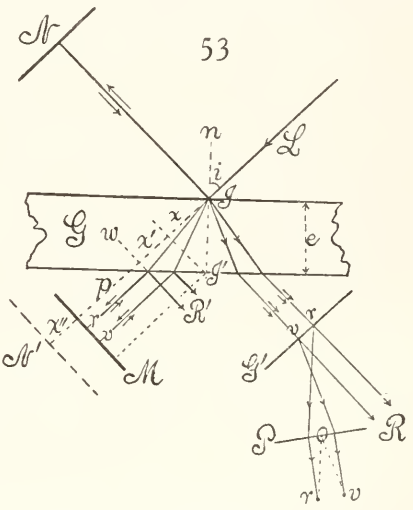
In all these classical cases there is a continuous succession of pairs of corresponding points (one of the pair in each slit of the doublet) between which interferences occur. The line of any two such points is rigidly normal to the direction of the slits. In the above experiments with spectra, however, the two points may not only have any relation to each other, but either point may be moved at pleasure. This gives rise to the bewildering variety of beautiful phenomena, some of them useful, which I have tried to describe in the present and preceding reports.

With the beams of like origin separated, it is next necessary to bring them together again. This requires at least one independently controllable reflection for each beam. In the interesting group of phenomena obtained with crossed rays, two reflections may be desirable, though with a change of apparatus a single reflection here also suffices. Thereafter the beams may be compounded in a manner inverse to the one by which they were produced, for instance, by the reflection of a silvered obtuse prism, by refraction toward the edge of a prism, by a grating, by polarization, etc. To observe the recom-

bined ray, the telescope is always the more convenient instrument, since its use is not restricted to definite distances from the system.

It has been shown that as a whole the above phenomena correspond very closely to the behavior of the ellipses encountered in displacement interferometry. Thus the cases of non-reversed spectra, of inverted spectra, etc., if we disregard certain exceptional accompaniments for the moment, can be at once so classified. The shift of ellipses behind a narrow slit in an opaque screen and observed in front of it, for instance, would exhibit all the rotational occurrences.

39. Displacement interferometry. Equations.—It is thus desirable to adduce the equations of displacement interferometry in a somewhat different way, but in the main as taken from my earlier reports. In figure 53, G is a thick plate of glass on which the blade-shaped pencil of white light L from a collimator impinges at an angle i. M and N are the opaque mirrors of a Michelson device. G' is a plate grating by which the white beam R (feeble spectrum) is resolved, P the principal plane of the objective of the telescope, rv the image seen through the ocular. The plate disperses the white light L into the spectrum rv, as shown in the figure. The direct reflection at R' is not used. For convenience in discussion the mirror N and its component ray may be rotated 180° around the trace of the grating G as an axis, into the position N', where IN becomes $x+x'+p+x''$, intercepted between normals. If perpendiculars be let fall from I to N or N' and I' to M, their difference of length is



$$N=x+x''=e\cos i+x'' \tag{1}$$

N is an important coördinate used throughout, below, since it is independent of color (λ and μ). In (1) i is the angle of incidence, R of refraction of the plate of thickness e and index of refraction μ.

If we draw the wave-front w, the path-length of the red ray through glass to M, for instance, is $e\mu/\cos R+p$. The path of the ray through air (only) to mirror M is

$$x+x'+p+x''=e\cos i+e\sin i\tan R+p+x''$$

If $\sin i=\mu\sin R$ be introduced, the path-difference thus becomes, after reduction,

$$n\lambda=2N-2e\mu\cos R \tag{2}$$

or

$$n\lambda=2e\left(\mu-\cos(i\text{-}R)\right)/\cos R \tag{3}$$

the first equation being more practical. N, therefore, is the differences in distances of the extremities I, I' of the normal n at the point of impact I from the mirrors N and M respectively; x'' is the air-distance apart of the two mirrors (after rotation).

To find the change of wave-length per fringe, $d\lambda/dn$ may be deduced.

$$2\frac{d\lambda}{dn} = \frac{\lambda^2}{N - e(\mu \cos R + \lambda(d\mu/d\lambda)/\cos R)} \tag{4}$$

This equation has a maximum when

$$N = N_c = e\left(\mu \cos R + \frac{\lambda}{\cos R}\frac{d\mu}{d\lambda}\right) \tag{5}$$

and this is the coördinate N_c for centers of ellipses on any given spectrum line λ. $N = N_c$ in equation (2) gives

$$n_c = \frac{2e}{\cos R}\frac{d\mu}{d\lambda} \tag{6}$$

In general $\mu = A + B/\lambda^2$; $\frac{d\mu}{d\lambda} = \frac{-2B}{\lambda^3}$ is adequate for experimental work. Thus if $B = 4.6 \times 10^{-11}$, $e = 1$ cm., $R = 0$, then $n_c = 880$, or 880 sodium wave-lengths are expended in the path-difference at the elliptic center.

If n' fringes pass at a given color λ for a displacement ΔN of the mirror M

$$\lambda = 2\Delta N/n' \tag{7}$$

If n' fringes lie between two given colors λ and λ' for the same position N of the micrometer mirror M

$$n' = 2e\left(\frac{\mu' \cos R'}{\lambda'} - \frac{\mu \cos R}{\lambda}\right) - 2N\left(\frac{1}{\lambda'} - \frac{1}{\lambda}\right) \tag{8}$$

or if δ is the differential symbol

$$n' = 2e\delta\frac{\mu \cos R}{\lambda} - 2N\delta\frac{1}{\lambda}$$

The question next of interest is the change of the angle of altitude of the ray per fringes transversely to the spectrum. Light is homogeneous, N therefore constant. Let α be the angle of altitude of an oblique ray in the horizontal plane L, figure 53, impinging at I. If i' and R' are the corresponding angles of incidence and refraction, then i', i, α make up the sides of a spherical triangle, right-angled at the angle opposite i'. Hence

$$\cos i' = \cos i \cos \alpha, \text{ and } \mu \cos R' = \sqrt{\mu^2 - 1 + \cos^2 i \cos^2 \alpha} \tag{9}$$

With this introduction of R' for R, equation (2) is again applicable, since nothing has been changed in N, e, μ, λ, or i. Hence

$$n\lambda = 2N - 2e\sqrt{\mu^2 - 1 + \cos^2 i \cos^2 \alpha} \tag{10}$$

To determine the change of altitude per fringe,

$$\frac{d\alpha}{dn}=\frac{\lambda\sqrt{\mu^2-1+\cos^2 i\cos^2\alpha}}{e\cos^2 i\sin 2\alpha} \tag{11}$$

and this is a maximum when $\alpha=0$; *i.e.*, in the plane of figure 53. In this case equation (2) is reproduced from (10), so that a double maximum occurs for $\alpha=0$ and

$$N_e=2e\left(\mu\cos R+\frac{\lambda}{\cos R}\frac{d\mu}{d\lambda}\right)$$

The other practical datum is the shift of a given fringe per centimeter of displacement of the mirrors. Here n and e are constant while N, λ, μ, R vary, so that

$$\frac{d\lambda}{dN}=\frac{2}{n+\frac{2e}{\cos R}\frac{d\mu}{d\lambda}} \tag{12}$$

This is a maximum when $n=n_e=-\frac{2e}{\cos R}\frac{d\mu}{d\lambda}=4eB/\lambda^3$, or when $N=N_e$. In other words, there is a minimum displacement relative to wave-length shift of fringe at the centers of ellipses.

Equation (10) is thus inclusive. If $i=0$, which is nearly the case, experimentally, in my work and no restriction on the apparatus, and since α is always very small, equations (10), (11), (12), etc., may be simplified. Hence approximately ($i=0$)

$$n\lambda=2N-2e\sqrt{\mu^2-\alpha^2} \tag{13}$$

$$\frac{d\alpha}{dn}=\frac{\lambda}{2e\alpha}\sqrt{\mu^2-\alpha^2} \tag{14}$$

$$2\frac{d\lambda}{dn}=\frac{\lambda^2}{N-e(\mu+\lambda.d\mu/d\lambda)} \tag{15}$$

$$\frac{d\lambda}{dN}=\frac{2}{n+2e.d\mu/d\lambda} \tag{16}$$

where n is the order of the fringe at λ for N, e, μ, α. Again, $n_e=-2e.d\mu/d\lambda$.

Equation (13) admits of an interpretation in terms of the approximately elliptic locus found for constant n. The equation may be written, if μ is treated as a mean constant,

$$\frac{e^2(\alpha/\mu)^2}{e^2}+\frac{(\lambda-2N/n)^2}{(2e\mu/n)^2}=1$$

Here e (α/μ) and λ may be regarded as the coördinates of a curve described on the face of the plate of glass toward the observer, so that the equation is an ellipse referred to an eccentric axis of ordinates. The axes of this ellipse are $2e\mu/n$ horizontally and e vertically. Of course, the telescope converges all this to a

single white image of the slit; but the grating G reproduces the spectrum and enlarges it, in which case, however, not absolute position but the direction of rays is the determining factor.

40. Continued. Reversed spectra, etc.—The equation underlying the greater number of experiments in the work with reversed spectra is of the form

$$n\lambda = 2e \cos \delta/2 \tag{17}$$

where δ is the double angle of incidence at either opaque mirror and e is the effective distance apart of the two mirrors—*i.e.*, the distance between the faces when one is rotated 180° about the axis of symmetry into parallelism with the other. In the present case, therefore, e corresponds to N in § 39. The angle $\delta = \theta_2 - \theta_1$, where θ_2 and θ_1 are the angles of refraction of the collecting and the dispersing grating, respectively, so that $\sin \theta = \lambda/D$ if D is the grating space. If the silvered right-angled reflecting prism is used for alining the separated pencils, $\delta = 90° - \theta_1$.

From the above equation the change of λ per fringe is

$$\frac{d\lambda}{dn} = -\frac{\lambda^2}{e(2 \cos \delta/2 + \lambda(d\delta/d\lambda) \sin \delta/2)} \tag{18}$$

Since $\lambda d\delta/d\lambda = \lambda/D \cos \theta = \tan \theta$

$$\frac{d\lambda}{dn} = -\frac{\lambda^2}{e(2 \cos \delta/2 + \sin \delta/2(\tan \theta_2 - \tan \theta_1))} \tag{19}$$

This is a maximum if $e = 0$, as the quantity in the parenthesis can not vanish for very acute angles, such as θ and δ must be.

If $\delta = 0$, or $D_1 = D_2$, $d\lambda/dn = -\lambda^2/2e$.

Similarly, since e is now the micrometer variable or coördinate, and n constant,

$$\frac{d\lambda}{de} = \frac{2\lambda}{e(2 + \tan \delta/2(\tan \theta_2 - \tan \theta_1))} \tag{20}$$

from which the similar conclusions may be drawn with regard to the motion of a given fringe. There is a maximum for $e = 0$. The equation, it will be seen, is quite cumbersome, so that further treatment is inexpedient. Nevertheless equation (20), if θ and δ are expressed in terms of λ, should admit of integration, at least approximately.

The equation $n\lambda = 2e \cos (90° - \theta)/2$ for reflecting prisms needs special treatment, since 90° is not derived from θ. The coefficients after reduction become

$$\frac{d\lambda}{dn} = \frac{-\lambda^2 \sqrt{2D(D+\lambda)}}{e(2D+)\lambda} \tag{21}$$

and

$$\frac{d\lambda}{de} = \frac{2\lambda(D+\lambda)}{e(2D+\lambda)} = \frac{2}{C}\frac{(D+\lambda)^{3/2}}{2D+\lambda} \text{ with the aid of (23).} \tag{22}$$

In both cases there is a maximum for $e = 0$.

Equation (22) may be integrated, and if C is an experimental constant,

$$e^2 = C^2 \frac{\lambda^2}{D+\lambda} = e_0^2 \frac{\lambda}{D+\lambda} \text{ if } e = e_0 \text{ for } D = 0 \tag{23}$$

There remains the equation for crossed rays or achromatic conditions,

$$n\lambda = 2e \cos \frac{180^\circ - 2\theta}{2} = 2e\lambda/D$$

or

$$e = nD/2 \tag{24}$$

in which there should be no motion of fringes throughout the spectrum, but for secondary reasons.

It is now possible to consider the above results on the increase of the range of displacement within which interferences are visible, with the dispersion of the grating. In this case the equations in $d\lambda/de$, viz, Nos. 20, 22, as well as 23 and 24, may be consulted. Since $\sin \theta = \lambda/D$, all of them involve the dispersion $1/D$, where D is the grating space. In the case of No. 24 the range of displacement should be indefinite, since the locus of fringes is stationary in the spectrum. It is found to be exceptionally large, but limited by special diffraction. Equation (20) is cumbersome, but otherwise similar to equation (22), which may be treated first. The displacement of any given fringe in wave-length increases with $f = 1/D$, the number of lines per centimeter. If a fringe travels between any two wave-lengths λ and λ' and if D is large relative to λ, equation (23) shows that approximately

$$\Delta e = e - e' = C\sqrt{f}\,(\sqrt{\lambda} - \sqrt{\lambda'})$$

The range of displacement should therefore be roughly proportional to the square root of the dispersion, and one is not at once at liberty to conclude that the uniformity of wave-trains is enhanced by dispersion.

In fact, if D is not large compared with λ, as in the higher orders of dispersion, the full equation must be taken. Unfortunately the data of Chapter I, § 25, table 12, which are the most complete, do not easily admit of computation in full. I have compared them both with $e = e_0\sqrt{\lambda/(D+\lambda)}$, in which the ratios of e observed and computed run up with D, regularly, from 1 to 7; and with $2de/d\lambda = C(2D+\lambda)/(D+\lambda)^{3/2}$, in which the regular change of ratios for the same D (as D decreases) is again from 1 to 7. In other words, the observed values of e varying with D decrease enormously faster than coefficients of this type, as they should. In view of the equation

$$e = e_0\sqrt{\lambda/(D+\lambda)}$$

it follows that

$$\frac{de}{dD} = \frac{-e_0}{2}\sqrt{\frac{\lambda}{(D+\lambda)^3}}$$

and the comparison of the e observed in table 12 with this coefficient is therefore crucial.

To determine D from table 12 we have $D=D'/n=1/(\cos\theta_n\cdot d\theta_n/d\lambda)$, where n is the order of the spectrum and $d\theta_n/d\lambda$ its dispersive power, like θ_n is given in the table. In this way the data of table 15 were obtained.

TABLE 15.—Ratio of the range of displacement e observed in table 13 and de/dD, computed.

Order.	$D\times10^6$	10^3e observed.	$\sqrt{\lambda/(D+\lambda)^3}$	Ratio $e_{obs}/\sqrt{\lambda/(D+\lambda)^3}$
0	1,320	38	151	2.5
1	335	200	980	2.1
2	204	420	1,800	2.3
3	158	520	2,400	2.2
4	142	580	2,690	2.2

In view of the *character* of the results for e, the ratio $e/\sqrt{\lambda/(D+\lambda)^3}$, where e is the observed range of displacement, may be considered constant. The enormous variation of the range e with the dispersive power, as observed, must therefore be regarded as in keeping with the theory of the phenomenon, although the computation is not direct. The latter would require an integration of equation (22) which may be written

$$e=\frac{e_0}{2}\int_0^\infty \frac{2D+\lambda}{\sqrt{\lambda(D+\lambda)^3}}\,d\lambda$$

but the simpler comparison given was regarded adequate.

Data bearing on equation (20) are given in table 11 and may after reduction be written as in table 16 ($\theta_2=19^\circ\,30'$, $D^2=177\times10^{-6}$).

TABLE 16.

Range e observed.	θ_1	$D\times10^6$	δ	$\tan\delta/2\times(\tan\theta_2-\tan\theta_1)$
0.33	2° 36′	1,320	16° 54′	0.0459
.52	9° 39′	352	9° 51′	.0156

The value of the term in the last column is thus small in comparison with 2 and may be neglected, as a first approximation. Hence roughly

$$e=C\lambda=n\lambda/2$$

and the range of displacement should be nearly independent of the dispersion. As it is not, some corresponding principle must here be active, and this has already been found in the shift of one illuminated strip on the collecting grating relative to the other, when either of the opaque mirrors is displaced.

For the same reason the effect produced by making $\delta=0$, as in §24, is not marked, so far as equation (20) is concerned. If $\delta=0$ rigorously, the original experiment with but a single grating did in fact show large ranges of displacement, in view of the absence of sliding.

We thus return to the special diffraction already mentioned in §38. When two spectra from the same source coincide, horizontally and vertically, throughout their extent, they will interfere at every point. The interference

will be visible within a certain range of path-difference. If one spectrum shrinks longitudinally on the other, the strip carrying fringes rapidly diminishes in breadth; but interference is still marked near the transverse line of coincident wave-lengths. If one spectrum is reversed with reference to the other on a transverse axis, the interferences are reduced to a single nearly linear strip coincident with the line of symmetry. The width of this strip is independent of the dispersion of the system. It depends on the breadth of colored region which contributes rays to the strip in question. Hence, if, beginning with both ends of the spectrum, rays are cut off except those very near the line of symmetry, the linear phenomenon rapidly increases in size until all light is extinguished. This is what one would expect from the theory of the diffraction of wave-fronts broad or slender, with the generalization as to the rotation of fringes to which I have already referred.

The association of the two diffractions is well illustrated by the experiments with inverted spectra. Here the edge of the reflecting prism is horizontal and normal to the interfering beams. When this edge is moved normal to itself, path-difference only is introduced. To compensate a plate 0.434 cm. thick the motion should be about 0.243 cm. The displacement found was $2y = 0.247$ cm., the difference being referable to insufficiently accurate dispersive constants. When either of the opaque mirrors moves, the corresponding beam slides along the edge of the prism and the displacement $2e = 0.370$ cm. of mirror was found, corresponding to the path-difference $x = 2e \cos \delta/2 = 0.282$ cm. About 14 per cent *more* path-difference is thus needed with sliding (x) than without ($2y$).

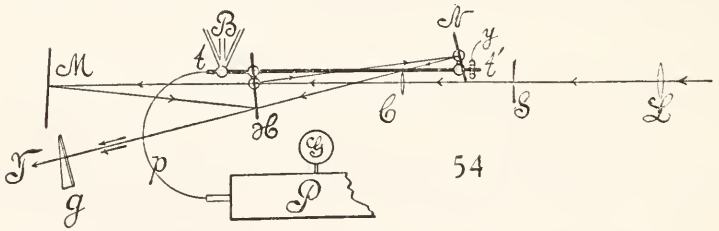
If now the reflecting prism is turned 90°, so that the edge is vertical, the corresponding beams slide normally to or from the edge of the prism when the opaque mirrors are moved. The corresponding data were then found to be $2y = 0.250$ cm., $x = 0.235$ cm. Here about 6 per cent *less* path-difference is needed with sliding (x) than without ($2y$). The smaller effect in the latter case is to be expected, since the two corresponding rays slide toward each other in the same plane and can not pass through each other. In the former case they pass in marked degree across or through each other and must therefore essentially contribute to the rotation of fringes. But the sign of the effect is precisely the opposite to what one would expect. Investigations such as these and the corresponding question of the width of strip carrying interference fringes in case of crossed rays call for apparatus with better optical plate, or for more rigorous instrumental adjustment than I have been able to utilize in the present papers. It is best, therefore, to waive them for the present, however interesting the theoretical results with which they are associated.*

* I have since treated the outstanding difficulties of the text rigorously and the results will be given in a future report.

CHAPTER III.

ELONGATION OF METALLIC TUBES BY PRESSURE AND THE MEASUREMENT OF THE BULK MODULUS BY DISPLACEMENT INTERFEROMETRY.

41. General method and apparatus.—About 25 years ago* I obtained satisfactory results in the measurement of pressures of the order of 1,000 atmospheres by the expansion of steel tubes of suitable thickness. The tube in this case was inclosed in a snugly fitting glass tube filled with water and the volume expansion measured by an attached capillary tube, the system being submerged in water to obviate thermal discrepancies. The whole subject has since been transformed by the famous experiments of Prof. P. W. Bridgman, and I merely touch it here with the purpose of testing the optic apparatus involved and with a view to the experiment explained in the final paragraph of this paper. In the present experiments I shall attempt to measure the increase of length of a steel tube due to internal pressure, by the displacement interferometer. The experiments will lead to an independent method for the measurement of the bulk modulus (Tait) and to a procedure for studying the thermodynamics of the adiabatic expansion of liquids.



54

The interferometer used was of the linear type (fig. 54). Here L is a weak lens, about 2 meters in focal distance and 12 cm. in diameter, concentrating a beam of sunlight on the slit s. c is the objective of the collimator, being a spectacle lens of about 1 meter focal distance. It is particularly advantageous to have rays of slight obliquity here if a brilliant and wide spectrum is to be seen in the telescope at T. H is the half-silvered plate of the interferometer, N and M (on a micrometer) are the opaque mirrors, each about 2 meters from H. The rays reaching the telescope T would therefore show two white slit images from N and from M, which are to be placed in coincidence both horizontally and vertically by the adjustment-screws on M and

* Phil. Mag. (5), xxx, p. 338, 1890; Bull. U. S. Geol. Sur., No. 96, 1892; *cf.* Am. Acad. Arts and Sciences, xxv, p. 93, 1890; for effect of pressure on electrical conductivity of liquids, see Am. Journal, xl, p. 219, 1890, and on the mercury pressure-gage, Am. Journal, p. 96, xlv, 1893.

N. To bring out the interferences, a direct-vision prism grating *g* is placed in front of the objective of *T*, whereupon, when the path-difference *HM*, *HN* is annulled, magnificent ellipses may be seen in the bright spectrum in the field of the telescope.

The steel or other tube whose elongation under pressure is to be measured is shown diagrammatically at *t t'*. The end *t'*, moreover, is closed by a tinned-steel plug-screw, while *t* communicates, by aid of a thick-walled ½-inch tube *p* of small bore, with the screw-compressor *P* described in my earlier papers (*l. c.*). It is here that the thick hydrocarbon oil is forced into the tube *t t'* and the pressure measured by a Bourdon pressure-gage *G*, reading in steps of 10 atmospheres to 1,000 atmospheres.

The parts of the interferometer are attached directly or indirectly to a brick pier in the laboratory. *M* is separately so attached; so is also the end *t* of the steel tube by the bracket at *B*, this being fixed rigidly. The other end, *t'*, which must be free to expand, is to be supported on knife-edges or rollers of a vertical pendulum hanger *y*, the supports of which are in turn rigidly fixed to the pier. This will presently be further described. It was found that long vertical wires, supporting intermediate parts of the tube, were desirable and quite as good as more complicated arrangements.

With the tube *t t'* thus fixed except as to linear expansion toward the right, the mirror *N* is clamped by a horizontal lateral arm at the end *t'*, and the half-silvered plate *H* by a similar arm on the other side, at the end *t*. Thus the length *HN* varies with the pressure and the increment is compensated at *M* by bringing the center of ellipses back to the *D* lines in the field of the telescope. Accessories like water-jackets, etc., are left out of the figure for clearness and will not be used in these experiments.

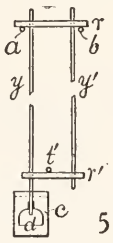
To obviate friction, the end *t'* of the tube *t t'* was suspended from a rectangular yoke or pendulum consisting of two vertical rods *y* and *y'*, figure 55, and horizontal smooth round brass cross-rods *r* and *r'*. The latter roll on the round horizontal rods *a* and *b* suitably anchored at the same level in the pier. The rod *r'* supported the free end *t'* of the pressure tube.

To counteract vibrations the rod *y* carries a bell-shaped damper, *d*, below, submerged in oil in the cup *c*. The middle of the tube *t'* is similarly damped at its center by a bell-shaped damper in oil (not shown), against lateral and vertical vibrations.

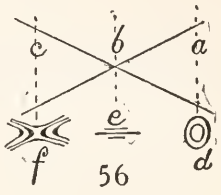
42. Remarks on the displacement interferometer.—As a rule the ellipses are not seen at their best in the principal focus. The ocular must be drawn out somewhat to focus them sharply; but usually the sodium lines are still visible for guidance. No doubt this is due to the fact that ordinary glass plate was employed at *M*, *N*, and *H*, figure 54, or that *H* was not optically plane parallel. Moreover, as *M* is displaced, the focus of fringes changes; but as the centers of ellipses are used in measurement this is no particular disadvantage.

A few trials were made with lens compensators, but the available combinations reduced the ellipses to horizontal sharp spindles or lines, without

passing into the hyperbolic patterns. However, a pair of plates of about the same thickness (0.7 cm.), but respectively of crown and flint glass, when inserted in the M and N beams, gave good hyperbolas.* It was interesting to notice that in the principal focus the fringe pattern was nearly circular or roundish elliptic, but the ellipses were not strong. On drawing the ocular out, these ellipses underwent continuous deformation, passing through horizontal bands finally into sharp and strong hyperbolic forms. The fringes obtained with the differently dispersing plates must therefore be referred to space loci in which, on passing along the axis, an elliptic cone becomes linear at the apex and symmetrically hyperbolic beyond. Thus in figure 56 the sections of the cone at a, b, c show fringes of the form d, e, f.



55



56

43. Observations. Thick steel tube.—The seamless steel tube in my possession had the following dimensions: Length between mirrors, 160.8 cm.; diameter inside, 0.515 cm.; diameter outside, 1.278 cm. Hence the inside cross-section is 0.208 square cm. and the cross-section of steel 1.075 sq. cm. Such a tube is therefore rather adapted for measuring very high pressures, whereas the following work will not go beyond 1,000 atmospheres; but it was admitted for trial. If the case is treated as simple traction with Young's modulus taken as 2.14×10^{12}, the elongation should be about 14×10^{-6} cm. per atmosphere, equivalent to a little less than half an interference ring. But this is obviously too large, as the tube expands in all directions by internal pressure. The case has been treated by Tait and will presently be referred to.

The experiments made proceeded with unexpected smoothness from the outset, barring the tremors of the laboratory, which made it difficult to set the ellipses. Comparing the steel gage with a standard Bourdon gage reading in steps of 10 atmospheres to 1,000 atmospheres, the first six series of experiments showed an elongation ΔL of tube per atmosphere of

$$10^6\Delta L = 7.5,\quad 8.0,\quad 7.0,\quad 8.0,\quad 7.0,\quad 7.5 \text{ cm.}$$

In the last series the individual results were:

Pressure.....	100	200	300	400	500		500	400	300	200	100 atmosph.
Micrometer at	93	87	79	71	65		65	73	81	89	96 cm./10^4
	$10^6\Delta L = 7.4\times10^{-6}$ cm.						$10^6\Delta L = 7.7\times10^{-6}$ cm.				

The data for decreasing pressures do not return into the preceding values for increasing pressures for incidental reasons which need not be discussed, but the mean rates are not very different. The discrepancies are probably in the setting of the Bourdon gage. They are not due to temperature here,

* Later experiments showed that the flint plate was slightly curved.

even though the tube was not jacketed with water. The data, as was to be expected, show an expansion less than was computed for the case of traction, being only about half as large, or equivalent to about a quarter of an interference ring per atmosphere. An arc lamp was used as a source of light and its flickering was very annoying.

Tait* in the *Challenger* reports justifies the expression

$$\frac{d\xi}{dx} = \Pi \frac{a_0^2}{a_1^2 - a_0^2} \quad \frac{1}{3k}$$

where $d\xi/dx$ is the elongation due to the internal pressure Π, in case of a tube of sectional diameters a_0 and a_1 and bulk modulus k. This merely replaces Young's modulus by the linear equivalent of the bulk modulus. Hence for the tube of length $x = 160.8$ cm. and $a_0 = 0.515$ cm., $a_1 = 1.278$ cm., if for tool steel $k = 1.84 \times 10^6$ and pressure is given in atmospheres (10^6 dynes/cm.^{2}) the elongation per atmosphere is

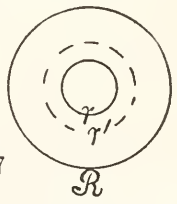
$$\frac{160.8 \times 0.265}{1.368 \times 5.52 \times 10^6} = 5.65 \times 10^{-6} \text{ cm.}$$

This is smaller than the value found, probably because the tube is made of mild steel. If k be computed for the tube, since the elongation per atmosphere is 7.5×10^{-6}

$$k = \frac{160.8 \times 0.265}{1.368 \times 3 \times 7.5 \times 10^{-6}} = 13.9 \times 10^6$$

which is about the order of value given by Everett† for wrought iron. Voigt gives 1.46×10^6 for steel (see Landolt and Boernstein's Tables, 1905, p. 45).

44. Further experiments.—The washer of the screw of the compressor, in the default of marine glue, was a perforated disk of pitch. This proved to be quite inadmissible for further work. The behavior of pitch was very peculiar and in itself interesting. The perforated disk was found to adhere without slip to the screw at the inner edge r, figure 57, and to the wall of the stuffing-box at its outer edge R. On turning the screw a smaller coaxial disk r' of pitch broke out of the larger disk, and the turning proceeded on this surface, r', without leakage. It was found nearly impossible to force the screw with the adhering pitch into the socket without serious injury to the screw. The sharp edges of the threads were in fact planed off flat and it was only by leaving fore-and-aft room for play in the stuffing-box that the compressor could be used at all. The part of the screw turning in pitch was ruined.



57

* Tait: Challenger Reports, II, 1882, App. A, p. 26.

† See Everett tables, 1879, p. 53, containing original experiments of the author.

The pitch washer was therefore removed and replaced by one of *tallow* slightly hardened with a little resin or wax, the two being melted together. This functioned perfectly within 1,000 atmospheres and was easily inserted in parts which could then be molded into a disk within the stuffing-box on forcing the gland into it.

The measurements given in table 17 were made in steps of 100 atmospheres. ΔL denotes the elongation per atmosphere.

TABLE 17.

Series.	Pressure range.	$10^6\Delta L$ (pressure increasing).	$10^6\Delta L$ (pressure decreasing).
7	100 to 500 atm.	8.3 cm.	6.5 cm.
8	100 600	9.2	6.1
9	100 700	7.9	6.2
10	100 800	7.9	7.1

An example of the individual results may be given in case of series 9:

Pressure 100 200 300 400 500 600 700 700 600 500 400 300 200 100 atm.
Micrometer reading 1.01 9.4 8.6 7.9 7.0 6.2 5.5 5.4 6.3 7.0 7.7 8.5 9.1 9.8 cm./10^3

The elongation here is always greater when pressures increase, although time is allowed for dissipation of temperature, than when they decrease. Four reasons may be assigned for this result: (1) the temperature increase on increasing pressure and *vice versa;* (2) permanent set imparted to the tube; (3) elastic warping of the tube owing to the end-thrust of internal pressures and consequent disadjustment of the interferometer; (4) viscosity of steel. Probably all of these discrepancies are present. That there was set I infer from the gradual displacement of the reading of the interferometer for 100 atmospheres at the beginning and end of a series, though this may be due to new adjustments. The incidental displacements are particularly shown in the values of ΔL when pressure increases and are specially marked in series 7 and 8. They are also apparent in the change of form of the ellipses. As sunlight was used in the above work the annoyances of a flickering arc do not occur. The ellipses were not centered.

To obtain some notion of the relation of these discrepancies we may proceed as follows: The difference between the elongation per atmosphere during the phases of increasing and decreasing pressures in the four series given is, respectively, 1.8, 3.1, 1.7, 0.8 cm./10^6, or 1.8×10^{-6} cm. per atmosphere of compression. For a tube-length of 160.8 cm. and a coefficient of expansion 12×10^{-6} this is equivalent to a rise of temperature 9.3×10^{-4}, or, roughly, 10^{-3}° C. per atmosphere of compression.

Supposing the compressibility of the oil to be $dv=100\times10^{-6}$ per atmosphere per cubic centimeter and the mean pressure $p=500$ atmospheres, the work done is pdv or

$500\times10^6\times100\times10^{-6}=5\times10^4$ ergs per atmosphere per cubic centimeter at 500 atmospheres

Since the preceding datum corresponds to both increasing and decreasing pressures, the work done must be reckoned per 2 atmospheres or it will be 10^5 ergs. Taking the specific heat of oil as 0.5 and the mechanical equivalent as 42×10^6, the rise of temperature of the oil should be

$$\frac{10^5}{0.5 \times 42 \times 10^6} = 5 \times 10^{-3}\ ^\circ \text{C., nearly}$$

Hence the residual temperature discrepancy found, 0.001 C., would be but one-fifth of the full temperature discrepancy to be anticipated—*i.e.*, four-fifths of the heat would have dissipated by conduction, etc., during the waiting between successive compressions.

The residual temperature is thus adequate to account for the full discrepancy, and if a tube of this kind is to be used as a pressure-gage, the tube should be made of "invar" or other metal without thermal expansion. True, a water-jacket surrounding the tube would improve the apparatus, but the thermal increments in question are so small that the device would not be trustworthy. If, however, a temperature discrepancy is shown by the optic gage it should also be shown by the more sensitive Bourdon gage, which is not the case. Thus a residual effect of temperature is improbable. The optical difficulties are slight and could be overcome by suspending the yoke, which in figure 55 rolls loosely on the cylinder *a*, *b*, *t'*, from steel pivots bearing on jeweled cups. Elastic and particularly slow viscous yieldings to persistent pressure are thus the probable reason for the errors. This also accounts for the displacement of the fiducial reading.

Two further experiments were now made in which the ellipses were *centered* before each observation (table 18). In the second set (series 12) the tube was attached to the yoke and the latter to the hangers by soft adhesive wax, applied in the molten state. This proved quite adequate.

TABLE 18.

Series.	Range.	$10^6 \triangle L$ (pressure increasing).	$10^6 \triangle L$ (pressure decreasing).
11	100 to 600 atm.	7.2	7.2
12	100 600	7.7	7.7

The zeros were regained and the results were marked improvement on the preceding series. The same mean elongation is found for increasing and decreasing pressure; but the values are not identical in the two series. The following data give the details of series 11:

Pressure.....	100	200	300	400	500	600	500	400	300	200	100 atm.
Micrometer reading	50	43	34	28	20	15	21	28	36	43	50 cm./10^4

A few units in the cm./10^4 place are thus uncertain. The graph is shown in figure 58.

45. Brass tube.—A somewhat thinner seamless tube of soft brass was next tested within 600 atmospheres. The dimensions were: length, 161 cm.; diameter within, 0.485 cm.; diameter outside, 0.960 cm. Hence

$$k = \frac{161 \times 0.235}{(0.9216 - 0.2352)3\Delta L} = \frac{18.36}{\Delta L}$$

The ellipses were centered throughout and the yoke was given additional stability by soft adhesive wax, as above. The tube showed extraordinary variability, but during the trials under increasing and decreasing pressure and in the lapse of time the viscous changes somewhat subsided, as will be seen from table 19.

TABLE 19.

Series.	Range of pressures.	$10^6\Delta L$ (pressure increasing).	$10^6\Delta L$ (pressure decreasing).
1	100 to 500 atm.		15.6 cm.
2	100 500	13.6 cm.	16.5
3	100 500	13.5	17.0
4	100 600	13.7	16.7
Mean..		13.6	16.7

Disregarding the first series, which was preliminary, the remaining data are consistent. Hence k from the mean $10^6\Delta L = 15.2$ is relative to atmospheres

$$k = 10^6 \frac{18.36}{15.2} = 1.21 \times 10^6$$

Voigt's value for brass is but 0.61×10^6, *i.e.*, but half this. Throughout these experiments the reading for 100 atmospheres wandered continually, creeping over 7×10^{-3} cm. during the time interval of the experiments. The following individual data show this for the fourth series:

Pressure.....	100	200	300	400	500	600	600	500	400	300	200	100 atm.
Micrometer reading	320	301	290	274	263	250	252	270	290	305	321	336 cm./10^4

One would naturally refer this to the viscosity of the brass tube, but, curiously enough, the march is a contraction. Apparently the tube continually contracts in the lapse of time under internal pressure. The contraction occurs, however, for the case of a tube which was not rigorously straight.

Optically, apart from the tremor of the laboratory, one would have no fault to find with the measurements, allowing a micrometer accuracy of a few 10^{-4} cm. Interference rings could easily have been utilized, but this would have required two observers.

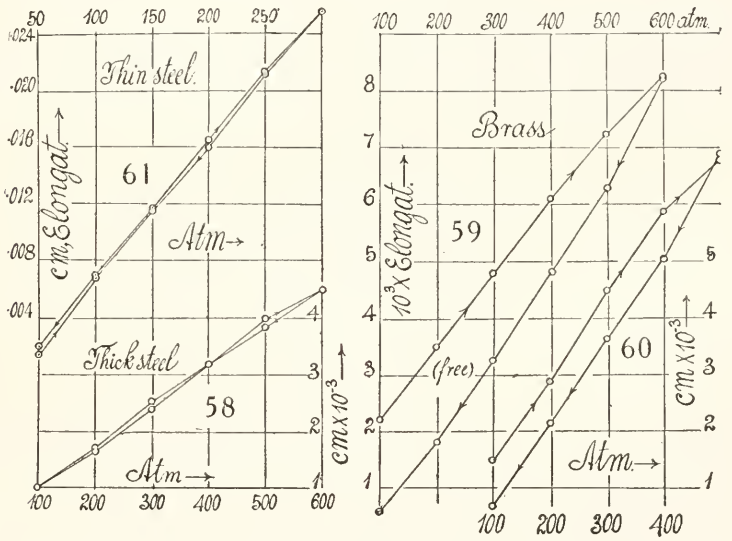
Two more series of experiments were made with the brass tube (table 20), in one (5) of which it was supported only at the ends with its original curva-

ture convex upward; in the sixth series the tube was additionally supported in the middle on a large pendulum-like wire or hanger.

TABLE 20.

Series.	Range of pressure.	$10^6\Delta L$ (pressure increasing).	$10^6\Delta L$ (pressure decreasing).
5 (free).....	100 to 600 atm.	12.3 cm.	15.2 cm.
6 (supported)...	100 500	13.6	15.2

The individual results are shown in figures 59 and 60. It will be noticed that an error was introduced when pressures passed from the increasing to the decreasing phase at the highest pressure, and this was particularly the case when a slight leak developed. If the highest pressure is omitted, $10^6\Delta L = 14.7$, both for increasing and decreasing pressures in the case of the suspended tube. Hence $k = 1.250 \times 10^6$, not differing essentially from the above. The unsupported tube is highly subject to viscosity.



The large effect resulting from viscosity is also shown in the initial and final readings (100 atmospheres) in figures 59 and 60. It is in both cases again an apparent contraction and is present even in the supported tube. The viscous effect in the lapse of time is directly given in the following independent measurements of apparent contraction. The tube was kept charged with an internal pressure of 100 atmospheres.

Time.....	$9^h\ 30^m$	$10^h\ 5^m$	$12^h\ 12^m$
Length, L.....	0.0173	0.0183	0.0206 cm.

It is difficult to understand, however, how anything of the nature of viscous longitudinal contraction can occur under internal pressure. One might

suppose that the cylindrical tube as a whole is gradually progressing toward an ultimate spherical form, but this seems far-fetched. It is more reasonable to suppose that the viscosity is simply flexural. The tube is curved slightly convex upward and therefore the end mirrors N and H, figure 54, rotate continually towards each other on a horizontal axis, under the end-thrusts of the internal pressure. The component beams and HNH and HMH are thereby each modified in length. Though it is difficult to specify why the former should be shortened relative to the latter, such a result is easily conceived.

46. Thin steel tube.—The steel tube in §§43 and 44 was adapted for high pressures only, showing but 0.2 interference ring per atmosphere. In contrast with this a thin steel tube was now inserted, adapted for lower pressures. This was more sensitive than the Bourdon gage, the other tube being on the whole less so. The dimensions were: length, $L=161$ cm.; diameter inside, $a_0=0.799$ cm.; diameter outside, $a_1=0.951$ cm. The outside diameter was calipered. A short length was then cut off and slit open and the wall thickness similarly found (0.076 cm.). The tube was not quite straight. Snugly fitting brass plugs were carefully soldered into the ends, and these were then tapped to receive the tubes conveying pressure.

The observations shown in table 21 were recorded, the steps of pressure being 50 atmospheres in the first two and 100 atmospheres in the last two series.

TABLE 21.

Series.	Pressure range.	$10^6\triangle L$ (pressure increasing).	$10^6\triangle L$ (pressure decreasing).
1	50 to 200 atm.	89 cm.	100.1 cm.
2	50 300	95.3	95.5
3	100 400	97.3	100.0
4	100 400	95.2	100.7

At 400 atmospheres the tube developed a slight leak at the ends. At 750 atmospheres one of the soldered end-plugs was blown out. It is remarkable that the plugs held so well.

An example of the individual data may be given for the second series. In figure 61 these data are shown, positively.

Pressure.....	50	100	150	200	250	300	300	250	200	150	100	50	atm.
Micrometer reading	260	210	164	115	67	23	24	67	120	163	212	266	cm./10^4

Very little viscosity is, therefore, in evidence, but there is some displacement or irregularity, probably in the reading of the Bourdon gage.

Pressure increments and decrements slightly rotated the mirrors in opposite directions around both a vertical and a horizontal axis. These were compensated by adjustment at the mirror M before each reading. As the mirrors inclined towards each other for pressure increments the tube must have been slightly convex upward, and therefore successively straightened as pressures

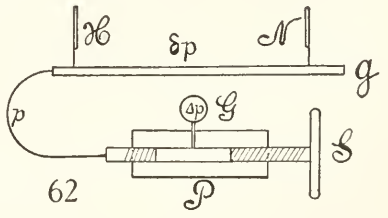
increased. The mean elongation per atmosphere is $10^6\Delta L = 97$ cm. and the bulk modulus may be computed as

$$k = \frac{a_0^2}{a_1^2 - a_0^2}\,\frac{L}{3\Delta L} = \frac{0.6384 \times 161}{(0.9044 - 0.6384) \times 3 \times 97 \times 10^{-6}} = 10^6 \times 1.33$$

In spite of the large difference of dimensions, this datum is of the same order of value as the above ($k = 1.39 \times 10^6$) for the thick tube, particularly as the present ΔL, from the occurrence of flexure, is probably slightly large.

A tube of this kind with well-sealed ends (brazed probably), quite straight, and supported at different points of its length by wire pendula, should make a good pressure-gage within at least 1,000 atmospheres. An individual reading about 10^{-4} cm. per atmosphere or over 3 interference rings would be uniformly available throughout.

47. Conclusion. Thermodynamic application.—The data given show that an independent method of measuring the bulk modulus of metals is quite within the province of the displacement interferometer. The annoyances encountered, resulting from the viscosity of the metal or from warping, may be considered eliminated in the mean of the pressure-increasing and pressure-decreasing phase of the experiment. The tubes should be supported at various points along their length. Even the temperature discrepancy, if sufficient time is allowed between the successive steps of pressure, seems not to be of serious effect on the mean data.



For the measurement of pressure, however, the device is promising. In such a case the tube section should be chosen to correspond with the pressures to be measured. Within 1,000 atmospheres a steel tube about 1 cm. in diameter, with walls about 0.75 mm. thick, gave fair results, showing the evanescence of about 3 interference rings per atmosphere. Such a tube must be rigorously straight, well supported, and if possible of non-expanding (temperature) steel.

It is interesting to consider the case of the adiabatic expansion of liquids in relation to such a gage. The available thermodynamic equation is

$$\Delta\theta = \frac{\alpha\theta}{J\rho C_p}\Delta p$$

where $\Delta\theta$ is the temperature increment corresponding to the adiabatic compression Δp at the temperature θ, in case of a liquid whose coefficient of expansion is α, density ρ, and specific heat C_p., J is the mechanical equivalent of heat. In an apparatus like figure 62, in which P is the screw compressor (with tinned or waxed screw S) filled with the liquid in question, G the Bourdon gage, pressures may be suddenly applied without leakage by turning the

screw S. These are also measurable at the interferometer gage g, H being the half-silvered and N an opaque mirror, as in figure 54. The subsidence of pressure due to cooling adiabatic compression is, however, also measurable at g in terms of the delaying pressure. For we should have (v denoting volume, k the bulk modulus)

$$\frac{\Delta v}{v} = \alpha \Delta\theta; \quad -\frac{\Delta v}{v} = \frac{\delta p}{k}$$

or, apart from signs, $\Delta\theta = \frac{\delta p}{k\alpha}$, where δp is the subsidence of pressure due to the cooling $\Delta\theta$, after adiabatic compression. Hence the original equation takes the form

$$C_p = \frac{k\alpha^2\theta}{J\rho} \quad \frac{\Delta p}{\delta p}$$

an equation for measuring the specific heat of constant pressure of the liquid at temperature θ and pressure $\frac{2p+\Delta p}{2}$. The observations thus consist in measuring Δp (in displacement) and δp in interference rings, both at the gage g.

One may estimate the value of δp per atmosphere of Δp, for alcohol, by way of illustration. Here in c.g.s. units,

$$k = 1.21 \times 10^{10}; \ \alpha = 1.1 \times 10^{-3}; \ \theta = 20^\circ; \ \rho = 0.79; \ C_p = 0.58$$

Hence

$$\delta p = \frac{1.21 \times 10^{10} \times (1.1 \times 10^{-3})^2 \times 20 \times 10^6}{42 \times 10^6 \times 0.79 \times 0.58} = 1.52 \times 10^4 \ \frac{\text{dynes}}{\text{cm.}^2}$$

or

$$\delta p = 0.015 \text{ atm. per atm. of } \Delta p$$

Hence, if $\delta p = 200$ atmospheres, the above gage would show about 10 rings for δp. Similarly a pressure dropping adiabatically from 1,000 atmospheres would show about 50 rings, residually, after closing.

The present research was planned to be pursued at much greater length; but owing to the annoyances of a quivering pier, which are particularly marked during the term weeks, and to the injury of the screw before the tallow washer was inserted, it was thought wise to discontinue it at present. If the micrometer is to be set to 10^{-4} cm., the ellipses must be reasonably quiet, and in case of long-distance interferometry such a condition can be realized only during the summer months.

CHAPTER IV.

REFRACTIVITY DETERMINED IRRESPECTIVE OF FORM BY DISPLACEMENT INTERFEROMETRY.

48. Introductory.—Some time ago* I made a number of experiments on the use of curvilinear compensators in connection with the displacement interferometer. It is obvious that the curvature in such a case must be very small, so that single lenses for the purpose are not easily obtained. The use of a doublet of two lenses of the same glass, but respectively convex and concave, meets the case fairly well, the necessary refracting power being received by spacing the doublet. Lenses of about 1 diopter each gave the best results, bringing out fringes of quasi-elliptic and hyperbolic symmetry in great variety.

Later it appeared as if plates of different varieties of glass, as for instance crown and flint, if placed in the two component beams *MH*, *NH*, figure 54, would produce the same phenomena. The flint plate used, however, proved to be inadequately plane, so that the result is in doubt.

More recently I have endeavored to secure similar results by submerging the lens (convex or concave) in a liquid of about the same index of refraction. This method would seem to be interesting in other respects, for it is probable that the index of the solid may be determined in this way irrespective of form.† If, for instance, the liquid and the solid have the same index, one would be tempted to infer that the latter may be removed or inserted without displacing the center of ellipses at the particular wave-length under consideration. The index of the liquid in place is then determinable by the interferometer to a few units in the fourth place.

If experiments of the present kind are to be accurate, it is obvious that the walls and cavity of the trough in which the lenses are to be submerged must be *optically* plane parallel; otherwise some compensating adjustment must be made at the opaque mirrors of the interferometer, and for this no adequate allowance is at hand. It did not, however, seem worth while to provide expensive apparatus before the method had been worked out in detail. Accordingly the present experiments were conducted with troughs of ordinary plate-glass put together by myself, and little attention will be given to absolute values of index of refraction, as such.

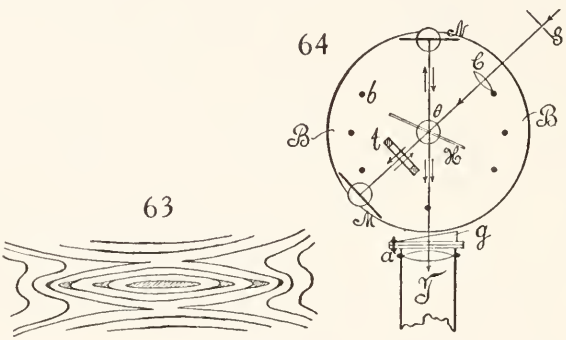
49. Preliminary experiments.—The first experiments were made on a large linear interferometer (see fig. 54) with distances of nearly 2 meters between

* Carnegie Inst. Wash. Pub. No. 249, 1916, chapter IX; *cf.* Amer. Journ. Science, XL, pp. 299–308, 1915.

† Mr. R. W. Cheshire (Phil. Mag., XXXII, 1916, pp. 409–420) has recently used Töpler's method for the same purpose with marked success.

the mirrors. The rays in such a case are all very nearly parallel. Sunlight, arc light, and the Nernst filament were each available for illumination. If the latter is used, the adjustment must be made by aid of the two white slit images, which are to coincide horizontally and vertically. Otherwise the sodium lines are available. With a very long collimator (2 meters) and a wide single-lens objective (10 cm. or more), the Nernst filament may be used directly in place of the slit. If the beam passing the objective is not wider than 1 cm. (opaque slotted screen), very perfect ellipses may be obtained.

On inserting the trough with a thickness of 1.3 cm. of CS_2 solution normally into the *MH* beam, the original very large ellipses were reduced in size and rounded as usual to smaller circles. Submerging a convex lens (1 diopter) into the liquid until the beam passed symmetrically through it changed these circles to very long horizontal spindles. A concave lens similarly produced horizontally very eccentric hyperbolæ. With water in the trough, only the convex lens showed observable fringes, these being very long, practically linear horizontal spindles. All these fringes lie considerably in front of the principal focal plane of the telescope (fig. 54, *T*), and the abnormal forms are necessarily relatively faint. They change in shape and intensity with the focal plane observed.



On mixing CS_2 with kerosene (about equal parts), types of fringes shown in figure 63, but with many more lines, were obtained. This is a combination of both spindles and hyperbolæ. Probably three layers of liquid are chiefly in question, viz, kerosene, kerosene + CS_2, CS_2, and the three stages of form and the sinuous lines correspond to them. Fringes were sharp only if viewed in front of the principal focal plane of the telescope. By submerging convex or concave lenses, the hyperbolic parts or the spindles of the fringes could often be removed. Similar results were obtained with mixture of CS_2 and sweet oil, though this solution is more homogeneous.

50. Apparatus.—To obviate the tremor of apparatus which is inevitable in the case of the long-distance interferometer, the parts were now screwed down at short distances in the cast-iron block *B*, figure 64. Here the ranges *MH*, *HN* of half-silvered plate *H*, and opaque mirrors *M*, *N*, did not exceed

14 cm., but this gives ample room for the manipulation of the trough t placed normally in the beam MH. White light enters by way of the collimator SC at any convenient angle θ (as this does not enter into the equations), and $\theta = 60°$ was used. The opaque mirrors M (and preferably also N) are on micrometers with screws normal to their faces, and each must be provided with adjusting-screws relatively to horizontal and vertical axes. An elastic fine adjustment is desirable. The block contains a number of screw-sockets, b, for attaching subsidiary apparatus. The trough t should preferably be attached to an independent supporting arm, not connected with B, and be revolvable about two axes normal to each other. In such a case the position *normal* to the beam of light may be found from the reverse of motion of the interference rings, while the trough is slowly rotated in a given sense.

The telescope T (relatively much enlarged in the diagram) is not attached to the block. It is to be used both as a simple telescope for the adjustment of the white slit images to horizontal and vertical coincidence, and as a direct-vision spectroscope. The most convenient attachment for this purpose is the direct-vision prism grating G (film grating) just in front of the objective of T. Two perforated thin disks of brass are useful for this purpose, one disk being firmly attached (like the cap) to the objective, the other to the flat face of the grating with the prism outward. A swivel bolt a, between the disks, thus allows the observer to throw out the grating and use the telescope. A stop arrests the motion of the grating when it is rotated about a, back again, for viewing the spectrum. This plan worked very well, and the ellipses obtained were magnificent. It was almost possible to control the micrometer M manually, and all hurtful quiver is absent. The fiducial line to which centers of ellipses, etc., are to be returned is always the sodium doublet present in sunlight and the arc and artificially supplied by an interposed burner in case of the Nernst lamp. The telescopic lens need not be more than 2 cm. wide, and cross-hairs are not needed. For measuring dispersion the Fraunhofer lines B, C, D, E, b, F were used.

51. Equations.—The useful equations for present purposes are given in a preceding report,* and the following cases only need be repeated here. If e is the thickness of glass plate of index of refraction μ for the wave-length λ, and if the equation $\mu = A + B/\lambda^2$, where A and B are constants, be taken as sufficient,

$$(1) \qquad \mu - 1 = \Delta N/e - 2B/\lambda^2$$

where ΔN is the displacement of the micrometer at the opaque mirror M or N due to the insertion of the plate normally to the component beam in question. To determine μ, B must be known at least approximately. It may be measured in the same adjustment, however, if two Fraunhofer lines are used fiducially. Let δN be the displacement of micrometer to pass the center of

* Carnegie Inst. Wash. Pub. No. 229, 1915, §§ 40, 41, 42.

ellipses from wave-lengths λ to λ'. Then if e' is the thickness of the half-silvered plate H, and R the angle of refraction within it,

$$\delta N = B\left(e + e'\cos R + 2\left(e + \frac{e'}{\cos R}\right)\right)\left(\frac{1}{\lambda^2} - \frac{1}{\lambda'^2}\right) \tag{2}$$

If $e = 0$,

$$\delta N_a = B\left(e'\cos R + \frac{2e'}{\cos R}\right)\left(\frac{1}{\lambda^2} - \frac{1}{\lambda'^2}\right) \tag{3}$$

which may be called the corresponding air displacement. Hence

$$B = \frac{\delta N - \delta N_a}{3e\left(\frac{1}{\lambda^2} - \frac{1}{\lambda'^2}\right)} \tag{4}$$

Here $$\delta N = \delta N_a = N - N' - (N_a - N'_a) = N - N_a - (N' - N'_a)$$

so that the difference of the corresponding positions of micrometer for a given Fraunhofer line, with and without the plate, are to be found. The method is quite accurate, as will be seen below. More than two constants A and B may be taken, if desirable.

To return to equation (1), remembering that $2B/\lambda^2$ is small, it is seen that the percentage accuracy of $\mu - 1$ and ΔN are about equal. Now ΔN, for a plate 5 to 6 mm. thick and ordinary glass, is about 0.3 cm. This may be measured within 10^{-4} cm. or 3 parts in 10^4 of ΔN or one or two units in the fourth place of μ, the index of refraction of the glass. A much more serious consideration is the consistent measurement of the thickness of plate e, which must be given to 10^{-4} cm. if the same accuracy is wanted. Naturally this presupposes optic plate. Hence the data below will be inaccurate as to absolute values from this cause. The plates used frequently showed increases of thickness of several 10^{-3} cm. within a decimeter of length. Absolute values are, however, without interest in this paper.

To show that less than 10^{-4} cm. is guaranteed on the micrometer in the placing of elliptic centers at the sodium line, the pairs of results given in table 22, made at different times and with entirely independent adjustments, may be cited. The screw-pitch was 0.025 cm. and the drum divided into 50 parts with a vernier to 0.1 part.

TABLE 22.

Fraunhofer line.	Pitch, drum.	Pitch, drum.	Difference.
B	x 85 17.1	74 33.2	0.25000+0.01695 cm.
C	85 23.3	74 39.3	+ .01700
D	85 41.0	75 7.0	+ .01700
E	xx 86 14.9	75 30.9	+ .01700
b	86 19.2	75 35.2	+ .01703
F	*f* 86 36.6	76 2.6	+ .01703

x Ellipses long horizontally. xx Circles. *f* Ellipses long vertically.

The total difference is less than 10^{-4} cm. and probably due to the width of the Fraunhofer lines with deficiency of light at the ends of the spectrum.

Apart from measurement of the thickness e, therefore, the method is guaranteed for fourth-place work.

52. Observations.—At short distances the ellipses are always rounder and present in all focal planes of the telescope. Doublet lens compensators of relatively large focal power are available. Using the CS_2-sweet oil solution, the submergence of convex and concave lenses in it made but very little difference in the position and definition of the ellipses. There must, therefore, have been approximate equality of the conditions of refraction. With glass in water this was naturally not the case.

A number of experiments were made with the well-known mercury-potassic iodide solution as obtained from Eimer & Amend. The index of refraction in the concentrated state (floating glass) exceeds 1.7. The slight straw-color is no disadvantage.

A plane-parallel trough of ordinary plate-glass, 0.293 cm. internal width, was now constructed, only just large enough to receive a glass plate or a convex lens. With the plate or lens submerged centrally, therefore, the excess of path-difference over the empty trough would be nearly constant. The liquid was then gradually diluted until the excess of path-difference of the liquid over the glass content passed through zero into a deficiency. Considerable stirring was needed to insure homogeneity on each dilution. The results are given in table 23 for the plate and in table 24 for the lens. So long as the diluted solution was effectively more refracting than the glass, the ellipses were nearly circular and very clear both for the submerged plate and lens, as well as for the liquid, but when the solution began to effectively refract less than the glass, the ellipses were washed and could not be obtained strongly. On submerging the lens in these cases it was necessary to so adjust its position horizontally and vertically that the white images (obviously in different focal planes) coincide as nearly as possible. This insures a symmetric position for the lens, after which the spectrum is to be examined and the ellipses placed by moving the micrometer. Unfortunately, as neither the trough nor the plate was optically plane parallel, some readjustment for this was necessary at each observation, an operation which introduces the error in the results shown in tables 23 and 24, so far as absolute values are concerned, which has been alluded to above.

TABLE 23.—Submergence of plate-glass (thickness 0.284 cm.) in mercury-potassic iodide solution. Thickness inside of trough, 0.293 cm. Sodium line. $2B/\lambda^2=K$. Glass, $B=4.5\times10^{-11}$; $2B/\lambda^2=0.0262$.

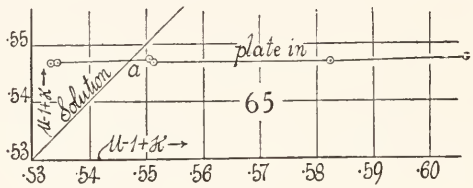
Solution.	Liquid ΔN	Glass in ΔN	Liquid $\mu-1+K$	Glass in $\mu-1+K$
	cm.	*cm.*		
6	0.1640	0.1468	0.6064	0.5476
7	.1570	.1466	.5824	.5469
8	.1494	.1466	.5564	.5469
9	.1478	.1468	.5505	.5475
10	.1430	.1466	.5345	.5470
11	.1426	.1466	.5333	.5468

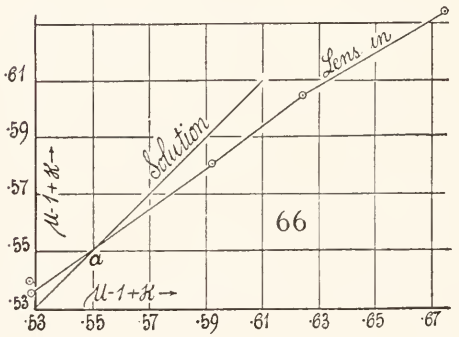
TABLE 24.—Submergence of glass convex lenses in mercury-potassic iodide solutions. Thickness of the trough inside, 0.293 cm. Focal power, 1 diopter. Sodium line. $K=2B/\lambda^2$. Glass, $B=4.5\times10^{-11}$; $2B/\lambda^2=0.0262$.

Solution.	Liquid $\triangle N$	Glass in $\triangle N$	Liquid $\mu-1+K$	Glass in $\mu-1+K$
	cm.	*cm.*		
1	0.2069		0.7525	
2	.1841	x 0.1722	.6746	0.6340
		.1742		.6410
3	.1692	.1638	.6239	.6055
4	.1599	.1565	.5921	.5805
5	.1412	xx .1432	.5283	.5352
	.1411	*f* .1445	.5280	.5396

x Focal power 2 diopter. xx Washed ellipses. *f* Concave lens.

In both these series the trough was not fixed with adequate rigidity, so that errors crept in from this source. Nevertheless, if the data are con-





structed graphically ($\mu-1+K$ for solution as abscissa and for submerged glass as ordinate), the results (figs. 65 and 66) show a very definite trend and show also that slight interpolation would be possible. It would be hasty, however, to infer that the intersection at *a* of the graph for submerged glass with the line at 45° through the origin is the index of refraction of the glass, in so far as the data for the liquid are trustworthy. The method seems to be deserving of notice; but before discussing the matter further it will be necessary to determine the dispersion involved in B.

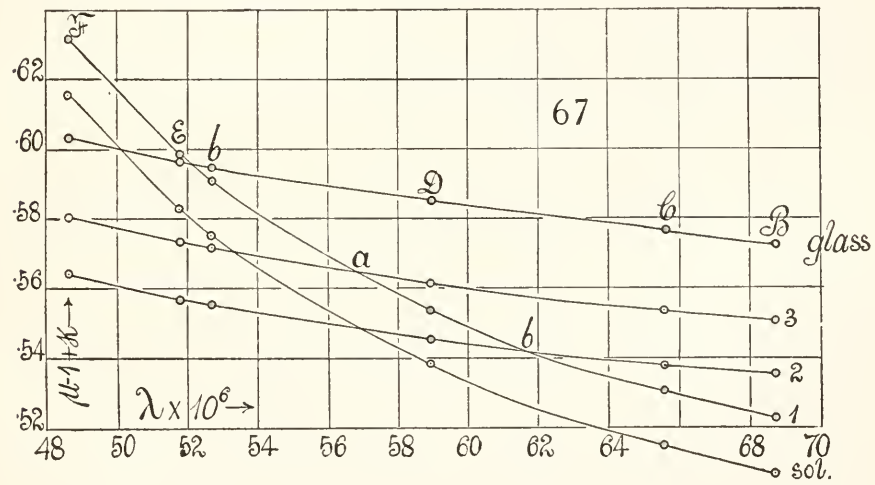
53. Dispersion constants.—As shown in §51, the constant B is found by passing the center of ellipses between Fraunhofer lines, both in the presence and absence of the plate to be tested. In the case of liquids the empty and

the filled trough are similarly compared. Data of this kind for a dilute solution of mercury-potassic iodide and two kinds of glass are given in table 25. N_a is the micrometer reading at M for the half-silvered plate alone. In case of the solution, it is to include the glass plate of the trough. $N-N_a=\Delta N$.

TABLE 25.—Dispersion constants.

Fraunhofer line.	$\lambda\times10^6$	N_a	(1) Solution. $e=0.293$ cm. $N-N_a$	(2) Trough glass. $e=0.562$ cm. $N-N_a$	(3) Glass plate. $e=0.434$ cm. $N-N_a$
	cm.				
B	68.7	0.0152	0.1530	0.3008	0.2390
C	65.63	.0173	.1554	.3023	.2403
D	58.93	.0220	.1622	.3065	.2436
E	52.70	.0284	.1731	.3121	.2481
b	51.77	.0296	.1753	.3130	.2488
F	48.61	.0342	.1851	.3171	.2520

The computed values $\mu-1+K=(N-N_a)/e=\Delta N/e$ are given in the graph figure 67 (series numbered), from which the characteristic difference in the dispersion of the solution and of the glass is apparent.



If, now, the value of B is computed by equation (4), between successive Fraunhofer lines $B-E$, $C-b$, $D-F$, the results come out as in table 26 and the coefficient B should be correct to about 1 per cent. For instance, in the case of the solution $(N-N_a)\lambda-(N-N_a)\lambda'=\delta N=0.0201$, 0.0200, 0.0229, respectively.

TABLE 26.

Fraunhofer lines.	(1) Solution. $B\times10^{11}$	(2) Trough glass. $B\times10^{11}$	(3) Glass. $B\times10^{11}$
B–E	15.38	4.50	4.71
C–b	16.02	4.49	4.65
D–F	19.22	4.62	4.76

It thus appears that in case of the solution the equation $\mu = A + B/\lambda^2$ is far from sufficient up to the Fraunhofer F line. Nevertheless even here the mean of the first two results may be regarded as holding in the region of the D line. The large value of B as compared with the glasses is particularly noteworthy, and from this a reason for the poor ellipses obtained with dilute solutions is suggested. If for two media the $\Delta N/e$ are identical, as at a and b in figure 67, this implies merely that

$$\mu + 2B/\lambda^2 = \mu' + 2B'/\lambda^2$$

Hence, when the coefficients B differ as largely as is the case for the solution and the glass, the indices μ are far from equal. In the above case, if $\mu - \mu' = 0.071$, the solution should show no displacement at the D line when the glass is submerged. But this difference in the indices of refraction of the glass and the solution is enormous, and if the submerged body is a lens, the corresponding images in the telescope will be thrown quite out of focus. Thus the ellipses are necessarily washed. Conversely, when the indices of lens and solution are nearly equal at the sodium line, the displacement is $2(eB - eB')/\lambda^2$, and therefore considerable (0.035 cm. above, in the example taken); but the ellipses are now sharp and strong. Unfortunately, therefore, displacement is no criterion for equality of μ, and mere dependence on the sharpness of fringes is insufficiently accurate. The only resource left is to compute B and B' for two spectrum lines and adjust the solution for this displacement. Again, this is not convenient, particularly when but a single spectrum line is at hand.

54. Further observations.—A somewhat wider trough was now constructed of the same plate-glass as above. The following dimensions were found by calipering: Glass wall plates, top 0.290 cm., bottom 0.283 cm.; internal thickness (liquid plate), top 0.564 cm., bottom 0.563 cm. As the light passed through near the bottom of the trough, the second data are to be taken in each case. The observations were made with sunlight and at each of the Fraunhofer lines B, C, D, E, b, F. In case of a hazy sun the lines B and F were often less strong than desirable; but in other respects the work throughout progressed smoothly, showing magnificent ellipses beginning at the B line with the horizontal axis longer and ending at the F line with the vertical axis longer. Circles occur earlier as the refraction is greater. $N - N_a$ in table 27 is the coördinate referring to the difference of micrometer reading for the presence and absence of the plate under observation. If the glass walls of the trough alone are to be taken, the N_a refers to the half-silver plate alone. If the solution is in question, N_a refers to the half-silver and the trough walls taken conjointly and in place. The trough is, of course, not to be moved; but some adjustment is needed when the liquid is introduced, which mars the absolute result. In series 5 a glass plate $e = 0.293$ cm. thick was submerged in the solution without readjustment. Hence of the resulting refraction $293/563 = 0.5024$ belongs to the glass and $270/563 = 0.4796$ to the solution surrounding it. Table 16 contains ten series of results with the

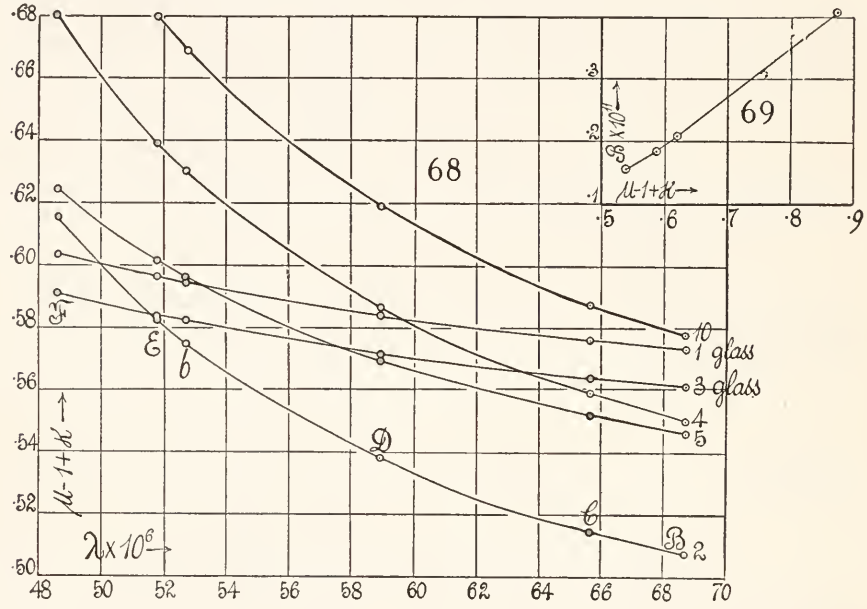
TABLE 27.—Refraction of glass and of mercury-potassic iodide solutions. New trough. Glass walls, $e=0.283$ cm. thick, each; solution, $E=0.563$ cm. thick; $K=2B/\lambda^2$. Figure 68 is an exhibit of the more important of these results.

Series.	Fraunhofer line.	$\lambda\times10^6$	$N_a\times10^3$	$\triangle N$	$\mu-1+K$	$\delta N\times10^4$	$B\times10^{11}$
		cm.	*cm.*	*cm.*		*cm.*	
(1) Glass plate. $e=0.566$.....	B	68.7	8.1	0.3247	0.5737	BE, 117	4.65
	C	65.63	9.7	.3263	.5766	Cb, 111	4.65
	D	58.93	14.4	.3306	.5841	DF, 110	4.78
	E	52.70	* 20.8	.3364	.5943		
	b	51.77	22.0	.3375	.5963		
	F	48.61	26.6	.3416	.6035		
(2) Dilute solution.....	B	Same as above		0.2855	0.5071	BE, 382	15.26
	C			.2899	.5149	Cb, 382	16.01
	D			.3031	.5384	DF, 435	19.00
	E			.3237	.5750		
	b			.3281	.5828		
	F			.3466	.6156		
(3) Glass plate. $e=0.566$ cm...	B	Same as above		0.3178	0.5616	BE, 116	4.63
	C			.3194	.5643	Cb, 111	4.63
	D			.3237	.5719	DF, 109	4.74
	E			.3295	.5822		
	b			.3305	.5839		
	F			.3346	.5912		
(4) Stronger solution.....	B	Same as above		0.3098	0.5503	BE, 450	17.99
	C			.3151	.5597	Cb, 446	18.75
	D			.3304	.5869	DF, 524	22.89
	E			.3548	.6303		
	b			.3598	.6391		
	F			.3828	.6800		
(5) Glass plate in solution 4. $e=0.293$ cm...	B	Same as above		0.3077	.05465	BE, 279	11.16
	C			.3110	.5525	Cb, 276	11.59
	D			.3207	.5697	DF, 309	13.52
	E			.3356	.5962		
	b			.3387	.6016		
	F			.3517	.6247		
(6, 7) Glass plate. $e=0.566$ cm...	B	Same as above	8.0	.03193	0.5641	BE, 114	4.53
	C		9.7	.3207	.5666	Cb, 107	4.48
	D		14.5	.3249	.5740	DF, 108	4.69
	E		21.0	.3307	.5843		
	b		22.2	.3315	.5858		
	F		26.8	.3357	.5931		
(8) Strong solution.....	B	Same as above		0.4474	0.7947	BE, 1000	39.94
	C			.4582	.8139	Cb, 1003	42.03
	D			.4916	.8732	DF, 1224	53.47
	E			.5474	.9723		
	b			.5585	.9920		
	F			.6140	1.0906		
(9) Strong solution.....	B	Same as above		0.4474	0.7953	BE, 999	39.90
	C			.4584	.8143	Cb, 1004	42.06
	D			.4918	.8736	DF, 1216	53.14
	E			.5476	.9727		
	b			.5589	.9927		
	F			.6135	1.0897		
(10) Dilute solution.....	B	Same as above		0.3255	0.5782	BE, 509	20.32
	C			.3309	.5879	Cb, 514	21.56
	D			.3487	.6194	DF, 601	26.25
	E			.3764	.6687		
	b			.3824	.6792		
	F			.4088	.7261		

* Circles.

same trough but with different solutions, dilute and nearly concentrated. To place the trough normal to the beam, the reflection of the latter from the face of the trough was made to coincide with the spot on the half-silver. This is inadequate for fine work, but the interferometer method of retrogressing fringes is not applicable unless the trough is separately mounted.

From the data obtained the constant B was computed from pairs of Fraunhofer lines, B and E, C and b, D and F. Apart from the effect of the thickness e, it should be correct in case of the solutions to about a few tenths per cent. In case of the concentrated solutions, however, the ellipses already begin to move sluggishly and are much smaller.



From $\mu-1+2B/\lambda^2$ and B, the corresponding indices of refraction in table 27 are easily computed; but these data are of little value here, because the thickness e of the ordinary plate-glass used is not constant to the degree necessary. It is, however, worth while to exhibit the B for the different mercury-iodide solutions in terms of either μ or, what is equally serviceable and more convenient, in terms of $\mu-1+K$; for this quantity is directly given by the displacement measurement $\Delta N/e$. If we regard the mean B for the B to E lines, and C to b lines as applying to the D line, the coördinated values are:

	(2)	(4)	(8)	(9)	(10)
$\mu-1+K$	0.5384	0.5869	0.8732	0.8736	0.6194
$B\times10^{11}$	15.63	18.37	40.99	40.98	20.94

For solutions of small concentration the ratio of B and $\mu-1+K$ changes but slowly (29 to 34) as shown in figure 69, so that B may be predicted from the latter, always remembering that our equation with two constants ($\mu=A+B/\lambda^2$) is inadequate at the outset.

To take the case of the submerged glass-plate series 5, if e' be the thickness of plate and e'' of solution, so that $e'+e''=e$, the thickness of trough,

$$\frac{e'}{e}(\mu'-1+K')+\frac{e''}{e}(\mu'-1+K'')=\frac{\Delta N}{e}$$

Thus, 0.5204 of the data of series (3) added to 0.4796 of the data of series (4) should reproduce series (5). The results are given in table 28.

TABLE 28.

	B	C	D	E	b	F
3, 4 Computed....	0.5561	0.5621	0.5791	0.6052	0.6104	0.6338
5 Found.....	.5465	.5525	.5697	.5962	.6016	.6247
Difference....	.0096	.0096	.0094	.0090	.0088	.0091

These differences are nearly constant and due to the orientation of the glass plate with which its effective thickness (assumed 0.293 cm.) will vary.

55. Conclusion.—It appears, therefore, that the expectation of recognizing the equality of refraction of a submerged solid and a solution, at any given wave-length, from the fixity of the fringes in the presence and absence of the solid has not been fulfilled, at least for the mercury-potassic iodide solution. The reason is found in the enormous difference of the dispersions of the solution and ordinary glass. When the ellipses are not displaced, $\mu-\mu'=2(B'-B)/\lambda^2$, and this difference may even approach a unit in the first decimal of μ. The troughs in which such experiments are to be made must be *optically* plane parallel, as otherwise an inadmissible error due to thickness of plates is introduced. With such a trough, however, the ease and accuracy with which the dispersion constants may be found, at least for the solution, are noteworthy.

When the solution is more refracting than the glass, it is curious that the ellipses are not seriously distorted or vague, even when the symmetrically submerged solid is lenticular. Hence the equation just stated is available for a wide variation of form. Furthermore, if ΔN is the displacement at the micrometer corresponding to the presence and absence of glass of the thickness e,

$$\mu-\mu'+\frac{2}{\lambda^2}(B-B')=\frac{\Delta N}{e}$$

But as μ', B' for the solution are known, μ and B for the glass may both be computed from observation at a number of wave-lengths, λ, provided $\mu=A+B/\lambda^2$ for glass, which is sufficiently nearly so to the fourth place of decimals. Hence if $\Delta N/e+\mu'+2B'/\lambda^2=x$ is known,

$$B=\frac{x-x'}{3(1/\lambda^2-1/\lambda'^2)}$$

and $\mu = x + 2B/\lambda^2$. Data of this kind are given in table 29, the absolute values depending wholly on the correctness of the thickness E of the solution and e for the submerged lens. The ellipses were excellent, sharp, and strong. $\mu - 1 + 2B'/\lambda^2$ is found directly and ΔN is negative as the solution is stronger.

TABLE 29.—Refraction of lenses. D line. Thickness of solution, $E = 0.563$ cm.; $K' = \mu' - 1 + 2B'/\lambda^2$; $2B/\lambda^2 = 0.0260$ for glass. $\mu - 1 = K' - \Delta N/e$.

Lens.	e	K'	$\Delta N \times 10^3$	μ	Remarks.
	cm.		*cm.*		
1 diopter.....	0.138	0.6140	7.8	1.5315	Ellipses strong.
2 diopters....	.200	.6140	10.7	1.5345	Ellipses strong.
5 diopters....	.248	.6140	*18.7	1.5126	Ellipses vague.
10 diopters....	.447	.6343	*20.5	1.5625	Ellipses vague.

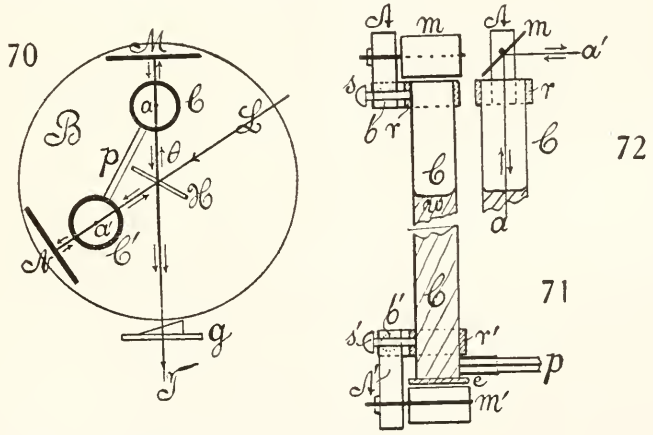
* Probably not adequately centered.

But such a method is not as convenient as was anticipated at the outset, while it may fall short of the needed accuracy if rigorously carried out. The only escape out of the difficulty would be the use of a liquid of about the same dispersion constants as the glass. In this case the corrections would be minimized and the experimental work simpler.

CHAPTER V.

DISPLACEMENT INTERFEROMETRY IN CONNECTION WITH U-TUBES. JAMIN'S INTERFEROMETER.

56. Introduction.—A variety of constants in physics may be found from the relative heights of two communicating columns of liquid. This is, for instance, the case in the classical experiment of Dulong and Petit on the thermal expansion of liquids. Again, if one of the tubes is subject to a special force acting in the direction of its axis, this force in its bearing on the liquid may be evaluated from the resulting difference of heads of the columns. Thus one tube may be surrounded by a magnetizing helix and the effect of the axial magnetic field on the liquid in question (*i.e.*, the susceptibility) found from the displacement of its surface by the presence and absence of the field, etc. It seemed to me worth while, therefore, to test whether it would be possible to measure small displacements of this kind by passing the two component beams of a displacement interferometer axially *through* the two columns respectively, and to measure the differential effects in question in terms of the resulting displacements of fringes.



57. Apparatus. Michelson interferometer.—The interferometer first used was of the same form as that described above (§ 2, fig. 3), *B*, figure 70, being a heavy iron block, 1 foot in diameter and 1.5 inches thick, on which the mirrors *M*, *N* (the latter and preferably both on micrometers) are securely mounted with the usual direct rough and elastic fine adjustment for horizontal and vertical axes. A beam of parallel white rays *L* arrives from a collimator (not shown) and impinges on the half-silver plate *H*, to be reflected and transmitted at a convenient angle θ (about 60°), thus furnishing the two component beams which are to traverse the limbs of the U-tube.

The vertical columns of this tube are shown at C and C' (with accessory mirrors removed), and they are joined to the capillary tube p near the bottom of C and C'. Details will be given in connection with figures 71 and 72.

The ray HM strikes a mirror symmetrically at 45° to the vertical below C, is thence reflected upward along the axis a, striking another mirror above, also symmetrically at 45° and parallel to the former, whence it is reflected to the opaque mirror M. The latter reflects the ray normally back, so that it retraces its path as far as H, by which plate it is now transmitted to be observed by the telescope at T. Similarly the transmitted component ray HN is guided by suitable reflectors at 45°, so as to take the path $Ha'Na'HT$, thus passing axially (a') through the tube C'.

It is necessary that the U-tube CpC' be mounted independently of the block B on suitable bracket or arm attached to the pier. Otherwise any manipulation at N will disturb the surfaces of water in C and C'. Ordinary clamps admit of raising or lowering or rotating CC' satisfactorily, always providing that it shall not touch B. The telescope at T is also mounted apart from B on the table below. The direct-vision prism grating g is placed immediately in front of the objective and swiveled as described in figure 64, Chapter IV, so that either the white slit images or their spectra may be seen in the field of view, according as g is rotated aside or is in place.

In figure 71 a front sectional elevation of one of the shanks of the U-tube is given with all appurtenances, and a similar sectional elevation at right angles to the former is added in figure 72 for the top of the tube. In figure 71 the mirrors m' and m are on horizontal axes and the component ray coming from behind the diagram strikes m' below, is reflected axially upward through CC, impinging on the mirror m (also on a horizontal axis), whence it is reflected horizontally toward the front of the diagram. The ray a and mirror m are given more clearly in figure 72. The lateral capillary tube appears at p and the tube C is closed below with a plate of glass e, cemented in place.

To mount the mirrors m, m', snugly fitting rings r and r' encircle the tube C near its top and bottom and can be fixed by the set-screws s and s'. In virtue of these rings, the mirrors m, m' may be rotated at pleasure around the vertical axis a of CC. The horizontal axis of the mirrors m, m' rotates at pleasure in the vertical arms A, A' of square brass tube. A, A' in turn may be slightly swiveled about the horizontal axis b, b', in a rigid lateral projection of the rings r, r'. Thus m, m' are capable of rotation around three axes normal to each other and adequately clamped in any position.

The component ray HN may be adjusted to the center of the lower mirror m' by placing the collimator L and then guided axially by m', m, N as described, each being adjustable. The component ray HM may be similarly adjusted to the center of the lower mirror m' (at 45°) by slightly rotating the half-silver plate H (on horizontal and vertical axes) and then guided axially by m', m, M. As a whole the adjustment is difficult, though it need not be much refined. Clear white slit images in the telescope T are an adequate criterion.

In the absence of a liquid in CC, figure 71, the fringes are easily found after

careful preliminary measurement, and they are strong and satisfactory. When this adjustment is given, the presence of liquid in *CC*, if the two columns are of nearly equal length, does not much modify the adjustment. In fact, the fringes were found much more easily than I anticipated, and in quiet surroundings they are strong and fine. It is necessary, however, that the tube *CC* should be of sufficient width to avoid all curvature due to capillarity, at least in the axis. Tubes 2 cm. in diameter and 10 cm. long of thin brass were first tried, but proved to be too narrow. No sharp slit images could be obtained with reasonable care as to setting the mirrors. Thereafter tubes 4 cm. in diameter were used, but even these are somewhat too narrow. Slit images, however, were sharp and parallel and could be easily brought to coincide.

With the wide tubes, however, the mobility of the liquid in *CC* increases enormously, so that only under exceptionally quiet conditions could the fringes be seen, and never quite without quiver. The wind beating on the house, for instance, threw them nearly out of view, so that only a suggestion of their presence remained. In spite of the very promising beginnings, therefore, it became a serious question whether, with the apparatus as here devised, the purposes of the research could be reached in this laboratory.

Finally, the flickering of the arc lamp may be a grave inconvenience; for if the columns *C*, *C'* as usual are virtually prisms, the coincidence of spectra will for this and other reasons be destroyed by the displacement of the arc.

58. Equations.—Some estimate of the increments to be anticipated may be given here, and expressed in terms of the Dulong-Petit experiment. If α is the mean coefficient of expansion of water at the temperature in question and ΔH the increment of the head H corresponding to the temperature difference Δt between the columns,

$$\Delta H = \alpha H \Delta t \tag{1}$$

Again, if ΔN corresponding to ΔH is the displacement of centers of ellipses at the wave-length λ, and μ the index of refraction of water, so that $\mu = A + B/\lambda^2$, nearly,

$$\Delta H = \frac{\Delta N}{\mu - 1 + 2B/\lambda^2} \tag{2}$$

Hence Δt may be computed as

$$\Delta t = \frac{\Delta N}{(\mu - 1 + 2B/\lambda^2)\alpha H} \tag{3}$$

Since the value of ΔN is within 10^{-4} cm. and $H = 10$ cm. in the above apparatus, we may further write at mean temperatures (25°)

$\alpha = 2.5 \times 10^{-4}$ $\mu = 1.333$ $B = 10^{-11} \times 3.1$ $2B/\lambda^2 = 0.018$ at the *D* line.

Thus $\mu - 1 + 2B/\lambda^2 = 0.351$ and $\Delta t = 10^{-4}/0.351 \times 2.5 \times 10^{-4} \times 10 = 0.114°$. In other words, in case of tubes 10 cm. long, the effect of a difference of tempera-

ture of about 0.1 degree between the tubes should be easily observable by mere displacement, whereas a difference of less than 0.03 would be equivalent to the passage of one interference ring.

Again, from equation (2), if $\Delta N = 10^{-4}$ cm., then $\Delta H = 10^{-4}/0.351 = 10^{-4} \times 2.8$ cm., or about 9×10^{-5} cm. per vanishing interference ring are the displacements to be anticipated. These are equivalent to pressures of about 0.3 and 0.1 dyne per square centimeter.

59. Observations.—A large number of observations were made with the apparatus described, but as under present surroundings the fringes always quivered violently, no quantitative results of value were obtained. Naturally such experiments imperatively demand a laboratory remote from traffic, since the undulation of mobile liquid surfaces is introduced in addition to the tremors of solid appurtenances.

An attempt was made to register the pressure near an electrically charged point, but no results could be obtained. Again, though the attraction of an electrically charged surface for the free surface of water in either tube was recognized, on using adequately high potentials to measure the forces the surface became troubled and the fringes vanished. In this case, if p is the pressure, V the difference of potential in volts, and d the distance apart of surfaces in centimeters, $f = 4.4 \times 10^{-7} \times (V/d)^2$ dynes/cm.^{2} if $f = 0.3$ can just be determined by the displacement method, and if $V = 80$ volts (roughly) is the smallest potential difference discernible for quiet fringes. Finally, Dulong and Petit's experiment gave very definite results even for small ranges of temperature, subject to the conditions stated.

By surrounding the top of the tube C, figure 71, with a close-fitting helix, the upper face of which reached just below r, while the surface of liquid within, w, lay at its center, an attempt was made to detect the susceptibility k of water, etc. If the field of the coil be written roughly $H = 0.4\pi in/l$, where i is the current in ampères, n the number of turns, and l the length of the helix, we may write

$$\rho g . \Delta h = H . kH = kH^2$$

Since $\rho = 1$, the increment of head, h, becomes

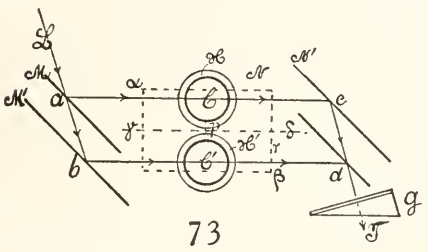
$$\Delta h = kH^2/g = (0.4n\pi/l)^2 i^2 k/g$$

Hence if roughly $k = 10^{-6}$, $g = 10^3$, $i = 1$ am., $n/l = 35$ as in the helix used,

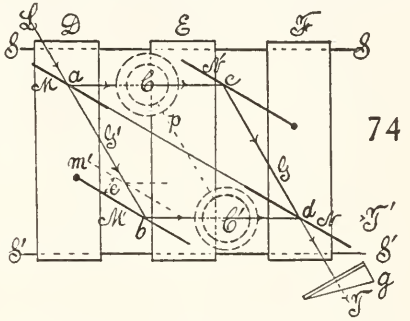
$$\Delta h = 44^2 \times 10^{-9} = 1.9 \times 10^{-6} \text{ cm.}$$

Thus if $i = 10$ ampères, $\Delta h = 2 \times 10^{-4}$ cm., nearly, and easily determinable by the displacement of ellipses, or from interference rings. The experiment was tried, but the quiver of rings was such as to admit of no decision. In case of the magnetic solutions, k is of course much larger; but under the circumstances it did not seem worth while to attempt further work. This will be done with other apparatus in the course of this paper.

60. Jamin's interferometer.—The ease with which the Michelson interferometer may be adjusted and its remarkable adaptability have led to its general preference over the older form of Jamin. Nevertheless, the latter furnishes two parallel rays which for such purposes as the present are desirable. Hence if the four faces of the interferometer be separated in the manner suggested by Mach (shown in fig. 73), a very available form of interferom-



73



74

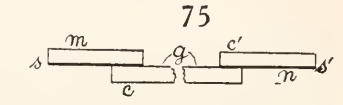
eter is obtained. Here M and N are half-silvered plates, M' and N' the opaque mirrors. The white light L impinging from a collimator thus furnishes the two component beams ac and bd, which are observed with the telescope at T, after passing the direct-vision prism grating g. If either mirror M' or N' is displaced a distance e, moving parallel to itself, the path-difference $2e \cos \theta$ is introduced with the corresponding shift of ellipses. The U-tubes C, C', with their helices H, H', and connecting pipe p are now conveniently installed as shown. But the trouble with the arrangement is the difficulty of adjusting the *four* surfaces. Not only are the centers of ellipses liable to be remote from the center of the field, but it is often hard, without special equipment, to even find the fringes.

If, however, the device which I suggested in the preceding report is adopted—*i.e.*, if (fig. 74) the half-silvered plates M, N are at the ends of a single strip of plate-glass, so that rays terminating in $M, M' N N'$ after adjustment necessarily make a rhombus-like figure symmetrical to MN—the fringes are found at once; for they appear when the white slit images in T coincide horizontally and vertically and the rays bd and cd intersect in the common point d. Hence the mirrors M', N' should be on carriages D, F, adapted to move on parallel slides S, S'. M, N may also be put on a carriage E, though this is not necessary. S, S' need not be parallel to ac or bd. If the mirrors M' and N' are wide, considerable latitude of adjustment is thus obtained.

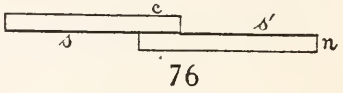
If MN is half-silvered on the same side (*i.e.*, toward N') a compensator is needed in ac or cd if path-difference is to be annulled (symmetry). If, however, M is half-silvered on the N' side and N on the M' side, no compensator is required. In the latter case, however, if ordinary plate-glass is taken, M and N are not quite parallel and the ellipses will be eccentric. This, however, is not necessarily a disadvantage, unless the strip MN is excessively wedge-shaped.

The ellipses obtained are usually long vertically—*i.e.*, quite eccentric—so that the fringes soon become straight and the rotation is extremely rapid whenever the center of ellipses is out of the field. It is therefore possible to adjust relative to horizontal fringes (parallel to the shadow of wire across slit), as these incline very obviously for a displacement of less than 10^{-4} cm. and rapidly become vertical. For this reason it makes little difference in practice whether the half-silvers are on the same or on opposite sides, or whether observation be made at T (cd prolonged) or at T' (bd prolonged). Moreover, the plate MN may be conveniently constructed, as in figure 75, of two mirrors m, n, attached to the clear strip of plate-glass g by aid of strong steel clips at c, c'. With the half-silvers s, s', on the same side, the wedge-angle of the glass is excluded. For shorter diagonals, the plan of figure 76, with the silver surfaces s, s' held together by clips at c, is preferable.

75



76



If the mirror M', figure 74, is displaced a distance e, where a glass-plate compensator of thickness E and refraction constants μ and B is introduced normally either into ab or bd, the equation is easily seen to be, at wavelength λ,

$$E(\mu-1)+2B/\lambda^2=2e\cos\theta$$

where θ is the angle of reflection at M. Using the plate $E=0.434$ cm. treated above, the first member is 0.2428 cm. Values of e of 0.2420, 0.2409, 0.2427 were roughly obtained. Hence the mean value of θ should be about 60°, as it actually was.

The occurrence of this angle and the shift of the beam bd along the mirrors M' and N are the main objections to the method of figure 74, for the rhombus is not necessarily perfect. If the ends of the plate MN are silvered on the same side, the compensator must have double the plate-thickness to annul path-difference. Finally, the half-silvering does not, for large θ, sufficiently exclude the reflection of bd from the naked face of the plate, so that the fringes are never quite black. These difficulties may be met by making MN, figure 74, the *short* diagonal of the rhombus and using the strip, figure 76. In such a case θ at M' is small, and in view of the nearly normal reflection at M and N relatively little reflection comes from naked glass, sliding is largely avoided, and no compensator is necessary. In this case the fringes for no path-difference are actually strong black horizontal lines on a colored ground and far enough apart that 0.1 fringe could easily be estimated. A test experiment with the above plate showed $e=0.1244$ cm., corresponding to the small angle θ, a little over 12°.

When the U-tube $C\,C'$, figures 71 and 74, is introduced, the strip MN will have to be at a considerable angle (about 45°) to the horizontal, so as to raise the N end about 15 cm. above the M end, corresponding to the height of m above m' in figure 71. The new condition, however, in no way changes

the general procedure. In case of figure 74, the mirror N' must be high and M' low. This is usually less convenient than the case when both mirrors are high (C placed at G) or where both mirrors are low (C' placed at G'). In the former case, again, the rays have considerably diverged in a vertical plane and the fringes are less marked. If C' is at G' the whole of each component beam may be caught and passed through the respective shanks of the U-tube. The fringes are strong, easily found, and large, so that the center of ellipses is not far outside of the field of the telescope. It is obvious that to facilitate adjustment the mirrors m and m', figure 71, must be nearly parallel. They are made so by the aid of a broad beam of sunlight and then clamped firmly in position at about 45° to the respective axis of the U-tube.

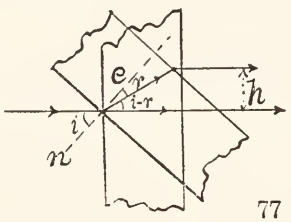
Finally, if the connecting-tube p is nearly horizontal when in place, the fringes are usually found at about the same position of the micrometer (at M') after the liquid is introduced into the U-tube. Here it is advantageous and usually permissible to make a part of the connection p of flexible rubber tubing. But unless the free surface w, figure 71, is very nearly parallel to the plate e, the center of ellipses is liable to be far outside of the field of the telescope and the fringes correspondingly small. The difficulty of adjustment for large fringes is now considerable, because of the two mobile liquid surfaces in the U-tubes. For this reason I did not attempt to make measurements, although the fringes themselves were surprisingly steady and strong and would have been quite available, apart from laboratory tremors. Slight changes in density, due to solution or temperature changes in one shank of the U-tube, were well recorded, after stirring, with curious effects of surface-tension and viscosity.

The fringes being very clear, a number of other promiscuous experiments were tried. Thus, a tube with plate-glass ends and filled with water was made the core of a powerful magnetic helix. The tube, 26 cm. long, was placed in one of the component beams and compensated by a column of glass in the other. Good fringes were easily found; but not the slightest displacement could be detected by alternations of presence and absence of the magnetic field. The water was now replaced by a solution of nickel sulphate. Fringes were again easily found and strong in the green, but the effect of the magnetic field was quite as inappreciable as before. Magnetic fields were thus totally ineffective.

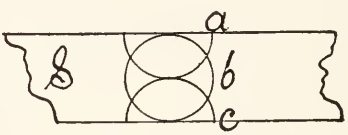
In a set of experiments of a different kind the attempt was made to observe the gradual deposition of silver on plate-glass. Böttger's solutions were poured into a plane-parallel clean glass trough normal to one of the component beams (cd, fig. 74) and compensated by a plate of glass in the other (bd). Large fringes were produced by setting the micrometer and observed during the formation of the two silver films on the opposite faces of the trough, until they became quite opaque. It was astonishing to find that fringes were still faintly visible long after a highly reflecting mirror had been deposited. But no displacement larger than a fraction of a fringe could be detected, showing the extraordinary thinness of the silver film even when practically opaque.

Similarly, the silver deposit on plate-glass was removed in parallel strips, so that the film had the appearance of a grid. The results when this plate was placed normally in one of the component beams were the same.

61. Vertical displacement of ellipses.—If the fringes are too small when horizontally centered by the micrometer, the center of ellipses may be brought into the middle of the field of the telescope by sliding one component beam vertically over the other without appreciably changing the direction of the rays. In other words, one illuminated spot at *d*, figure 74, is to move vertically relative to the other by a small amount. This may be done by placing a thick plate-glass compensator, such as is shown in figure 77, in each of the component beams *abd* and *acd* and suitably rotating one plate relative to the other, each on a *horizontal* axis. Very little rotation is required. In the same way elliptical fringes may be changed to nearly linear horizontal fringes when desirable. If the fringes are to be sharp the slit must be very fine. When sunlight is used with a slit not too fine, each of the coincident sodium lines (D_1D_2) frequently shows a sharply defined helical or rope-like structure, the dark parts in step with the fringes of the spectrum. It looks like an optical illusion of slanting lines or a shadow interference of two grids (fringes and sodium lines respectively); but later experiments showed it to be an independent phenomenon. (*Cf.* § 63 *et seq.*, 68, 70.)



77



78

The first result is particularly interesting, inasmuch as it is thus possible to displace the centers of ellipses not only horizontally as usual relative to the fixed sodium lines in the spectrum, but also *vertically* relatively to the fixed horizontal shadow in the spectrum due to the fine wire across the slit. The following experiment was made to coördinate the vertical displacement of the component rays and centers of elliptic fringes: A glass plate $d=0.705$ cm. thick was placed nearly normally in the beam *ac*, figure 74, and provided with a horizontal axis and graduated arc. The amount (i) of rotation of the plate, corresponding to the vertical displacement of one central fringe in the telescope (*i.e.*, passage of fringe *a* into *b*, into *c*, in the duplicate spectrum *S*, fig. 78), was then found to be, if i is the angle of incidence,

	i	h
No fringes.....	3.5°	0.0149 cm.
One fringe.....	5.0°	.0214
Two fringes.....	6.5°	.0281

where h is the corresponding vertical displacement of the rays *ac*, figure 74, and computed from (μ index, r angle of refraction)

$$h=d(\sin i-\cos i\tan r)$$

Thus the vertical displacement of rays corresponding to the vertical semi-axes of the central ellipse or one fringe is between 0.0065 and 0.0067 cm.—*i.e.*, on the average below 7×10^{-3} cm. Hence $h=N\times0.007$ for N such central fringes. It was difficult to get a closer result, owing to quiver.

The interesting question is now suggested, in how far such an arrangement would fall short of being able to exhibit the drag of the ether in a rapidly rotating body, should such drag occur. In figure 73, let $\alpha\beta$ be a cylinder of glass with plane-parallel ends, capable of rotating on the axle $\gamma\delta$. If l is the length of the cylinder, μ its index of refraction, and r the distance of either component ray (ac, bd) from the axis $\gamma\delta$, n the number of turns per second, and V the velocity of light, we may write, using the above excessive estimate, N being the number of fringes displaced,

$$h=\tfrac{1}{2}N\times0.007=2\pi nrl\mu/V$$

since ac rises while bd falls. If

$$n=200, \qquad r=10 \text{ cm.}, \qquad l=100 \text{ cm.}, \qquad V=3\times10^{10}, \qquad \mu=1.5,$$

$$N=\frac{6.3\times2\times10^{2}\times10\times10^{2}\times1.5}{3.5\times10^{-3}\times3\times10^{10}}=0.18, \text{ nearly}$$

It would thus be necessary to estimate about one-sixtieth of a fringe, which is just beyond the limit of certainty, even if nr can be increased and l multiplied by reflection. The device suggested is nevertheless of interest and deserves further consideration. It will appear much more promising in connection with the achromatic fringes described below.

62. Displacement interferometer. Jamin type.—These considerations induced me to devote further study to the Jamin type of interferometer (fig. 73). The mirrors M, N' were put on one pair of long slides (1.5 meters long) parallel to ac and the mirrors M', N on similar slides parallel to the former. In this way any distance ac or bd was available. The beams were about 16 cm. apart, corresponding to a normal distance between the end mirrors (NN', MM') of about 12 cm. But these distances could also be increased from nearly zero (M and M' nearly contiguous) to about 20 cm. in view of the width of mirrors used. The angles at a, b, c, d were each about 45°, so that a rectangle of rays is in question. (See figure 88 or 93 below.)

The adjustment proved eventually to be greatly facilitated by using a horizontal beam of sunlight with *weak* condenser-lens and collimator. A thin wire is to be drawn across the slit. M and M' are first set for parallelism in the absence of N and N', by adjusting the images of the slit at the same level (horizontal) on a distant wall. The images or shadows of the wire specified on the wall are to be equally far apart, with the beams ac and bd at the mirror. The mirrors N and N' are next put in place with the distances acd and abd about equal. The two images seen in the telescope at T (g removed) are then made to coincide both horizontally and vertically by adjusting N and N',

and these are then slid by a small amount on their slides (direction *ac*) until the rays are coincident at *d* to the eye (light strips on the mirror coincide).

If, now, the grating *g* is inserted, very fine oblique fringes will usually be seen. These may be enlarged to a maximum by moving the micrometer controlling the displacement *M'* normal to itself. Somewhat coarser *horizontal* lines are thus obtained.

Finally, the distant centers of the ellipses are brought into the center of the telescope by aid of the thick glass compensator, like figure 77 (the equivalent air-path of the other ray being correspondingly lengthened) by rotating the glass plate on a horizontal axis.* It is desirable to have an excess of glass-path in one beam, as otherwise the ellipses are so large as to be unwieldy.

The ellipses so obtained with common plate-glass and a film grating at *g* were magnificent. A rough test of the displacement interferometer was made by using the above plate-glass of thickness $E=0.434$ cm., where $z=E(\mu-1)+2B/\lambda^2=0.2428$ cm. In two experiments agreeing to within 10^{-4} cm., $2e=0.3448$ cm. were the displacements obtained. Assuming that $\theta=45°$, $2e\cos\theta=0.2438$ cm. This agrees with z as nearly as may be expected, unless θ is specifically measured.

Experiments were now made (as above) with thick plate-glass compensators inserted in one component ray (*bd*) only, to determine the rotation of compensator ($i°$) necessary to raise the center of ellipses in steps of half the diameter of the first ring (see *a*, *b*, *c*, fig. 78). The initial angle i is already large and shows the rotation of compensator from the vertical needed to bring the ellipses into the field. Two sets of experiments were made with plates respectively $d=0.965$ cm. and $d=0.705$ cm. in thickness, with the results given in table 30.

TABLE 30.

Experiment I.			
d	i	h	$\triangle h$
0.965 cm.	9.0°	0.0529 cm.	
	10.1	.0596	0.0067 cm.
	11.4	.0676	.0080
Experiment II.			
d	i	h	Δh
0.705 cm.	2.6°	0.0100 cm.	
	3.3	.0139	0.0039
	3.9	.0165	.0026

The equation of the preceding section is used for h. The first case shows about the same order of sensitiveness (Δh per half-ring). In the second case, for the thinner plate, the sensitiveness has been more than doubled. This

* The same result may be obtained in the absence of the compensator by rotating N and N' on a horizontal axis, successively by small amounts, into parallelism with M and M'.

is in a measure not unexpected, because the amount of displacement, *caet. par.* (*i.e.*, the mobility and size of ellipses), increases in marked degree as the plate compensator is thinner. But apart from this Δh is in some way, yet to be stated, associated with the obliquity of rays in a vertical plane.

In case of the rotating compensator, vertical and lateral displacement of centers of ellipses go together. It is therefore next in order to determine the ratio of vertical and lateral displacement.

The equation deduced in § 8, which follows easily from figure 77, may be put in the form (for a single passage of light through the plate)

$$n\lambda = 2e(\sin^2 i/2 - \mu \sin^2 r/2)$$

or into the approximate form for small angles

$$n\lambda = e(\mu - 1)i^2/2\mu$$

From the former equation

$$\frac{di}{dn} = \frac{\lambda}{e(\sin i - \cos i \tan r)}$$

or approximately, again,

$$\frac{di}{dn} = \frac{\lambda\mu}{e(\mu - 1)i}$$

Hence, if Δi corresponds to x fringes,

$$\Delta i = x\frac{di}{dn} = x\,\frac{\lambda\mu}{ei(\mu - 1)} \text{ roughly}$$

Again, for the corresponding normal displacement ΔN of the micrometer at the opaque mirror,

$$x\lambda = 2\Delta N \cos\theta$$

Hence

$$x = \frac{ei(\mu - 1)\Delta i}{\lambda\mu} = \frac{2\Delta N \cos\theta}{\lambda}$$

The data given in table 31 were found from successive positions of the plate $e = 0.705$ cm., while the center of ellipses moved as in figure 78, at the D line.

TABLE 31.

	Center at			$10^4 N$	$10^4 \triangle N$	x	
	i	$\triangle i$	x				
Bottom.....	13.6°	...	..	19 cm.	...	...	$\theta = 45°$
Middle.....	12.5	1.1	18	28	9	22	$x = 1.27 i \triangle i$
Top.....	11.5	1.0	15	35	7	17	$x = 24{,}000 \triangle N$
Bottom.....	7.5	...	..	111	...	...	$10^6\lambda = 59$; $\mu = 1.53$
Middle.....	6.7	0.8	7	115	4	10	
Top.....	5.9	0.8	6	119	3	8	

In view of the small values of ΔN and Δi and the estimated μ and θ, the two sets of values of x are no more divergent than would be expected. The

values of i are very different in different adjustments, because the ellipses may also be raised and lowered by rotating one of the opaque mirrors, as M, around a horizontal axis, though in this case with rapid loss of sharpness. Here the rotation of both mirrors of a pair, M' and M for instance, by the same amount, is required as an equivalent to the rotation of the compensator, as has been stated. The aim is to render both parallel pairs themselves parallel.

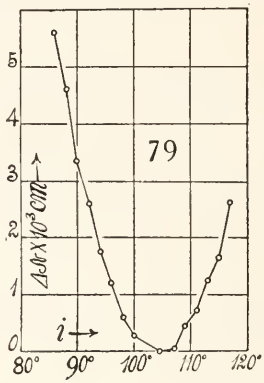
If $x\lambda$ is eliminated from the two equations on the preceding page,

$$\mu = \frac{1}{1 - 2\Delta N \cos\theta / ei\Delta i}$$

The above data are inadequate for evaluating μ, but they nevertheless indicate a value entirely too low. It seems, therefore, as if some essential term has been left out of sight. This is also to be inferred from the values of x, which differ systematically on the two sides of the table 31.

TABLE 32.—Refraction of a glass plate. $e = 0.434$ cm. $\mu = 1.53$. Rotation around vertical axis. Jamin type displacement interferometer. $\theta = 45°$.

i	$\Delta N \times 10^3$	μ	i	$\Delta N \times 10^3$	μ
	cm.			cm.	
+12.5°	2.60	1.56	− 6.5°	.60	
10.5	1.65	1.47	− 8.5	1.20	1.56
8.5	1.25	1.51	−10.5	1.75	1.52
6.5	.70		−12.5	2.60	1.56
4.5	.45		−14.5	3.35	1.51
2.5	.05		−16.5	4.60	1.57
± 0.0	.00		−18.5	5.60	1.55
− 4.5	.30				



In view of the discordant results obtained here and elsewhere with this type of rotating compensator, the provisional parts of the apparatus were improved by mounting a more accurate graduated circle with vertical axis and tangent screw. A good plane-parallel plate of thickness $e = 0.434$ cm. and refractive index $\mu = 1.53$ was then adjusted normal to the ray passing through it, by noting the position of reversal of motion of the ellipses both when the plate was rotated around a vertical and around a horizontal axis. The data of table 32 and figure 79 were found while the plate was rotated on its vertical axis both in a clockwise and counter-clockwise direction from the normal position. In the former case (left side of curve) the normal position showed the same constants before and after. In the latter this was not quite the case, the micrometer being not sufficiently refined for such purposes.

The results for μ were computed from the full equation

$$\Delta N \cos\theta = e \sin^2 \frac{i}{2} \cdot \left(1 - \frac{1}{\mu}\right)$$

They are as good as the small values of ΔN and the impossibility of obtaining the zero of i with sufficient sharpness admit, and they show that the latter cause adequately explains all the irregularities encountered.

The equations are liable to be cumbersome in the cases of greatest interest. I therefore proceeded experimentally to obtain a limit of Δh or Δx per fringe, using thinner glass compensators. The results are given in table 33. The ellipses were now so large and distorted that it was difficult to define the center of irregular rings. The transverse displacement is therefore largely referred to the top, middle and bottom of the spectrum band, which took up about one-third of the height or diameter of the field of the telescope. The angular width of the latter being about 3°, the corresponding angular height of the spectrum is thus about 1.0°. In view of the large rings, moreover, the displacement ΔN at the micrometer of the mirror M' is difficult to obtain and the data given are estimates. Experiments like the present must be made with optic plate-glass, so that sharp rings nearly circular may be obtained, if the data are to be quite satisfactory. In table 33, Δh thus corresponds to a transverse displacement of one component ray parallel to itself, equivalent to a displacement of the centers of ellipses of about 0.5° at the sodium line.

TABLE 33.—Vertical (transverse) displacement of ellipses. Glass-plate compensators $\mu = 1.53$. Horizontal axis. Angle of telescopic field 3°; angular height of spectrum about 1.0° or 0.175 radian. Vertical diameter of first fringe in excess of height of spectrum.

Fringe centers at	e	i	h	$\Delta h \times 10^4$	$\Delta N \times 10^4$
	cm.		*cm.*	*cm.*	*cm.*
Top of spectrum.....	0.300	0.4°	0.0007	−26	...
Middle of spectrum..		1.9	34	0	...
Bottom of spectrum..		2.6	47	+13	...
Bottom of spectrum..	.300	2.3	.0042	+22	...
Middle of spectrum..		1.1	20	00	...
Top of spectrum.....		0.0	00	20	...
B.....	0.434	40.8°	0.1274	+15	0
M.....		40.2	.1259	00	7
T.....		39.2	.1217	−42	22
B.....	.434	8.1	.0213	+12	0
M.....		7.6	.0200	00	0
T.....		f 7.1	.0187	−13	2
B.....	.434	6.5°	.0170	+29	0
M.....		5.4	.0141	00	2
T.....		4.3	.0112	−29	7
B.....	.434	f 3.3	.0087	+19	0
M.....		2.6	.0068	00	4
T.....		1.5	.0039	−29	4
B.....	.020	20.0	.00253	+14	...
M.....		9.4	.00115	00	...
T.....		−3.6	−.00044	−16	...

The mean result of all data is here about $\Delta h = 0.002$ cm., and this is not influenced in a discernible way, either by the thickness of plate e or by the rotation angle of the compensator i. The smallest value $\Delta h = 0.0012$ cm. appears incidentally and not when the system of four mirrors is most nearly in parallel adjustment. The transverse displacement of ellipses changes sign with the sign of the rotation of i in all cases and is independent of the normal position. The longitudinal displacement reverses at the normal position.

63. Broad slit interferences. Achromatic fringes.—Some allusion has been made above to a type of interferences totally different in size from the regular fringes and seen in the broadened slit. These were finally isolated and show exceedingly interesting properties. They appear to best advantage, in the absence of the spectroscope, in the broad white field of a very wide slit. The latter may be removed. They have the appearance when vertical of regular Young or Fresnellian fringes, very sharp and fine, achromatically black and white at the middle of the grid, colored and fainter outward. They are vertical when the enormously larger spectrum fringes discussed above are centered. Like these, they partake of displacement here through the broad white slit image, and this displacement is extremely sensitive in relation to the displacement of the opaque mirror M' (fig. 73) to which it is due. Thus a displacement of $\Delta N = 10^{-4}$ cm. of the latter corresponds to a march of fringes through about 0.017 of the telescopic field of 3°; *i.e.*, to 0.05°. This comprises two fringes or $\Delta N = 5 \times 10^{-5}$ cm. per fringe. Now, these fringes are so sharp and luminous that it should be possible on proper magnification to measure a few hundredths of this with an ocular micrometer. It is from this point of view that I regard the new fringes important. They supply the fine fiducial mark in displacement interferometry for which I have long been seeking. They appear in a white field, thus requiring no spectrum resolution nor monochromatic light. Moreover, the source of light need not be intense.

To have a distinctive name for these fringes which will be much used in the work following, I shall refer to them under the term "achromatic fringes." If not too large, the central fringes are straight and almost quite black and white.

The displacement of fringes with ΔN at the mirror (when $n\lambda = 2\Delta N \cos \theta$) is so rapid that if they are lost it is difficult to find them, unless the centered large spectrum fringes in the spectroscope are first reëstablished. The latter are easily found. A removal of the prism grating g, figure 73, and a widening of the slit show the achromatic fringes. The datum for sensitiveness may be found directly as follows: The displacement at the mirrors corresponds to about two residual fringes. Thus a single fringe (distance apart of the intensely black lines at the center which can be distinguished and used as fiducial lines for this very reason) corresponds to a displacement of mirror of $\Delta N = 50 \times 10^{-6}$, as above. The white pattern, as a rule, appears but once and is not usually present rhythmically, as is the phenomenon in the next section for homogeneous light.

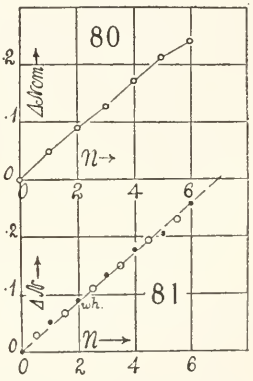
As a clue to the nature of the residual fringes, one may note in the first place that they may be recovered in the principal focal plane, if the two white slit images which may have separated be put in coincidence. Without such coincidence they are seen sharply in other focal planes.

Later, on more careful adjustment as to parallelism by the auxiliary normal method described below, periodic reappearance of the achromatic fringes was in fact obtained. The central set was exceedingly strong and sharp as usual. To the right and left of it similar patterns or groups rapidly decreasing in strength were discovered. Not more than two patterns on each side of the

central set could be seen. The white field between the patterns was several times the width of the fringed field. Each group as a whole resembles the fringes of the biprism, as usual, and they differ appreciably only in intensity and in their focal planes. It is difficult to account for this periodic reappearance; but it must be due to reflections at the half-silver surfaces. The reflections from the uncovered surfaces are indeed just visible, and naturally, since they are duplicates, they also carry the fringes. But they are easily differentiated by the relative faintness of field and have nothing to do with the recurrences in question.

Ordinary daylight is quite adequate to show the residual fringes in the complete absence of the collimator. They are superimposed on the field of view (landscape, etc.) and hence will subserve other purposes than are here given. When the adjustment for parallelism is not sharp, the fringes may often be found strong in continuously varying focal planes.

64. Wide slit. Homogeneous light. Sodium flame.—A further clue to the nature of the residual fringes will be obtained when white light is replaced by homogeneous light. A strong, large sodium flame near the mirror M, figure 73, suffices. The fringes now appear of the same size in yellow light, naturally spread over a much larger area of field. But on moving the mirror M' (ΔN increasing continually) forward very gradually, the homogeneous fringes alternately vanish and reappear, each time, however, enlarged in size (nearly doubled but still straight) until at an intermediate position of symmetry enormous round ovals cover the yellow field. The fringes then diminish symmetrically in the same way. The following data for the micrometer position corresponding to the clearest demarcations of fringes are illustrative. At least six periods (n) are easily detected on each side of the ovals ($n=0$). Thus (originally small fringes, vertical, increasing in size to huge ovals)



$n=6$	5	4	3	2	1	0, etc.
$\Delta N\times 10^3=0$	49	90	127	171	214	243 cm., etc.

These intervals, since it is impossible to establish the maximum states of presence or absence of fringes quite sharply, are practically equidistant, as figure 80 indicates. Thus the mean period of reappearance is $\Delta N=0.042$ cm.; or a path-difference of $2\Delta N\cos\theta=0.059$ cm.; or a shift of ray parallel to itself ($2\Delta N\sin\theta=0.059$ cm.) of the same amount.

The reason for this rhythm can only be the two wave-lengths of the D_1 and D_2 lines of the sodium flame, originally detected in the colors of thin plates by Fizeau. Hence a relatively enormous shift of micrometer of nearly 0.5 mm. is equivalent to the wave-length interval $\Delta\lambda=6\times 10^{-8}$ cm., or $\Delta\lambda/\Delta N=6\times$

$10^{-8}/42\times10^{-3}=1.4\times10^{-6}$. Treating the case in terms of the interferences of thin plates and two wave-lengths, λ and $\lambda+d\lambda$,

$$n\lambda=\text{constant}, \quad \text{or} \quad \frac{\Delta\lambda}{\lambda}=\frac{\Delta n}{n}=\frac{1}{n} \text{ for each period}$$

while

$$n\lambda=\frac{\lambda^2}{\Delta\lambda}=2\Delta N\cos\theta \quad \text{or} \quad \Delta N=\lambda^2/2\Delta\lambda\cos\theta$$

since ($\theta=45°$) approximately,

$$\lambda=60\times10^{-6} \text{ cm.}, \quad \Delta\lambda=6\times10^{-8} \text{ cm.}, \quad \cos\theta=0.71, \quad \Delta N=0.041 \text{ cm.}$$

agreeing as nearly as may be expected with the experimental datum. The apparatus thus serves incidentally for investigating such properties of spectrum lines as Michelson in particular has detected. Finally, with the sodium arc the data of figure 81 were found, where black dots denote fringes, open circles a clear yellow field. The mean trend is about $\Delta N=0.043$ cm. per period or wave-length gained. White fringes coincided with $n=2$.

With white light the interference grid does not usually reappear rhythmically, nor does it correspond to the zero period of figure 80—*i.e.*, to the ovals for sodium light. It was exactly of the size of the fourth period, in yellow light; it always coincides with the central ellipses of the spectroscope as stated, but does not require sharp horizontal and virtual coincidence of the superposed images. The reappearance of the achromatic fringes obviously depends on conditions different from the case of sodium light.

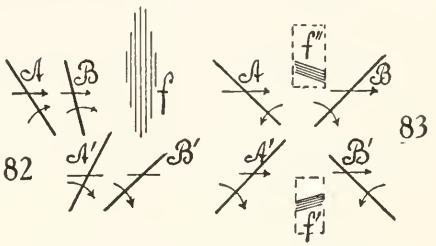
In a flash of the arc, showing many sharp spectrum lines in all colors, each of the lines gives evidence of the phenomenon—*i.e.*, if the residual fringes are oblique, each such line is strongly helical in appearance.

If a single compensator (*i.e.*, a glass plate in one interfering beam) is used and the path-difference annulled, the fringes are visible again, but very rapidly grow smaller with the increase of glass-path. If compensators of nearly like thickness and glass are used in both beams, they nearly neutralize each other if at the proper angle one to the other. But there is almost always an outstanding micrometeric difference in thickness (if ordinary glass plate is used) of great importance in modifying the residual phenomenon. The following experiments, for instance, were made with a compensator 0.944 cm. thick in the rear and 0.958 cm. thick in the front beam, both of the same glass. The half-silver mirrors were 0.7 cm. thick. The wide-slit experiments are supposed to start after the spectrum ellipses first to be found (fine slit) have been centered. The fringes are always clear and very sharp when the white slit images accurately coincide.

With the compensators A, B at the proper angle and rotating in the same direction (fig. 82), fringes of very slight enlargement were seen with the lines nearly vertical. If the compensators A, B were rotated at a proper pace in the opposite direction to each other, A, B, figure 83, the fringes f' and f'' grew rapidly smaller and turned toward the horizontal. Since the fringes are large circles and the beams here rise and fall, respectively, while a greater

glass thickness is introduced, this result is to be expected. It shows the importance of the differential glass-path.

The preceding thick half-silver mirrors (0.7 cm.) were now replaced by thinner half-silvers, the glass plates being each about 0.3 cm. thick. The fringes after being found had not appreciably changed. Another pair of half-silvers of the same thickness was then installed with like results. But now, on adding the compensators (0.944 and 0.958 cm.) as above, a marked enlargement of fringes resulted. Small differential thicknesses must here have been accidentally compensated. Opposite rotations, as in figure 83, rapidly produced very fine, nearly horizontal fringes $f'f''$. Rotation as in figure 82 left the vertical fringes nearly intact, but on passing from the position AB to $A'B'$ very marked enlargement occurred, as follows:



Mean angle of glass plates.	−45°	0°	+45°
Mean angle subtended by one fringe in the telescope.	0.0015 rad.	0.008 rad.	0.0005 rad.

The compensator plates were now exchanged and the fringes found after centering. They proved to be very much smaller, the angle subtended in the same telescope being only about 0.0002 radian. The preceding accidental compensator has therefore been destroyed by exchange.

On passing through the normal position of one plate in figure 82, the fringes usually incline toward one side or the other. Thus there can be little doubt that the fringes in question are due to slight difference of glass-path or extremely sharp glass-wedge excess in one or the other component beam. In fact, I found eventually that fringes could be enlarged by rotating the proper compensator around a vertical axis. Large fringes (up to 0.002 radian in the given telescope) are usually colored and curved and not so available as smaller fringes highly magnified. It is in this way (double rotation) that it was possible to make the white fringes coincide in order with the ovals of the fringes for homogeneous light ($n=0$), the orders met with above being the $n=2$ and $n=4$. The fringes resemble those of Fresnel's biprism; but as they are seen with a wide slit or in the absence of a slit only, as they coincide with the centered spectrum ellipses of a fine slit and as they are a definite order (second, for instance) of the fringes seen with a flame of homogeneous light, they are necessarily referable to the colors of thin plates.

Hence the equation for these fringes may be assumed to be (as may be seen from figure 84, where A and B are the compensators)

$$n\lambda=(e-e')\ (\mu\cos(r-\alpha)-\cos i)$$

when e and e' are the thicknesses of the two half-silver plates, μ their index of refraction, i the angle of incidence, r the angle of refraction of an incident ray, and where α is the outstanding angle between the faces of the differential

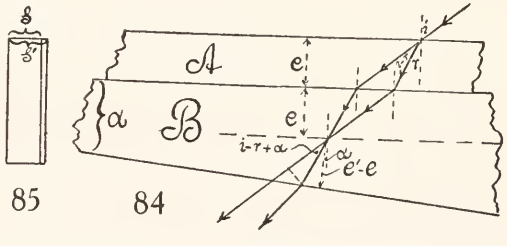
glass wedge, $e-e'$ thick at the ray in question. The possibility of throwing these fringes into any order of size, their small extent, sharpness, and great abundance of light constitute their value for measurement.

Thus it is furthermore obvious that the achromatic fringes must also be obtainable in Michelson's interferometer, in any order of size and in a field of white light. Tests were made with this object, beginning with the fine slit and the centered ellipses of the spectrum interferences. Removing the spectroscope and enlarging the slit indefinitely, the residual fringes appeared. They were never so strong and clear, however, in any order, as was the case with the Jamin interferometer, although many trials with different compensators were made. They would not be useful for measurement. Removing white light and replacing it by sodium light, the white fringes were found to be of exceedingly high order, more than 0.7 cm. of micrometer-screw being needed before the circles of the yellow field were approached. The latter were very vague and usually not seen in the principal focal plane of the telescope. Since the rays retrace their path in the Michelson interferometer, the raising and lowering of the spectrum ellipses is not possible; but the residual fringes may be put in any order by changing the differential glass-path of the rays. They appear but once, not rhythmically like the sodium fringes.

The equation for this phenomenon would thus be (since the rays retrace their paths)

$$n\lambda = 2e\mu \cos (r-\alpha)$$

where e is the thickness of the single half-silver and α its effective wedge angle, positive or negative.



To obtain the circular fringes in Michelson's interferometer with a wide slit and homogeneous light, the rays must rigorously retrace their path—*i.e.*, all reflection must take place at the same spot on the half-silver plate. When this is the case the fringes, even though obtained with common plate-glass and a sodium flame, are beautifully circular and sharp. This is due to the fact that so small a part of the plate is used. They are stationary and exhibit the Fizean periods due to the doublet D_1D_2, admirably. With white light the fringes are faint and useless. When the rays do not accurately retrace their paths—*i.e.*, when there are two spots of light on the half-silver one or more centimeters apart—the fringes are soon linear and very small, as above.

With regard to the last equation, if N is the *difference* of normal distances to the two opaque mirrors (M, N) of the Michelson interferometer, from the

two respective extremities of the normal to the half-silver, at the point where the incident ray impinges on it, the equation may be more completely written

$$n\lambda = 2e\mu \cos R - 2N \tag{1}$$

if α is temporarily disregarded. N is independent of color λ, but otherwise represents the difference of air-paths of the two interfering rays. From this equation

$$\frac{d\lambda}{dn} = \frac{\lambda^2}{2e(\mu \cos R - (\lambda/\cos R)(d\mu/d\lambda)) - 2N} \tag{2}$$

so that the center of ellipses is at λ in the spectrum when

$$N = N_c = e\left(\mu \cos R - \frac{\lambda}{\cos R}\frac{d\mu}{d\lambda}\right) \tag{3}$$

Furthermore,

$$\frac{d\lambda}{dN} = \frac{\lambda}{N - N_c} \tag{4}$$

and $$n = \frac{2e}{\cos R}\frac{d\mu}{d\lambda}$$ depends essentially on $\frac{d\mu}{d\lambda}$

On the other hand, in case of homogeneous light of wave-length λ,

$$\frac{di}{dn} = \frac{\lambda}{2\mu \cos R.\,(de/di) - 2e \tan R \cos i} = \frac{\lambda}{n\lambda(de/e)/di - 2e \tan R \cos i} \tag{5}$$

where de/di may be either positive or negative.

Centers occur when

$$\frac{de}{di} = \frac{e \tan R \cos i}{\mu \cos R} \quad \text{or} \quad \frac{de}{dR} = e \tan R \tag{6}$$

Thus di/dn is never independent of λ and the centers of equation (6) are, as a rule, quite different from those of equation (3). If the angle α is admitted, equation (6) takes the form

$$\frac{de}{dr} = e \tan R\,(1 - 2\alpha/\sin 2R) \tag{7}$$

The occurrence of the residual fringes for the same adjustment of the micrometer as the centered spectrum fringes is thus incidental. To obtain the latter the two superimposed spectra of a fine slit must coincide horizontally and vertically throughout their extent—*i.e.*, the two linear white slit images must coincide. If now the slit is indefinitely widened, there are two vertical lines in the superposed broad white images which are completely in coincidence. In case of ordinary plate-glass the remainder of the images will not be mutually in coincidence or generally there can not be coincidence in every color. The residual or achromatic fringes are found at and near the line of coincidence in question. Hence if either opaque mirror is slightly rotated on a vertical axis the residual fringes pass from edge to edge of the broad white slit images, S and S', figure 85, of slightly unequal width. Thus if the mean breadth is S and the difference of breadth $\Delta S = S' - S$, the very small

angle corresponding to ΔS is measured by the motion of the fringes over the relatively large angle S. Hence this is a sensitive method for measuring angles which will be utilized below.

Finally, the cause of displacement is to be given. If the fringes were homogeneous in light, they would fill the whole field and simply wander indistinguishably to or from the center of homogeneous circles when the micrometer is moved. But when white light is used the phenomenon is narrowed to a few fringes systematically grouped about two sharply distinguishable achromatic vertical fringes in the middle. The displacement of these is thus accurately measurable and they may always be brought back to the field of the telescope. Moreover, the distance apart of two black fringes must correspond to the mean wave-length of light—*i.e.*, if ΔN is the displacement of the micrometer mirror corresponding to a fringe-breadth for the angle of incidence i (here 45°),

$$2\Delta N \cos i = \lambda$$

or

$$\Delta N = \lambda/2 \cos i = 60 \times 10^{-6}/2 \times 0.707 = 43 \times 10^{-6} \text{ cm.}$$

agreeing reasonably closely with the above rough estimate of $\Delta N = 5 \times 10^{-5}$ cm.

If we take the equation for the residual fringes in the Jamin apparatus as

$$n\lambda = \epsilon(\mu \cos R - \cos i)$$

where $\epsilon = e - e'$ is the differential thickness of the compensators and the residual angle α is neglected (fig. 84),

$$\frac{di}{dn} = \frac{\lambda}{(\mu \cos R - \cos i)\,(d\epsilon/di + \epsilon \sin R/\mu \cos R)}$$

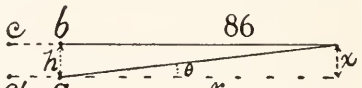
so that for large fringes the compensators must be so chosen that both ϵ and $d\epsilon/di$ may be small, where $d\epsilon/di$ may be either positive or negative.

The last equation may be written

$$\frac{di}{dn} = \frac{1}{\left(\frac{d\epsilon/\epsilon}{di} + \frac{\sin R}{\mu \cos R}\right)n}$$

and accounts for the rapid decrease of size of fringes with the differential thickness of the plate compensators.

65. Vertical displacement.—In conclusion, the rise and fall of spectrum fringes (*i.e.*, the transverse motion observed and utilized when a compensator of the form figure 77 rotates on a horizontal axis) must be considered. This method was used above for centering the spectrum fringes. Naturally the actual motion of centers is obliquely upward or downward, unless the increase of glass-path is compensated by the micrometer at the opaque mirror. The rays leaving the collimator are parallel in a horizontal plane only. They are not collimated in a vertical plane. Hence these rays intersect at the



conjugate focus of the objective of the collimator, usually somewhere between the mirrors $M\,M'$ and $N\,N'$ in figure 73. This intersection is nearly in a horizontal line, owing to the horizontal width of the collimated beam. Hence as in figure 86 there are two virtual linear sources of light, a and b, normal to the plane of the diagram, the rays from which may be treated for practical purposes as capable of interfering, since they come originally from the identical slit of the collimator. The effect of rotating the compensator (fig. 77) on a horizontal axis is thus to move these linear sources, a and b, through each other vertically, and hence their distance apart may be called h, where if d is the compensator thickness, i, r angles of incidence and refraction at the compensator, μ its index of refraction,

$$h = d\,(\sin i - \cos i \tan R) = di\frac{\mu - 1}{\mu} \text{ nearly}$$

The fringes will thus be larger as h is smaller (fig. 86), in accordance with the equation

$$\frac{\lambda}{h} = \frac{x}{r} = \theta$$

where x is the distance apart for the distance r and θ the angle between two fringes observed in the telescope, for instance.

Experiments were made to test the last equation by attaching an ocular micrometer to the telescope, so that if x is the distance and r the length of the telescope, θ is given. The distance between fringes in the same part of the field was then measured from different angles of incidence i at the compensator. The results were, if $\lambda = 6 \times 10^{-5}$ cm., $r = 19.5$ cm. (table 34).

TABLE 34.

i	$h \times 10^3$	$(\lambda/h) \times 10^3$	x	$(x/r) \times 10^3$
0°	0 cm.	0.0	(0.2) cm.	
3.6°	22	2.8	.05	2.6
6.6°	40	1.5	.03	1.5
8.6°	51	1.2	.025	1.3

These results for $\theta = \lambda/h$ and $\theta = x/r$ may therefore be considered as identical, since the fringes vary in size within the field of the telescope.

Finally, a displacement ΔN at the opaque mirror will move the virtual sources a and b in a horizontal plane, $2\Delta N \cos I$ in the direction of rays and $2\Delta N \sin I$ transverse to that direction if I is the angle of incidence. Hence b is usually found at some point c and moves into c' by the rotation of the compensator in question about a horizontal axis. The fringes do not therefore necessarily pass through infinite size unless c is at b, which would then pass through a. The condition of maximum sensitiveness in transverse displacement is therefore a large fringe-angle θ, a condition which requires use of optic plate. Fringes subtending 1° would admit of $\Delta h = 3.5 \times 10^{-3}$ cm.

per fringe, and that is about the mean value obtained in table 33 and elsewhere. In the present mode of treatment merely practical conveniences are aimed at. A more uniform method will be given in the next chapter.

66. Angular displacement of fringes.—Having for other purposes installed an ocular micrometer in connection with the telescope, it seemed worth while to make a direct test of the equations given elsewhere.* These are apart from signs

$$\frac{d\lambda}{dN_c} = \frac{\lambda e}{\cos R}\left\{\frac{\tan^2 R}{\mu}\left(\frac{d\mu}{d\lambda}\right)^2 + \frac{d^2\mu}{d\lambda}\right\}$$

When $\mu = A + B/\lambda^2$, $\lambda = D(\sin i - \sin\theta)$, and when two plates, the half-silver of thickness e and angles of incidence i (constant) and of refraction R, and a compensator of thickness E and at normal incidence are included, these may be changed to

$$\frac{d\theta}{dN_c} = \frac{\lambda}{(2B/\lambda^2)\, D\cos^2\theta}\left\{\frac{1}{\frac{e}{\cos R}\left(3 + \frac{2B}{\lambda^2}\,\frac{\tan^2 R}{\mu}\right)} + \frac{1}{3E}\right\}$$

Here $d\theta/dN_c$ is the displacement of the center of ellipses per centimeter of displacement of the normal micrometer at one opaque mirror of the Michelson device, for the wave-length λ. D is the grating constant and θ the angle of diffraction. In the apparatus used $D = 167\times10^{-6}$ cm., $\theta = 20°40'$ at D line, $i = 30°$, $R = 19°\ 5'$ in case of glass and $17°\ 52'$ in case of carbon-bisulphide plates; $\lambda = 58.93\times10^{-6}$ cm.; $B = 4.6\times10^{-11}$ or $2B/\lambda^2 = 0.0265$, $\mu = 1.53$ (glass). Under these circumstances the term

$$2B\tan^2 R/\lambda^2\mu = 0.0021$$

and may be neglected in comparison with 3. Thus the equation takes the simpler form

$$\frac{d\theta}{dN_c} = \frac{\lambda}{(6B/\lambda^2)\, D\cos\theta}\,\frac{1}{E + e/\cos R}$$

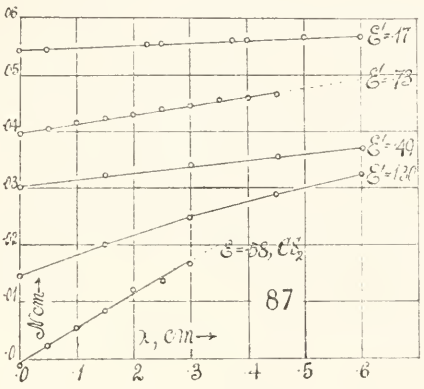
The values of E and e are given in table 35. The data marked $d\theta/dN_c$ (computed) in the table were found from the last equation.

TABLE 35.—Reduction of sensitiveness by glass thickness. $D = d/\cos r$. Incidence at $i = 30°$, $R = 19°\ 5'$ (glass), $17°\ 52'$ (CS_2), compensators normal. Glass: $\mu = 1.53$; CS_2, $\mu = 1.63$. Telescope 19.5 cm. long. $2B/\lambda^2 = 0.0265$. $D = 167\times10^{-6}$ cm. $\theta_D = 20°\ 40'$.

Detail.	e	E	Glass. $ed/\cos R$	CS_2 $E/\cos R$	Total $E' \pm E + e/\cos R$	$\frac{dx}{dN_c}$	$\frac{d\theta}{dN_c}$ observed.	$\frac{d\theta}{dN_c}$ computed.
	cm.	*cm.*	*cm.*	*cm.*	*cm.*			
Glass+CS_2...	+0.27 to 0.27	0.60	.0	0.63	0.63	33	1.70	
Glass+glass	0.695	.562	.735	.562	1.297	63	3.2	3.7
Glass.....	.695	.0	.735	.0	.735	126	6.5	6.5
Glass−glass	.695	.247	.735	.247	.488	182	9.3	9.7
Glass−glass	.695	.562	.735	.562	.173	500	25.64	27.6

* Carnegie Inst. Wash. Pub. No. 229, 1915, p. 74 *et seq.*, §§ 40, 41. In equations (13) and (18) $d\lambda/dN_c$ and $d\theta/dN_c$ should be inverted and $D\cos\theta$ in the latter put in the numerator.

If x is the displacement in centimeters in the ocular, $\theta = x/19.5$, the denominator being the length of the telescope. The successive values of x in terms of N, the mirror displacement, are given graphically in figure 87 for the different values of $E' = E + c/\cos R$ in question, and from them $d\theta/dN_c$ was taken graphically. All the curves are appreciably straight, except the one for $E' = 1.3$ cm., which is definitely curved.



The values of $d\theta/dN_c$ observed and computed obviously agree as closely as may be expected for mean conditions of the spectrum between green and red and of the mode of procedure. The small coefficient for carbon bisulphide is, moreover, in keeping with its large value of B or high dispersion. In a sensitive displacement interferometer B like $E'D$ should all be small; but unfortunately this implies large ellipses. The beautiful small ellipses obtained with the carbon-bisulphide plate are of little avail because of their sluggish motion. In fact, the small thickness of the carbon bisulphide layer and the reduced coefficient observed are quite striking in comparison with glass. Moreover, since for an order n

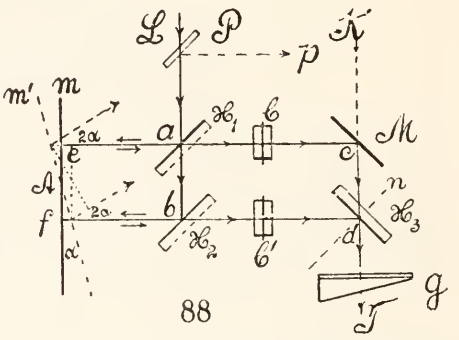
$$\frac{d\theta}{dn} = \frac{1}{2} \frac{\lambda^2}{D \cos\theta \,(\cos R + 2B/\lambda^2 \cos R) - N}$$

the effect of a large B, though it reduces the general size of ellipses, does so but slightly, since the term in B can not be more than a few per cent (3 to 6) of the other term in the binomial.

CHAPTER VI.

THE DISPLACEMENT INTERFEROMETRY OF SMALL ANGLES AND OF LONG DISTANCES. COMPLEMENTARY FRINGES.

67. Parallel rays retracing their path.—The following method was devised with a view to the micrometric measurement of angles. It will be used elsewhere in connection with an electrometer for reading microvolts. An interference method of a different kind for measuring small angles was developed some time since and used at length in connection with the deviation of the horizontal pendulum.* Again, the electrometer was treated in different ways† by the aid of the interferometer. The present method, however, will differ from all of these. In figure 88, L is a horizontal beam of white light from a collimator after passing through the auxiliary clear plate P (to be used preliminarily for parallelizing the mirrors of the system in a way presently to be shown), the beam is reflected at a and b by the half-silver plates H_1 and H_2 respectively, to the wide opaque mirror m. The rays now retrace their paths or nearly so, to be in turn transmitted at a and b by the half-silvers H_1 and H_2. These transmitted pencils similarly impinge on the opaque mirror M and the half-silver H_3 at c and d respectively, and pass thence (the ray from c being transmitted) into the telescope at T. The direct-vision grating prism g may be swiveled in place or removed at pleasure.



88

To bring the system of four mirrors into complete parallelism is here of considerable importance if the spectrum fringes or the achromatic phenomenon are to be adequately large for measurement. The presence of the common mirror m, however, suggests the procedure. When the clear plate P is in place, the rays ae and bf on returning are also again reflected at a and b toward L and may be clearly seen in a telescope at p. Hence if m is the standard plane and nearly vertical, the mirrors H_1 and H_2 will be parallel when the slit images seen at p coincide horizontally and vertically, while H_1, H_2, and m will have their common normal plane in the diagram. In the same way the mirrors M and H_3 may be parallelized with their common normal plane in the diagram. Again, the return rays aL and bL may be projected on the objective of the collimator, or on a small screen near it, by correspondingly focusing the collimator. The two sharp slit images are put in coincidence

* Carnegie Inst. Wash. Pub. No. 229, § 19 *et seq.*, 1915. † *Ibid.*, § 67 *et seq.*

horizontally and vertically. This is usually more convenient and as a rule adequate. Other methods are given below.

If the distances *ac* and *bd*, *ab* and *cd* have previously been made nearly equal and the angles approximately 90°, the fringes will usually be found on moving the micrometer-screw normal to H_3.

As the mirrors are thick glass plates, it is preferable that the half-silvered sides of H_1 and H_2 be toward L and the half-silvered side of H_3 toward T. In this case each ray passes the plates twice, as indicated in figure 88. With ordinary plate-glass the fringes when found are still apt to be small. They are then to be enlarged and centered, by compensator of clear glass C and C', in the two rays respectively, rotated in opposite directions around a horizontal axis until the center of ellipses is in the field of the spectroscope. It may be necessary to actuate the micrometer-screw at d to complete the adjustment. If m is adjustable on two axes, the compensators C, C' are superfluous, as will presently appear.

When the ellipses are centered, the direct-vision spectroscope g removed, and the slit widened or removed, the residual or achromatic fringes appear in sight and are ready for use. These are always strong. The spectrum fringes are apt to be less so, since the parts of the ray L pass through two half-silvered surfaces, $H_1 H_2$ or $H_1 H_3$, in succession. The spectrum fringes are only sharp when the slit is fine. If the white residual fringes are too dazzling, a single or two half-silvers may be placed before the objective of the telescope with advantage. Two plates with their half-silvered sides in contact and held so by a steel clip are excellent for this purpose, while they are at the same time protected from sulphur corrosion. This, in fact, is the best method of preserving silver mirrors (in pairs) when not in use.

If α is the fraction of light transmitted and $1-\alpha$ reflected, the fraction of the original light L reaching the telescope T will be $2\alpha^2(1-\alpha)^2$. This is a maximum if $\alpha = \frac{1}{2}$. Thus the illumination is reduced to $\frac{1}{8}$.

When the spectra are in coincidence and the fringes sharp, the mirror m may be rotated around a vertical axis at A into some position, m'. In such a case the two spectra will move through the field of the telescope at T, but their coincidence will not be destroyed. The D lines, for instance, will continue to be superposed throughout. Considerable path-difference is, however, introduced in this way, and hence the fringes will march through the spectrum at an *enormously* more rapid rate. The following data may be given, where α is the angle of rotation of the mirror m and N the reading of the micrometer at H_3 (screw in the normal dn) necessary to bring the center of ellipses back to the sodium lines. In both cases the centers were out of the field above or below, so that horizontal fringes were made the criterion for adjustment. This method is somewhat rough, but adequate for the present purposes.

(1) Fine thin fringes. Relatively large glass-path. Distance *ab*, figure 88, $2R = 21$ cm. Thickness of glass plates (half-silvers), $e = 0.70$ cm.

α	$=0°$	0.05°	0.20°	0.30°	0.40°	0.50°	0.60°
$N \times 10^3 =$	23	30	128	162	215	258	299 cm.

This is curve *a* in figure 89. From it the mean rate

$$\frac{\Delta N}{\Delta \alpha} = 0.47 \text{ cm./degree, or } 27 \text{ cm./radian}$$

may be found.

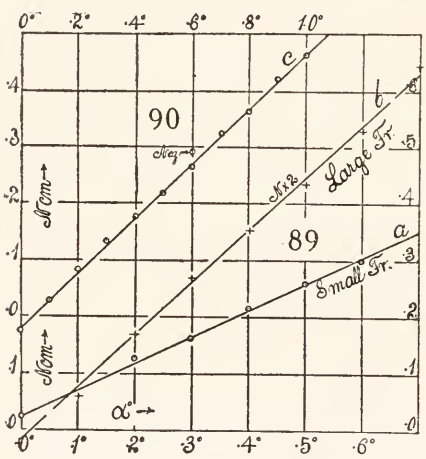
(2) Coarse large fringes. Smaller differential glass-path.

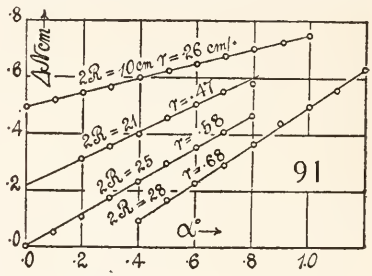
$\alpha =$	0°	0.1°	0.2°	0.3°	0.4°	0.5°	0.6°	0.7°	0.8°	0.9°	1.0°
$N \times 10^3 =$	−25	+29	84	134	176	217	265	323	365	420	467 cm.

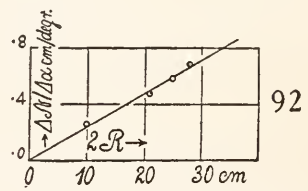
This is the curve given (with double ordinates for distinction) in curve *b*, figure 89, and in figure 90. Besides this the datum $\alpha = -0.6°$, $N = -0.320$ cm. was obtained. In figure 90 the mean rate is

$$\frac{\Delta N}{\Delta \alpha} = 0.465 \text{ cm./degree, or } 26.6 \text{ cm./radian}$$

agreeing with the preceding as closely as may be expected. We may thus estimate $\Delta N = 27 \times 10^{-6}$ of displacement at the micrometer at H_3 per micro-radian of turn α at the mirror m, which amounts to a little less than one interference ring per micro-radian (about 0.2 second of arc) of turn. Moreover, turns of α less than a few degrees are certainly measurable. Through-







out all this work the achromatic fringes are also available for precision in N, but for this reason are more difficult to manipulate if individual fringes are treated. They may, moreover, be much enlarged by rotating the mirror m and advancing the micrometer at H_3 in small steps in such a way as to produce contrary effects and thus keep the achromatic fringes in the field. If the fringes leave the principal focus, the micrometer at H_3 and its adjustment screws may be actuated together in the same way. This is the most available method for eliminating the glass-path, so that enormous spectrum ellipses are obtainable. Finally, three groups of achromatic fringes (on each side of the strong central group) were noticed, the distance apart of groups corresponding to about $\Delta N = 0.0014$ cm.

It is obvious that $2\Delta N \cos i$ will increase with $2R$, the distance apart of the parallel rays *ae* and *bf*, figure 88, as well as with the rotation α. But the relations are not obvious, and experiments were therefore made for the relation of ΔN and α in case of different distances apart ($2R = 10, 21, 25, 28$ cm.) of the rays in question. The results are given in figure 91, where the abbreviation $r = \Delta N/\Delta\alpha$. In figure 92 and table 35, furthermore, this value, as obtained from figure 91 graphically, is compared with $2R$. The results are not quite smooth; but as $2R$ is the distance apart of two spots of light, it can not be specified sharply. Moreover, a variety of other discrepancies of adjustment enter which need not be detailed here. From figure 92 it appears that on the average $r/2R = 0.024$ in terms of degrees or $= 1.35$ in terms of radian. Hence we may consider an equation of the form

$$2R\Delta\alpha = \Delta N \cos i$$

So computed $\cos i$ would be 0.73 instead of 0.71, but the difference is referable to the outstanding glass-path and outstanding air-paths which have not been included.

68. Groups of achromatic fringes.—With the good adjustment stated, a number of further experimental measurements of the mean position (ΔN) of the fringe patterns on the micrometer at H_3 were made, with results as follows: The size of the individual fringes was about $0.0225/35 = 0.00064$ radian in the telescope at T—*i.e.*, about 0.034° of arc. The fringe patterns will be designated primary, secondary, etc. The data are $10^3\Delta N$ cm.

Tertiary.....	+2.6	2.7	...	...	2.7 cm. $\times 10^{-3}$
Secondary.....	+1.3	1.2	1.3	1.4	1.4
Primary.....	±0.0	0.0	0.0	0.0	0.0
Secondary.....	−1.3	1.1	...	1.2	1.2

One group was visible on one side and two on the other and one or more frequently escaped capture by the micrometer. The wave-length difference of these positions is exceedingly small. Using the above expression, $\Delta\lambda = \lambda^2/2\Delta N \cos\theta$,

$$\Delta\lambda = \frac{36\times 10^{-10}}{2\times 1.3\times 10^{-3}\times 0.71} = 1.9\times 10^{-6} \text{ cm. nearly}$$

But there is no suggestion in this datum. The displacement ΔN is equivalent to a glass thickness e, where $\Delta N = e(\mu - 1)$, roughly. Hence $e = 1.3\times 10^{-3}/53 = 0.0025$ cm. This precludes the possibility of reflections from the two sides of the half-silver film, since this is about 1,000 times thinner, apart from its index of refraction.

Some experiments were also made with the primary achromatic fringes (treated as a single group and not individually, as the angle of measurement of α was not correspondingly delicate) to determine $\Delta N/\Delta\alpha$. Two series with different adjustments showed results as given in table 35 ($2R = 21$ cm.).

TABLE 36.

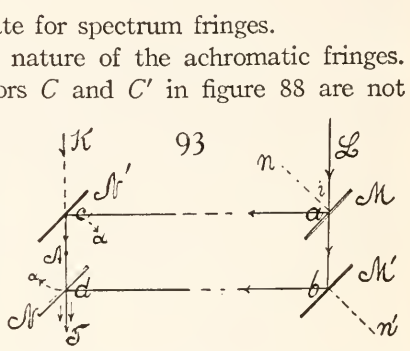
Fringes—	Series I.		Series II.	
	α	$N\times10^3$	α	$N\times10^3$
Smaller.....	−0.2	112	−0.2	114
Smaller.....	− .1	47	− .1	63
Very large.....	± .0	0	± .0	0
Smaller.....	+ .1	56		...
Smaller.....	+ .2	111		...
Smallest.....	+ .3	170		...

These data contain the new result that the achromatic fringes decrease in size with great rapidity in both directions of the increments from the central position ($\alpha=0$). Two sets were usually present. The rate of growth as well as the ratio $\Delta N/\Delta\alpha$ is not the same on both sides of the position of maximum size ($\alpha=0$). The mean coefficient may be found graphically as

$$\frac{\Delta N}{\Delta\alpha}=0.56 \text{ cm./degree or } 32 \text{ cm./radian}$$

which is larger than the preceding estimate for spectrum fringes.

This experiment bears directly on the nature of the achromatic fringes. It shows, moreover, that the compensators C and C' in figure 88 are not essential and that ellipses may be centered by rotating the mirror m on a horizontal and vertical axis. It is, in fact, possible to increase the achromatic fringes indefinitely in size in this way; but with ordinary glass they eventually become sinuous and no longer useful. When the slit is fine and the ocular out of focus, well-marked hyperbolic patterns may be recognized; but these become straight on returning to the wide slit in focus.



69. Measurement of small angles without auxiliary mirror.—This method makes use of the original apparatus, figure 73, but the two mirrors M and M' or N and N', figure 93, are rotated together as a rigid system around a vertical axis, at A, for instance. In view of the absence of auxiliary reflection, the method will be but half as sensitive as the preceding one, so that the equation

$$R\Delta\alpha=\Delta N\cos i$$

is sufficient to express the results. But on the other hand, if spectrum fringes are to be observed, there is greater abundance of light, since the half-silver film is penetrated but once by each component, ac or bd. When the achromatic fringes are used the light is always superabundant and must be reduced in intensity. To try this method the mirrors N and N' were mounted on a good divided circle so as to rotate together on a rigid arm over a small angle α. The achromatic fringes displaced in this way were restored by advancing

the mirror M' over the distance ΔN along the normal micrometer-screw at n'. The following is an example of the results of corresponding values of ΔN and $\Delta\alpha$, when the distance apart of the rays ac and bd was $2R=7$ cm.:

α	$=0.0°$	0.1°	0.2°	0.3°	0.4°	0.5°	0.6°	0.7°	0.8°	0.9°	1.0°
$\Delta N\times 10^3=$	0.0	8.0	16.6	25.6	34.9	42.7	50.7	61.7	70.5	78.5	90.6 cm.

These results as a whole are much smoother than above, for incidental reasons. From a graphic construction the mean rate $\Delta N/\Delta\alpha=0.088$ cm./degree or 5.0 cm./radian may be obtained. Hence, since $2R=7$ cm. $(\Delta N/\Delta\alpha)/2R=0.013$ in terms of degrees or 0.72 in terms of radians (table 37). This result is roughly half the preceding, if incidental errors be disregarded. From the above equation, since $I=45°$ nearly,

$$\frac{\Delta N}{\Delta\alpha}=\frac{2R}{2\cos i}=\frac{7.0}{1.41}=5.0 \text{ cm./radian}$$

agrees closely with the experimental result.

TABLE 37.—Values of $r=\triangle N/\triangle\alpha$ micrometer displacement per degree of mirror rotation.

A. Case of auxiliary mirror, fig. 88.				
Series No.	$\frac{\triangle N}{\triangle\alpha}$	$\frac{\triangle N}{\triangle\alpha}$	$2R$	$\frac{\triangle N}{\triangle\alpha}\Big/2R$
	cm./°	*cm./rad.*	*cm.*	*mean.*
6, 7; 1, 2	0.47	27	21	0.024[1]/ degree
8	.58	33	25	1.35[1]/ radian
9	.68	39	28	
10, 11	.26	15	10	
B. Case of rotating pairs of mirrors, fig. 93.				
1	0.088	5.0	7	0.0126[1]/degree .72[1]/radian

70. Complementary fringes.—Some additional attention was now given to the hyperbolic fringes of a fine slit and white light observed when the ocular is drawn outward or to the rear of the position for the principal focus and the spectroscope is removed. They appear and widen with the washed image of the slit. They are quite strong, sharp throughout, and gorgeously colored, the fields and shades, figure 94, *a*, being nearly complementary in color. The spectrum fringes must be centered if the others are to occur. The former, figure 94, *b*, are usually long ellipses or hyperbolic with their major axes horizontal, while the corresponding new fringes are hyperbolic with the major axes vertical. They are extremely sensitive to rotation of the micrometer mirror about a horizontal axis, rising or falling, but they soon vanish. When the micrometer mirror is rotated around a vertical axis, an operation which separates the white slit images if originally coincident, the new fringes move bodily by displacement from left to right, or the reverse, depending on the sign of the rotation, while they continually change their color-scheme. When the design is thus displaced as a whole the individual fringes move as shown

in figure 94, *a*. As a group the fringes closely resemble the lemniscates of a binaxial crystal in polarized light. The variation of the color-scheme is probably the same, since with sodium homogeneous light the design is in yellow and black. The pattern is not quite dichroic, but appears so, red-green, blue-yellow combinations with an intermediate violet-yellowish succeeding each other. In polarized light the figures are sharpened as a whole, but there is no discrimination. The pattern gradually vanishes with a wide slit, whereupon the achromatic fringes may be seen when the ocular is restored to the principal focal plane.

If the white slit images pass through each other (in consequence of the vertical rotation specified) the direction of fringes twice changes sign in rapid succession, and this probably occurs when the white slit images are coincident. Barring this inversion, the march is regularly proportional to the rotation.

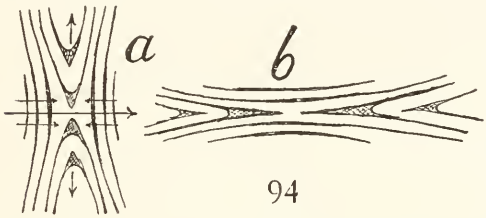
With the displacement (ΔN) of the mirror on the micrometer-screw normal to its face, the fringes pass through a continuous succession of color-schemes, but soon vanish, for they coincide in adjustment with the centered spectrum fringes. Similarly, if a pair of mirrors ($M\,M'$ or $N\,N'$, fig. 93) rotates about a vertical axis as a rigid system, the same continuous change of color-scheme and evanescence is apparent.

These interferences differ, naturally, from the spectrum interferences; they also differ from the achromatic interferences, which are much finer fringes, partaking of the regular fringe pattern seen with biprisms. They are a separate phenomenon, quite sharp and definite, occurring under like conditions of adjustment, but under different conditions of observation (ocular out of focus and fine slit). In the principal focus the two sharp, extremely bright slit images are alone present. They are absolutely identical in structure, however, and their spectra when superposed would interfere symmetrically throughout their extent. Under these circumstances the rays intersecting in the white slit images also interfere before and behind the principal focal plane of the telescopic images specified, and this interference is not destroyed when the slit images are separated (rotation of opaque mirror about vertical axis), or when the slit images are passed through each other. What is not easily seen, however, is the reason of the occurrence of large, sharp, definite hyperbolic forms instead of the usual Young or Fresnel fringes of two slits or slit images.

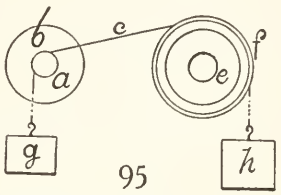
On the Michelson interferometer these fringes, like the achromatic fringes, are extremely faint and can hardly be detected except by putting them in slow motion. The spectrum fringes are equally strong in all cases. It appears, therefore, that the two half-silvers are favorable to evolving both the hyperbolic and the achromatic sets of fringes. The Michelson design is thus not useful here, nor for the measurement of small angles of rotation by the methods described, as the mirrors would have to be rotated in opposite directions.

Further work with the complementary fringes on different interferometers of the Jamin type showed that to produce the hyperbolics the fine slit images

must coincide horizontally and vertically. They do not in this case probably coincide in the fore-and-aft direction, for the plates, etc., are not optically flat. When the slit images are separated at the same horizontal level into two fine parallel lines, the complementary fringes in fact become Fresnellian fringes, finer as the slit images are more separated and as the ocular is more rearward or forward. This is precisely what should occur. We may conclude, therefore, that the complementary fringes are Fresnellian interferences of two slit images and that the central hyperbolic forms are due to outstanding front and rear positions of the two slit images, which seem to coincide in the field of the telescope. Differentiated from these, the achromatic fringes are referable to the colors of thin plates. I have, in fact, also succeeded in obtaining the complementary fringes in the shape of broad, straight, gorgeously colored vertical bars, without suggestion of hyperbolic contour.



94



95

An attempt was made to get quantitative estimates of the passage of fringes on rotating the paired mirrors over an angle α. To control the small angles the device, figure 95, was improvised and did good service. Here e is the tangent screw of a divided circle 6 inches in diameter. It is surrounded by a snug annulus of cork and holds the brass ring f, on whose surface a coarse screw-thread has been cut. Near this and with its axis in parallel is a quarter-inch screw a and socket (not shown) controlled by the disk b. A strong linen thread c is looped once around f in the grooves of the screw and once or twice around a, the string being normal to the cylinders and kept taut by two small weights, g about a half ounce and h about an ounce. The head b may be turned either way and the angle read off in minutes on the head of the tangent screw e.

The theoretical value, apart from glass-paths and other corrections, should be, per fringe vanishing,

$$2R\Delta\alpha=\lambda$$

where R is the radius of rotation corresponding to the angle $\Delta\alpha$ and λ the mean wave-length of light. In the given adjustment, $2R=10$ cm. was the normal distance apart of the two interfering beams. Hence

$$\Delta\alpha=\frac{\lambda}{2R}=\frac{60\times10^{-6}}{10}=6\times10^{-6}\text{ radians or }1.2''$$

per vanishing fringe. As the change of glass-path of one beam would have to be deducted from $2R$, a somewhat larger value would be anticipated. Testing the complementary fringes (white light), the passage of about 25

fringes completed the phenomenon, after which it paled to whiteness. These 25 fringes passed within $\Delta\alpha = 0.75'$, or per fringe about $0.03'$ or $1.8''$ of arc. Of course, this is merely an estimate from the small angles of turn involved.

The complementary fringes with sodium light are available indefinitely. I counted about 100 fringes for an angle of $2.7'$—*i.e.*, $1.6''$ per fringe.

Finally, using the spectrum fringes of the spectroscope, about 120 fringes were counted within $3'$—*i.e.*, $1.5''$ per fringe. All of these values are larger than the computed value $\lambda/2R$ without correction, but in view of the large number of fringes within exceedingly small angles $\Delta\alpha$, sharp agreement is not to be expected.

71. Equations.—To completely trace out the air- and glass-paths in the present apparatus would lead to complicated equations of no further interest here. I have, therefore, contented myself with the preceding experimental result, which is probably more accurate than it appears. To the first order of small quantities one may assert that the rotation of the mirror m (fig. 88) over an angle α (here to be called $\Delta\alpha$) cuts off the path $2R\Delta\alpha$ from the b ray and adds the same path to the a ray. Hence the total change of path is $4R\Delta\alpha$.

Again, though the additional glass-paths at H_1 and H_2 (being equally incremented for both the a and b rays) compensate each other, this is not true at H_1 and H_3 for the b and a rays. Since the b ray at H_3 receives no increment, the total glass-path increment at H_3 is effective. The glass-path z at H_3 may be written as heretofore,

$$2e\left(\sin^2\frac{i}{2} - \mu\sin^2\frac{r}{2}\right)$$

and hence if $\Delta i = -2\Delta\alpha$, since i is decreased by 2α at H_3, the glass-path incremented (dz/di), Δi may be found by differentiation to be

$$-2\frac{e\sin(i-r)}{\cos r}\Delta\alpha$$

Finally, the compensation at the micrometer-screw at d is $2\Delta N\cos i$. Hence when the center of ellipses is restored to the fiducial line,

$$\frac{\Delta N}{\Delta\alpha} = \frac{4R - 2e\sin(i-r)/\cos r}{2\cos i}$$

Here $2R$ is the normal distance between the a and b rays, e the thickness of the glass-plate H_3, and i, r the angles of incidence and refraction.

In the apparatus $2i$ was not measured, but made nearly 90° by eye adjustment. $2R$ was measured. Hence, in the first set of experiments,

$$i = 45°,\quad \mu = 1.53,\quad r = 27.5°,\quad 2R = 21 \text{ cm.},\quad e = 0.70 \text{ cm.}$$

and

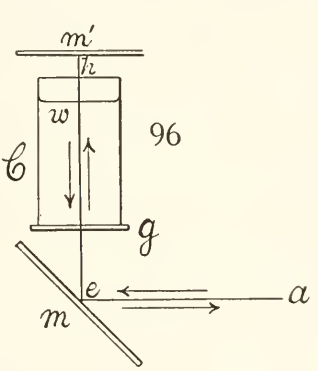
$$r = \frac{\Delta N}{\Delta\alpha} = \frac{42 - 2\times 0.70\times 0.30/0.89}{2\times 0.707} = 29.5\frac{\text{cm.}}{\text{radian}}$$

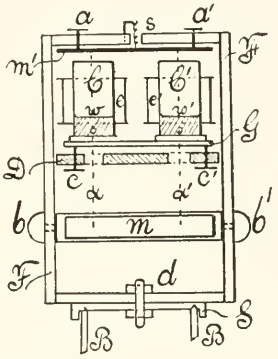
This is larger than the corresponding experimental value 27 cm./radian, but

no more so than the estimated data imply. In fact, the particular adjustment for achromatic fringes gave a larger result $r = 32$ cm./radian, for reasons not apparent. One may note that the correction for glass-path is small.

With regard to the application to the electrometer, we may come to the following conclusion: A good instrument of the quadrant or similar type should give about a radian of deflection per volt, or a microradian per microvolt. In the present interferometer the microradian is about equivalent to the passage of one interference fringe. Hence one fringe per microvolt is about the order of sensitiveness obtainable.

72. Separated rigid vertical system.—The method used above, of attaching the deflecting mirrors at 45° to the U-tubes, is faulty in design and difficult to adjust. It was, therefore, subsequently discarded in favor of the rigid deflecting system, figure 96, consisting of a wide mirror at 45°, m, and





a horizontal mirror m'. Both must be provided with adjusting screws for axes respectively parallel to the traces m and m' and normal to the diagram, if the fringes when found are to be centered and enlarged. It is particularly essential that the framework supporting m and m' be rigid, otherwise the quiver introduced here is superposed on and accentuates the corresponding tendency of the very mobile liquid column. This is contained in the brass tube C (with glass window at g) which is supported on an independent standard, rigidly. There are two of these tubes (C, C', fig. 97), side by side, parallel, and at the same level, one for each component beam. As the rays aeh are to retrace their path, the apparatus, figure 88, should be used, with the mirror m of that figure tilted up as in figure 96. Hence the two component beams ae and bf, figure 88, prolonged as at eh, figure 96, each penetrate a column C and are returned by the normal mirror m'. Thus one reflection of the old method is obviated and adjustment is facilitated, since both beams are reflected from the common mirrors m and m'. To assist in the preliminary adjustment, the rigid system m, m' should be capable of revolving roughly about a vertical axis. With a wide beam the rays may then be guided by the eye to retrace their path. Fine adjustment is made by the triple screws on m and m' already mentioned.

The fringes in coincident spectra should first be sought. When found they will usually be very small. They may then be centered by rotating the mirror m about the horizontal axis, cautiously. They may be enlarged by rotating m with the same caution around the axis parallel to its trace in the diagram. The latter operation (or both) succeeds best with the achromatic fringes of a wide slit (no spectroscope). The horizontal axis is employed for erecting them, the axis parallel to the diagram for enlarging them, use being also made of the micrometer-screw at d on H_3, figure 88, if the fringes escape. In fact, the achromatic fringes are so sharp and luminous that in a quivering system the fringes are distinctly seen at the two elongations, doubled by the quiver.

To adequately support the mirrors m and m' reasonably free from vibration, a rectangular wooden yoke $F\,F$, figure 97, is best, so long as the installation is not permanent. This yoke is made of inch boarding about 18 inches high, 15 inches broad, and 3 inches deep. It is bolted below at d to the iron carriage S, and thus capable of rotation around a vertical axis and of sliding normal to its face on the iron slides $B\,B'$ (about 1.5 meters long) of the base. S and $B\,B'$ are arranged like a lath-bed.

The mirror m', which is horizontal, is adjustably attached to the top of the frame $F\,F$; three adjustment screws (two seen at a, a') and the strong spring s (pulling upward) control the position of m' with the usual plane dot-slot mechanism and axes of rotation parallel to and normal to the plane of the frame.

The board carrying the mirror m may be roughly set at 45° to the vertical by rotation on the strong bolts $b\,b'$ and clamped in position. The mirror m is attached to it by three adjustment screws and a rearward-acting spring, as shown in the case of m'. The axes of rotation are parallel to the two edges of m, and all fine adjustment, together with the final rotation of fringes and changes of their size, are made here.

The columns of the U-tubes C and C' must be supported from an independent bracket, suitably braced from the wall or from a separate pier, if liquid surfaces are in question. A part of this free support, the table, also of wood, appears at D, and holes are cut in it sufficiently large for the passage of the two beams of light α, α', which retrace their paths between m and m', passing through C and C'. The table D is provided with three leveling screws (two shown at c and c') on which a plate of thick glass G may be mounted and made accurately horizontal by aid of a spirit-level. The two columns C and C', joined by a flexible rubber pipe and provided at the bottom with glass windows, are placed on G, so that the beams of light pass through their axes. The magnetizing helix of each is shown at e and e'.

It is obvious, therefore, that the two columns of liquid in C and C' are of the same height and their ends parallel, other things being equal. Hence, if the apparatus is adjusted for the achromatic fringes in the absence of the U-tube $C\,C'$, it will be nearly in adjustment when the columns are introduced; and this proved to be the case. The rigid system is easily adjusted for strong

vertical achromatic fringes. The fringes are found with a few turns of the micrometer after the liquid w has been poured in.

The fringes as seen through the liquid columns are still strong and clear, with scarcely any deterioration; but unfortunately in this locality they are in incessant and vigorous vibration. It is indeed astonishing that a phenomenon so sensitive can survive such relatively rough treatment.

With this apparatus the endeavor was again made to determine the susceptibility of water. Good fringes were first produced, but for all levels of the water-surfaces the effect of the presence or absence of a magnetic field was quite *nil*, so far as any appreciable displacement of fringes was concerned. They remained in place while the current in the helix was alternately closed and opened. The reason for this completely negative result I am unable to explain.

In a repetition of such experiments tubes much wider than 4 cm. should be used. At this diameter the liquid surfaces still show appreciable curvature, which is an annoyance.

The yoke, figures 96 and 97, is finally a considerable convenience in the measurement of vertical angles near the zenith. The rotation of the mirror m' around its two axes is here available. Horizontal achromatic fringes in all these cases may often be produced and used to advantage. In such a case the two adjustment screws of the mirror m' change their function, and the fringes travel up and down the wide slit image with changes of ΔN. As this image is more extended vertically than horizontally, the fringes are much longer in sight. Fringes are largest when the planes of symmetry of pencils of rays accurately retrace their paths. But as large fringes are apt to be irregular, a small angle of reflection at the mirror m' is preferable.

73. The displacement interferometry of long distances.—In the preceding paragraphs I suggested two methods for the measurement of small angles. The first (fig. 88) used an auxiliary mirror, and, apart from corrections, the angle $\Delta\alpha$ over which the auxiliary mirror m turns is

$$\Delta\alpha = \Delta N \cos i / 2R \tag{1}$$

where ΔN is the displacement of one of the plane mirrors parallel to itself necessary to restore the achromatic fringes to their former position in the field of the telescope, i the angle of incidence (conveniently 45°), $2R$ the normal distance apart (*ab* or *cd*) of the (parallel) interfering pencils in the fore-and-aft direction of the incident beam. In the second method (fig. 93) the auxiliary mirror is dispensed with and the rotation of a rigid system of paired mirrors is used. The sensitiveness is half the preceding.

Suppose that the paired mirrors near the telescope (figs. 88, 93) confront but a part of the area of the objective and that the telescope can therefore look over the mirrors directly into the region * beyond, as shown at K. The

* A series of small mirrors or reflecting prisms may be employed to the same purpose; or the mirrors may both be half-silvered and transparent.

telescope now contains two images, the first due to rays (K) entering it directly, the second due to rays (L) reflected into it by the mirrors of the interferometer. Suppose the object seen lies at infinity like a star, that its two images are made to coincide by adjusting the angle α, and that the achromatic fringes have been brought into the field by adjusting the micrometer displacement N.

Now let the angle α be changed by $\Delta\alpha$ until the two images of an object M at a measurable distance d coincide. Displace the micrometer mirror by ΔN until the achromatic fringes are restored to their former position. Let b be the effective distance apart (ac or bd) of the paired mirrors in the direction right and left to the observer or transverse to the impinging rays (L), and finally s the angle at the apex of the triangle of sight on the base b—*i.e.*, the small angle between the present rays KL. Then

$$d = b \operatorname{cotg} s = b \operatorname{cotg} 2\Delta\alpha = b/2\Delta\alpha \tag{2}$$

(nearly) by the laws of reflection. Hence from equation (1)

$$d = bR/\Delta N \cos i \tag{3}$$

Here $2bR$ is the area of the *ray parallelogram* of the interferometer (*abdc*, fig. 88). Using the constants of my apparatus, let $i = 45°$, $R = 10$ cm., $b = 200$ cm., $\Delta N = 10^{-4}$ cm., the latter being the smallest division on the micrometer. Hence

$$d = 200 \times 10/10^{-4} \times 0.71 = 2.8 \times 10^{7} \text{ cm.} = 280 \text{ kilometers}$$

or about 170 miles, is the limit of measurement of the apparatus.

Again, from equation (3) the sensitiveness $\delta(\Delta N)/\delta d$, since

$$\delta d = (d^2 \cos i/bR)\delta(\Delta N) \tag{4}$$

is inversely proportional to the square of the long distance d and the area of the ray parallelogram $2bR$. Thus with the above constants, if d is 2 kilometers, $\delta(\Delta N) = 10^{-4}$ cm.,

$$\delta d = (d^2 \cos i/bR)\delta(\Delta N)$$

Thus an object at about a mile should be located to about 30 feet. Per fringe of mean wave-length λ, moreover, since $\delta d = \lambda d^2/2bR$, the placement should be about 6 meters at 2 kilometers. I have stated the case, of course, merely for the interferometer, not for subsidiary optical appurtenances, nor for measurement by angular fringe displacement.

74. Theory.—To account for these phenomena theoretically the equations of displacement interferometry are available; for the center of ellipses of these and the central member of the achromatic fringes correspond to the same position, ΔN, of the micrometer mirror. In fact, the fine white slit image which produces the spectrum when observed through the spectroscope is the central achromatic fringe when the spectroscope is removed. We have, there-

fore, for the centers of ellipses in the spectrum fringes the equation heretofore deduced,

$$2\Delta N \cos i = e\left\{(\mu - 1)\cos R - \frac{\lambda}{\cos R}\frac{d\mu}{d\lambda}\right\}$$

where ΔN is the displacement of the micrometer to restore the center of fringes to their original position in wave-length λ, when the angle of incidence at the mirror is i, after a glass plate of thickness e and index of refraction μ is introduced in one component beam, at an angle of incidence corresponding to the angle of refraction R in the plate. This is equivalent to an equation in terms of the coördinates N, if $\mu = A + B/\lambda^2$ is assumed,

$$2N \cos i = e\mu \cos R + 2eB/\lambda^2 \cos R$$

But for the colors of thin plates we may write

$$n\lambda = 2e\mu \cos R$$

where n is the order of the fringe. If the rays, as in the present experiment, do not retrace their paths, the factor 2 is omitted, whence

$$2N \cos i = n\lambda + 2eB/\lambda^2 \cos R$$

Let N and n vary together, i, R, λ, e, B, μ remaining constant. Then

$$2 \cos i \cdot \Delta N = \lambda \cdot \Delta n$$

Now let $\Delta\varphi$ be the angular breadth of a fringe in the telescope, so that

$$n \cdot \Delta\varphi = \Delta\theta$$

In other words, the displacement $\Delta\theta$ of the group of fringes is due to the displacement of the individual fringes as usual; but as only those achromatic fringes which coincide in micrometer value ΔN with the centers of the elliptic spectrum fringes are visible, the displacement of the group is actually seen and thus determinable. It would not be so in case of sudden displacement and homogeneous light.

Finally, the relative sensitiveness of the measurement of the angle $\Delta\alpha$, directly in terms of ΔN and indirectly in terms of the displacement of achromatic fringes, must be presented. The given rough data in table 38 are as close as they could be obtained from the small displacements entering. The quantities to be compared are: ΔN, the displacement of the micrometer; $\Delta\alpha$, the corresponding rotation of the auxiliary mirror in the first method; $\Delta\varphi$, the angle subtended by a single fringe in the telescope, and $\Delta\theta$, the corresponding angle of the displacement of the fringes in the telescope. $\Delta\theta$ was constant throughout and measured about 3 mm. in the ocular of a telescope 33 cm. long.

TABLE 38.—Values of ΔN, $\Delta\theta$, $\Delta\varphi$, $\Delta\alpha$. All angles in radians, ΔN in cm.

$\Delta\theta \times 10^6$	$\Delta\varphi \times 10^6$	$\Delta N \times 10^6$	$\Delta\alpha \times 10^6$	$\Delta\theta/\Delta N$	$\Delta\theta/\Delta\alpha$	$\Delta\varphi\Delta N \times 10^6$	$\Delta\varphi\Delta\alpha \times 10^6$
9000	500	730	52	12.3	170	0.365	0.026
9000	1500	250	18	36.0	500	.375	.027

Here $\Delta\alpha$ is computed from equation (1), where $i=45°$ and $2R=10$ cm., about. The fringes of width 100″ and 300″ were both brilliant and capable of high magnification.

Thus it appears that the fringes travel faster in proportion to their width, or if $\Delta\varphi$ increases n times, ΔN (for the same telescopic excursion $\Delta\theta$) will decrease n times. Again, the fringes travel as a body over hundreds of times the angle described by the auxiliary mirror ($\Delta\alpha$), when both are observed in the telescope. In the table $\Delta\theta/\Delta\alpha$ is 170 to 500 and could be increased indefinitely for larger fringes. The rotation $\Delta\alpha$ seen in the telescope would be but $2\Delta\alpha$. This is the gist of the present method of measuring small angles—*i.e., the fringe index moves through the telescopic field many hundred times faster than the image of the slit which measures the change of* $\Delta\alpha$ *directly.*

Finally, for the same $\Delta\theta$ or displacement of the fringe group, $\Delta\alpha\Delta\varphi$ is a constant, say C, or

$$\Delta\theta = C\Delta\varphi \cdot \Delta\alpha = C'\Delta\varphi \cdot \Delta N$$

where

$$C=\frac{9000}{0.0265}=340{,}000 \qquad C'=\frac{9000}{0.370}=24{,}500$$

It is not necessary to obtain sharper data, because these constants can be found theoretically. It will presently be shown that

$$C=4R/\lambda, C'=\frac{2\cos i}{\lambda}$$

where R is the radius of rotation measuring α. Thus

$$\frac{\Delta\theta}{\Delta N}=\frac{\Delta n\Delta\varphi}{\Delta N}=\frac{2\Delta\varphi\cos i}{\lambda}$$

If the $\Delta\varphi$ in the table be used, and $\lambda=60\times10^{-6}$ cm., $i=45°$, the results are

$\Delta\varphi=500\times10^{-6}$	1500×10^{-6}	
$\Delta\theta/\Delta N=11{\cdot}8$	35·3	(computed)
$\Delta\theta/\Delta N=12$	36	(observed)

results which agree with the values of the table as closely as these subtle measurements permit.

A few words may be added relative to the size of fringes so far as the glass-paths are concerned, the air-path conditions having been stated. For this purpose the equation of the phenomenon may be written

$$n\lambda=2e\mu\cos R-2N\cos i$$

where N is the coördinate of the mirror at the micrometer. When the center of ellipses (or of achromatic fringes) is at wave-length λ, $N=N_c$, the value given for centers above. If n, i, R above vary, while e, μ, λ, N are fixed, since $\sin i=\mu\sin R$,

$$\Delta\varphi=\frac{di}{dn}=\frac{\lambda}{2N\sin i-2e\tan R\cos i}$$

so that the size $\Delta\varphi$ is influenced inversely as the effective thickness e (*i.e.*, the difference of thickness) of plates and depends on the position N of the micrometer. If $N=N_e=e\,(\mu\cos R+2B/\lambda^2\cos R)/\cos i$

$$\Delta\varphi=\frac{di}{dn}=\frac{\lambda}{2e(\mu\cos R\tan i-\cos i\tan R+2B\tan i/\lambda^2\cos R)}$$

$$=\frac{\lambda\cos R}{2e\tan i\left((\mu^2-1)/\mu+2B/\lambda^2\right)}$$

Since $i=45°$, $R=27°\,9'$, $\lambda=60\times10^{-6}$ cm.

$$\Delta\varphi=\frac{60\times10^{-6}}{2e(1.55\times0.89-0.513\times0.71+0.03)}$$

The parenthesis is 1.05. Hence

$$e=\frac{\lambda}{2\Delta\varphi}\text{ nearly}$$

which would make the effective glass thickness $e=0.06$ cm. and 0.02 cm. for $\Delta\varphi=5\times10^{-4}$ radian and 15×10^{-4} radian, as above. Moreover, the rays K, figure 93, entering the telescope from the foreground directly and the rays L reflected into it by the plates of the interferometer, will not be parallel when the fringes are of maximum size unless the plates M and N are equally thick. Finally, the size of fringes in general (apart from wedge-shape of plates) will be inversely as the effective differential thickness e of the plates used.

If we collect the above equations* we may write roughly (since $e=\frac{\lambda}{2\Delta\varphi}$ nearly),

$$\Delta\theta=\frac{4R}{\lambda}\Delta\varphi\Delta\alpha=2R\Delta\alpha/e \qquad \Delta\theta=\frac{2\cos i}{\lambda}\Delta\varphi\Delta N=\frac{\cos i}{e}\Delta N \qquad d=\frac{bR}{\Delta N\cos i}=\frac{bR}{e\Delta\theta}$$

so that the measurement of the long distance d depends ultimately on the area of the ray parallelogram $2bR$, the differential thickness e of the corresponding half-silvers, and the (relatively to $\Delta\alpha$) enormous displacement $\Delta\theta$ of the achromatic fringes.

Finally, if optic plate-glass were used for the half-silvered mirrors, the parallelism of rays KL would coincide with the occurrence of centered or circular achromatic fringes; while the whole preliminary adjustment of mirrors for parallelism would consist in bringing the image from $LMN'T$, figure 93, and from $LM'NT$, successively into coincidence with the direct image from K, in case of a very distant source of light.

The remarkable sensitiveness which accrues to the method, if the angular displacement of fringes is measured in the ocular of a long telescope, comes

* The text unduly accentuates the glass-paths, whereas the air-paths are more important. I shall give a rigorous deduction of all the path-differences in my next Report to the Institution, where they will be sustained in detail by experiments.

out clearly if the last equation for d is used. In case of corresponding increments δd and $\delta(\Delta\theta)$, this equation is equivalent to

$$-\delta d = \frac{d^2 e}{bR}\,\delta(\Delta\theta)$$

But if L is the length of the telescope and δn the micrometric displacement of fringes in the ocular corresponding to δd,

$$\delta(\Delta\theta) = \frac{\delta n}{L}$$

whence

$$\delta d = \frac{d^2 e}{bRL}\,\delta n$$

Thus if e, the difference in thickness of the corresponding half-silver mirrors, and δn be each even as large as 0.1 mm., and d a kilometer,

$$d = 10^5 \text{ cm.},\ e = 10^{-2} \text{ cm.},\ b = 200 \text{ cm.},\ R = 10 \text{ cm.},\ L = 50 \text{ cm.},\ \delta n = 10^{-2} \text{ cm.}$$

$$\delta d = \frac{10^{10} \times 10^{-2} \times 10^{-2}}{200 \times 10 \times 50} = 10 \text{ cm.}$$

With these very moderate estimates a distance of 1 kilometer should be measurable to 10 cm., so far as the glass-paths of the interferometer are concerned.

THE INTERFEROMETRY OF REVERSED AND NON-REVERSED SPECTRA

PART II

By CARL BARUS

Hazard Professor of Physics and Dean of the Graduate Department in Brown University



Published by the Carnegie Institution of Washington
Washington, 1917

MBL/WHOI LIBRARY
WH 18GV J